Numerical Methods for Time-Domain Boundary Integral Equations

---

Dissertation
zur
Erlangung der naturwissenschaftlichen Doktorwürde
(Dr. sc. nat.)
vorgelegt der
Mathematisch-naturwissenschaftlichen Fakultät
der
Universität Zürich
von

Alexander Veit
aus Deutschland

Promotionskomitee
Prof. Dr. Stefan A. Sauter (Vorsitz)
Prof. Dr. Michel Chipot
Prof. Dr. Joachim Rosenthal

Zürich, 2012

Abstract

In this thesis we are concerned with the development of numerical schemes for the solution of time-dependent acoustic and electromagnetic scattering problems in unbounded domains. In this setting the method of integral equations is an elegant approach which transforms the underlying partial differential equation to an integral equation on the bounded surface of the scatterer. The choice of the time discretization scheme for these equations is crucial for the stability and accuracy of the overall numerical method.
In the literature there exist essentially two approaches for which unconditional stability can be proved. The first is based on a Galerkin discretization of coercive space-time variational formulations. We propose new types of finite-dimensional spaces for the time discretization which allow variable time-stepping and variable order of approximation. Since the basis functions of these spaces are C^∞-smooth and compactly supported the quadrature problem arising in the generation of the system matrix is simplified substantially compared to the standard approach. In order to reduce the computational cost to evaluate the arising 4-dimensional integrals we propose a new quadrature technique based on low-rank tensor approximations. Numerical experiments for a spherical scatterer are presented. In order to have suitable reference solutions for these experiments we derive exact solutions of different boundary integral equations arising for Dirichlet and Neumann problems in acoustic scattering.
The second unconditionally stable approach for the time discretization of time-domain boundary integral equations is based on convolution quadrature. We apply Runge-Kutta convolution quadrature and a Galerkin method in space to the time-domain electric field integral equation arising in electromagnetic scattering. We derive an error analysis for the fully discrete scheme and perform numerical experiments.

Zusammenfassung

In dieser Arbeit beschäftigen wir uns mit der Entwicklung numerischer Verfahren zur Lösung von zeitabhängigen akustischen und elektromagnetischen Streuproblemen in unbeschränkten Gebieten. Die Methode der Integralgleichungen stellt hier eine elegante Herangehensweise dar, welche die zugrundeliegende partielle Differentialgleichung in eine Integralgleichung auf der beschränkten Oberfläche des Streuobjekts transformiert. Die Art der Zeitdiskretisierung dieser Gleichungen ist wesentlich für die Stabilität und Genauigkeit der gesamten numerischen Methode.
In der Literatur existieren hauptsächlich zwei Methoden, für welche uneingeschränkte Stabilität gezeigt werden kann. Die erste basiert auf einer Galerkin-Diskretisierung von koerziven Variationsformulierungen in Raum und Zeit. Wir führen eine neue Art von endlichdimensionalen Räumen für die Zeitdiskretisierung ein, welche variable Zeitschrittweiten und beliebige Approximationsordnungen erlauben. Da die Basisfunktionen dieser Räume unendlich oft stetig differenzierbar sind und ausserdem einen kompakten Träger besitzen, ist die Quadratur, welche zur Erstellung der Systemmatrix benötigt wird, deutlich einfacher als beim Standardverfahren. Um den Rechenaufwand zu reduzieren, der benötigt wird um die auftretenden vierdimensionalen Integrale auszuwerten, schlagen wir ein neues Quadraturverfahren vor, welches auf Tensorapproximation basiert. Numerische Experimente werden für die Streuung an einer Kugel durchgeführt. Um geeignete Referenzlösungen für diese Experimente zur Verfügung zu haben, leiten wir exakte Lösungen für verschiedene Randintegralgleichungen her, die bei Dirichlet und Neumann Problemen in der Akustik auftreten.
Die zweite, uneingeschränkt stabile Methode für die Zeitdiskretisierung von zeitabhängigen Randintegralgleichungen beruht auf Faltungsquadratur. Wir wenden Faltungsquadratur basierend auf Runge-Kutta Verfahren und eine Galerkin Methode im Raum auf die *electric field integral equation* im Zeitbereich an, welche bei elektromagnetischen Streuproblemen auftritt. Wir leiten eine Fehleranalyse für das diskrete Verfahren her und führen numerische Experimente durch.

Acknowledgement

First and foremost I would like to thank my supervisor Prof. Stefan Sauter for giving me the opportunity to write this PhD thesis in his workgroup. I am very grateful for his support, encouragement and expertise during my time at the University of Zurich. His great interest in my work led to numerous discussions and a frequent exchange of ideas creating a stimulating working atmosphere.

I am also deeply grateful to Lehel Banjai and Boris Khoromskij for inviting me several times to the Max-Planck-Institut in Leipzig. Their patience in answering all my questions and many insightful discussions were a great help for me. Here, I also want to thank Jonas Ballani, who helped me with various technical problems during my stays in Leipzig.

I also want to thank all my colleagues who worked with me at the University of Zurich, especially María López-Fernández for many fruitful discussions.

Special thanks go to Corina Simian for her friendship and support during the last two years.

Finally I would like to thank my family for their encouragement and support.

October 2011, Zurich Alexander Veit

Contents

Introduction

The accurate numerical simulation of wave propagation phenomena plays an important role in various application areas like detection, medicine, antenna design, underwater acoustics and many others. Most of these industrial applications lead to problems with a very large number of unknowns and therefore an enormous computational complexity for their numerical solution. The development and analysis of efficient, accurate and reliable numerical methods to treat such problems is therefore of great importance.
Acoustic and electromagnetic scattering problems play a significant role in the applications described above. They are governed by the scalar wave equation and the Maxwell equations respectively and are often posed as exterior problems in unbounded domains. The question of interest then reads: Given an incoming acoustic or electromagnetic wave that is propagating towards a bounded obstacle of arbitrary shape. Determine the field that is scattered by the obstacle from the knowledge of the incoming wave and the underlying physical laws of the wave propagation. The existing literature dealing with such scattering phenomena is in large part concerned with problems in the frequency domain. However, if an incoming wave is broad band it is often advantageous to compute directly in the time-domain since a wide range of frequencies is considered in only one experiment. The development and analysis of efficient methods for acoustic and electromagnetic scattering problems in the time-domain has gained growing attention in the last years and is the main topic of the present work. In the literature there exist different approaches to treat the arising equations numerically including domain methods like finite difference or finite element methods and methods based on boundary integral equations, which will be in the focus here. In this approach the unknown scattered wave which propagates in the unbounded domain is not computed directly. Instead the problem is reduced to an integral equation on the bounded surface of the scatterer which has to be solved for an auxiliary function. The actual solution of the scattering problem in the exterior domain can then be obtained via a cheap postprocessing. This approach has two important advantages compared to the domain methods mentioned above. First, since the problem is reduced to the boundary of the scatterer the space discretization has only to be performed for a two-dimensional surface instead of a three-dimensional domain. Second, since the surface of the obstacle is bounded there is no need to introduce artificial boundaries, which is necessary, e.g., for finite element methods in order to obtain finite computational domains. Therefore the difficult question how to choose suitable boundary conditions for this artificial boundary becomes superfluous.
Numerical methods based on time-domain boundary integral equations (TDBIEs), or alternatively retarded boundary integral equations, have now a 50 year history of development. Although they were unpopular in the beginning due to instabilities their importance increased with improved formulations and discretization techniques. This progress led to a successful application of these methods to various problems in, e.g., acoustics, electromagnetics or elas-

todynamics.
A successful numerical handling of TDBIEs is closely related to the question how to discretize these equations in time. In this context mainly two approaches are in the focus of current research for which unconditional stability can be proved. The first is due to A. Bamberger and T. Ha Duong and was introduced in 1986. They derived a coercive space-time variational formulation of the boundary integral equation arising in acoustic scattering and showed the stability of conforming Galerkin discretization schemes. Such formulations could also be found for electromagnetic and other wave propagation problems. The second approach to discretize TDBIEs in time that we want to mention here is based on convolution quadrature introduced by C. Lubich in 1988. This method exploits the fact that TDBIEs can be written as a convolution with respect to the time variable. The continuous convolution is then approximated by a discrete one only using the Laplace transform of the time-domain kernel function. This is an important advantage compared to methods which compute directly in the time-domain since frequency domain fundamental solutions are known for a wider class of problems which makes the method convenient for various applications. This and the excellent stability properties of the scheme led to an increasing interest in convolution quadrature based time discretizations for retarded potentials in recent years.
In the present work we will be especially concerned with the development and analysis of time discretization schemes for TDBIEs based on space-time variational formulations and convolution quadrature. The thesis is mainly based on a collection of four articles incorporated in different chapters having its own bibliography list. Solely Chapter 1 is an exception and serves as an introduction into the topic. Important boundary integral operators are defined such that the necessary boundary integral equations can be derived which will be needed in the following. In Chapter 2 we consider TDBIEs arising for different Dirichlet and Neumann problems in acoustic scattering. In the case of a spherical scatterer and specially chosen right-hand sides which are separable in space and time it is possible to reduce these equations to univariate problems in time. We solve these problems analytically which leads to exact solutions of the full scattering problems. In Chapter 3 we are concerned with the time discretization of space-time variational formulations of TDBIEs arising in sound-soft obstacle scattering. The standard Galerkin approach in space and time using piecewise polynomial basis function leads to difficult quadrature problems on complicated domains when evaluating the entries of the boundary element matrix. We therefore introduce C^∞-smooth and compactly supported basis functions in time which simplify this problem considerably. Furthermore they easily allow the use of a variable time-stepping and curved surface patches which is necessary to obtain higher order schemes. The benefit of this approach is demonstrated by numerical experiments in the setting of Chapter 2. Also in this approach the quadrature that is needed to compute the entries of the boundary element matrix and which has to be performed over the four dimensional unit cube is the most time-consuming part of the method. However, due to the smoothness of the integrand there exist various possibilities to evaluate the arising integrals efficiently. In Chapter 4 we propose a quadrature technique based on low-rank tensor approximations. We start from the standard tensor Gauss quadrature approach which requires the evaluation of the integrand on a four dimensional product grid. We show that the corresponding tensors can be compressed efficiently using the tensor train (TT) and quantized tensor train (QTT) format. The evaluation of the quadrature is then just a simple tensor operation involving the compressed tensor and a rank-1 coefficients tensor containing the weights of the Gauss quadrature. Various numerical experiments show the significant reduction of the computational cost that is needed to compute the arising

integrals accurately compared to the tensor Gauss quadrature approach. In Chapter 5 we are concerned with electromagnetic scattering problems. We consider the case of a perfectly conducting scatterer and discretize the time-domain electric field integral equation (EFIE) using convolution quadrature in time and a Galerkin method in space. Here we are especially concerned with convolution quadrature based on Runge-Kutta methods which became increasingly popular in recent years due to good stability estimates and the ability to obtain higher order schemes in time. We derive an error analysis for the fully-discrete scheme and illustrate the sharpness of the theoretical estimates by numerical experiments.

1

Time-Domain Boundary Integral Equations in Acoustics and their Discretization in Time

In this chapter we introduce the scattering problem and give a brief overview of classical acoustic scattering theory as presented, e.g., in [9, 12, 13]. We define the common boundary integral operators and the corresponding boundary integral equations which will be needed in the subsequent chapters. Furthermore we recall important properties of the Galerkin as well as the convolution quadrature approach for the time discretization of these integral equations. We restrict our presentation in this chapter to the acoustic case. For scattering problems arising in electromagnetics, which will be the topic in Chapter 5, similar boundary integral equations can be derived and analyzed (cf. [21, 7, 11]).

1.1 Acoustic Scattering Problems

The propagation of acoustic waves in a homogeneous medium in $\mathbb{R}^3$ is governed by the scalar wave equation

$$\frac{1}{c^2}\frac{\partial^2 p}{\partial t^2} - \Delta p = 0,$$

where p is the acoustic pressure and c is the speed of sound in the considered medium. In the following considerations we will always set $c = 1$. This second order partial differential equation describes the evolution of p as a function of position $x \in \mathbb{R}^3$ and time $t \in \mathbb{R}$. The wave equation is of hyperbolic nature which is reflected in the finite speed of the wave propagation. Disturbences, e.g., changes in the the initial or boundary conditions of such problems, do not have, unlike in elliptic or parabolic PDEs, an immediate effect on every point of the considered domain.
In order to study acoustic scattering problems we consider the following setting. Let $\Omega := \Omega^e \subset \mathbb{R}^3$ be an unbounded connected domain with bounded complement $\Omega^i := \mathbb{R}^3 \backslash \bar{\Omega}$ and Lipschitz boundary $\Gamma = \partial\Omega^e = \partial\Omega^i$. Suppose that the exterior domain Ω is occupied by a homogeneous medium and that an incident field u^i, propagating in Ω, hits the scatterer Ω^i at a certain time. Given this setting the direct scattering problem is to determine the acoustic

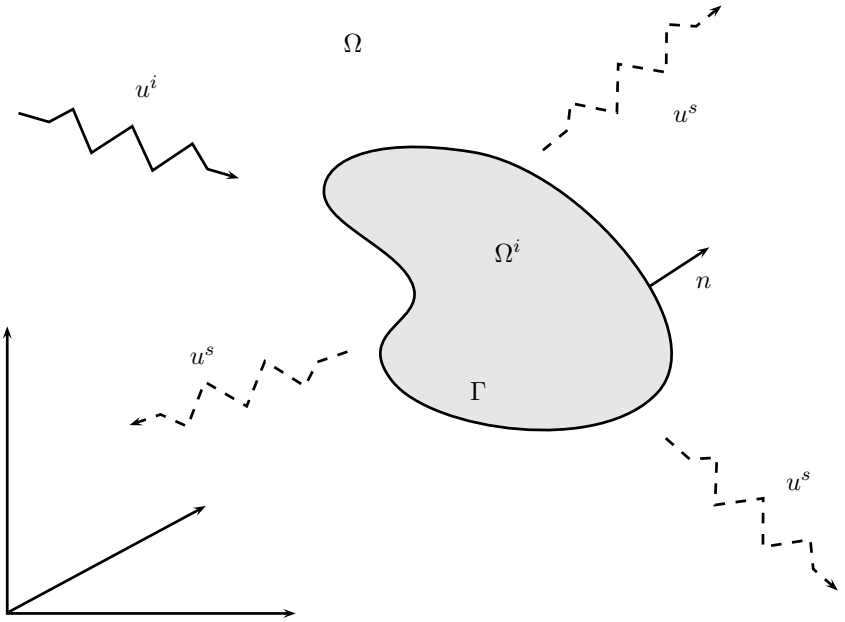

Figure 1.1: *Scattering of an incoming wave u^i at the obstacle Ω^i.*

pressure u^s of the scattered field from the knowledge of u^i and the underlying physical laws of the propagation, i.e., the wave equation (cf. Figure 1.1).

In order to solve this problem, suitable initial and boundary condition have to be employed. We assume that the incoming wave u^i has not reached the scatterer Ω^i at time $t = 0$, such that the scattered wave and its derivative at this time and before are zero in the whole exterior domain. The scattered wave u^s then satisfies the equations:

$$\partial_t^2 u^s - \Delta u^s = 0 \quad \text{in } \Omega \times [0,T]\,, \tag{1.1.1a}$$

$$u^s(\cdot,0) = \partial_t u^s(\cdot,0) = 0 \quad \text{in } \Omega, \tag{1.1.1b}$$

on a time interval $[0,T]$ for $T > 0$. Suitable boundary conditions depend on the material properties of the scatterer. In this thesis acoustically soft scatterers will be in the main focus which can be modeled with the Dirichlet boundary conditions

$$u^s = -u^i =: g \quad \text{on } \Gamma \times [0,T]\,. \tag{1.1.2}$$

An absorbing scatterer can be modeled by replacing the boundary conditions (1.1.2) by

$$\partial_n u^s - \alpha\, \partial_t u^s = -\partial_n u^i + \alpha\, \partial_t u^i \quad \text{on } \Gamma \times [0,T]\,, \tag{1.1.3}$$

where n is the outer unit normal vector and α is the impedance function of Γ. Assuming that $\alpha(x) \geq 0\ \forall x \in \Gamma$ it can be shown that the problem above is well posed (cf. [12, 13]). The case of a sound-hard scatterer results from the choice $\alpha \equiv 0$, i.e.,

$$\partial_n u^s = -\partial_n u^i =: h \quad \text{on } \Gamma \times [0,T] \tag{1.1.4}$$

and is mathematically therefore a Neumann problem.

In order to solve the scattering problem (1.1.1) together with suitable boundary conditions

we use the method of boundary integral equations. Especially in unbounded domains this approach shows its natural strength, reducing the original problem to a problem to the bounded surface of the scatterer. Suitable boundary integral formulations can be obtained with the following representation formula for the solution u of problem (1.1.1): Let $[v]$ denote the jump of a function v across Γ, then

$$\begin{aligned} u(x,t) =& \frac{1}{4\pi}\int_0^t \int_\Gamma \partial_{n_y} k(x-y,t-\tau)[u(y,\tau)] - k(x-y,t-\tau)[\partial_{n_y} u(y,\tau)] d\Gamma_y d\tau \\ =& \frac{1}{4\pi}\int_\Gamma \frac{n_y\cdot(x-y)}{\|x-y\|}\left(\frac{[u(y,t-\|x-y\|)]}{\|x-y\|^2} + \frac{[\partial_t u(y,t-\|x-y\|)]}{\|x-y\|}\right) d\Gamma_y \\ & - \frac{1}{4\pi}\int_\Gamma \frac{[\partial_n u(y,t-\|x-y\|)]}{\|x-y\|} d\Gamma_y \qquad \forall (x,t)\in \Omega\backslash\Gamma\times[0,T], \end{aligned} \tag{1.1.5}$$

where

$$k(z,t) := \frac{\delta(t-\|z\|)}{4\pi\|z\|} \tag{1.1.6}$$

is the fundamental solution of the wave equation and δ is the Dirac delta function. The knowledge of a fundamental solution of the underlying partial differential equation is an important requirement for the existence of such representation formulas. Their availability can be a serious restriction when using the boundary integral equation method for time-dependent problems, since such solutions are often not known explicitly or they are too complicated to handle. See, however, Section 1.2.2 for a way how to apply the method if only the fundamental solutions of the corresponding time-harmonic problems are known.

Formula (1.1.5) is a representation of u by so-called *retarded potentials*. Due to the causality of u, i.e., $u(x,t)=0$ in Ω for $t\le 0$, and due to the retarded time argument the integration has to be performed only on the intersection of the boundary Γ with the backward light cone. Note that such a simple representation by retarded potentials can in general not be obtained in situations where Huygens principle is not valid as e.g. for the wave equation in 2D or the dissipative wave equation.
In order to solve problem (1.1.1) with one of the boundary conditions (1.1.2)-(1.1.4) we need suitable boundary integral equations. For this purpose we define the *retarded single layer potential* by

$$S\phi(x,t) := \frac{1}{4\pi}\int_\Gamma \frac{\phi(y,t-\|x-y\|)}{\|x-y\|} d\Gamma_y \qquad \text{for } (x,t)\in\Omega\backslash\Gamma\times[0,T] \tag{1.1.7}$$

and the *retarded double layer potential* by

$$Dv(x,t) := \frac{1}{4\pi}\int_\Gamma \frac{n_y\cdot(x-y)}{\|x-y\|}\left(\frac{v(y,t-\|x-y\|)}{\|x-y\|^2} + \frac{\partial_t v(y,t-\|x-y\|)}{\|x-y\|}\right) d\Gamma_y \tag{1.1.8}$$

for $(x,t)\in\Omega\backslash\Gamma\times[0,T]$. Note that with these definitions the representation formula (1.1.5) reads:

$$u(x,t) = D([u])(x,t) - S([\partial_n u])(x,t). \tag{1.1.9}$$

Every function that can be written in terms of either a single or a double layer potential or a linear combination of both satisfies the wave equation (1.1.1a) and the initial conditions (1.1.1b). In order to obtain boundary integral equations these integral operators have to be extended to the boundary Γ.

Definition 1.1.1 (Time-domain boundary integral operators). *Let $(x,t) \in \Gamma \times [0,T]$. The single layer potential on the boundary is given by*

$$V\phi(x,t) := \frac{1}{4\pi} \int_\Gamma \frac{\phi(y, t - \|x-y\|)}{\|x-y\|} \, d\Gamma_y, \tag{1.1.10}$$

whereas the corresponding double layer potential is defined by

$$Kv(x,t) := \frac{1}{4\pi} \int_\Gamma \frac{n_y \cdot (x-y)}{\|x-y\|} \left(\frac{v(y, t-\|x-y\|)}{\|x-y\|^2} + \frac{\partial_t v(y, t-\|x-y\|)}{\|x-y\|} \right) d\Gamma_y. \tag{1.1.11}$$

Moreover, we define the normal derivative of the single layer potential as

$$K'\phi(x,t) := \frac{1}{4\pi} \int_\Gamma \frac{n_x \cdot (x-y)}{\|x-y\|} \left(\frac{\phi(y, t-\|x-y\|)}{\|x-y\|^2} + \frac{\partial_t \phi(y, t-\|x-y\|)}{\|x-y\|} \right) d\Gamma_y. \tag{1.1.12}$$

Finally the normal derivative of the double layer potential defines the operator

$$Wv(x,t) := \lim_{x^+ \in \Omega \to x} n_x \cdot \nabla_{x^+} Dv(x^+, t). \tag{1.1.13}$$

With these definitions we can characterize the jumps of the single layer potential (1.1.7), the double layer potential (1.1.8) and its normal derivatives when $x \in \Omega \backslash \Gamma$ is approaching the boundary Γ. Let $x \in \Gamma$ and

$$u|_{\text{int}}(x,t) := \lim_{x^- \in \Omega^- \to x} u(x^-, t), \qquad u|_{\text{ext}}(x,t) := \lim_{x^+ \in \Omega \to x} u(x^+, t).$$

Then, the following theorem holds:

Theorem 1.1.2. *Let ϕ and v be sufficiently regular density functions and $x \in \Gamma$. The single layer potential is continuous in $\mathbb{R}^3$, especially when crossing the boundary Γ. It holds*

$$S\phi|_{\text{int}}(x,t) = S\phi|_{\text{ext}}(x,t) = V\phi(x,t).$$

The normal derivative of S is discontinuous when crossing Γ. On the boundary it admits the values

$$\partial_n S\phi|_{\text{int}}(x,t) = \frac{\phi(x,t)}{2} + K'\phi(x,t),$$
$$\partial_n S\phi|_{\text{ext}}(x,t) = -\frac{\phi(x,t)}{2} + K'\phi(x,t).$$

The double layer potential is discontinuous when crossing Γ. The limit values are

$$Dv|_{\text{int}}(x,t) = -\frac{v(x,t)}{2} + Kv(x,t),$$
$$Dv|_{\text{ext}}(x,t) = \frac{v(x,t)}{2} + Kv(x,t).$$

The normal derivative of the double layer potential is continuous when crossing Γ. It holds

$$\partial_n Dv|_{\text{int}}(x,t) = \partial_n Dv|_{\text{ext}}(x,t) = Wv(x,t).$$

Note that the operator W contains a hypersingular kernel equivalent to $1/\|x-y\|^3$ and the integral has to be defined as a finite part *integral.*

The jump relations in Theorem 1.1.2 now lead to suitable boundary integral equations for the considered scattering problems. We begin with the case of a soft scatterer, i.e., Dirichlet boundary conditions. Assume that the boundary data $u|_\Gamma = g$ is given. The Dirichlet trace of (1.1.2) together with the representation formula (1.1.9) leads to the integral equation

$$V\psi = -\frac{g}{2} + Kg, \tag{1.1.14}$$

where $\psi = \partial_n u|_\Gamma$ is unknown. Taking the Neumann trace leads in the same way to

$$\frac{\psi}{2} + K'\psi = Wg. \tag{1.1.15}$$

The integral equations (1.1.14) and (1.1.15) are "direct" formulations. The unknown in this case is the physical quantity $\partial_n u|_\Gamma$. As mentioned before also the ansatz of the solution u as a single layer potential respectively as a double layer potential

$$u = S\phi \qquad \text{and} \qquad u = Dw$$

with unknown density functions ϕ and w, satisfies the wave equation and the initial conditions. Boundary integral equations based on these potentials therefore read

$$V\phi = g \tag{1.1.16}$$

and

$$\frac{w}{2} + Kw = g. \tag{1.1.17}$$

The integral equations (1.1.16) and (1.1.17) are referred to as "indirect" formulations.
Now we consider the case of an acoustically hard scatterer which can be modeled with Neumann boundary conditions. We assume that the boundary data $h := \partial_n u|_\Gamma$ is given and that the Dirichlet trace $v := u|_\Gamma$ is unknown. The last definition leads together with (1.1.9) to the integral equation

$$\frac{v}{2} - Kv = -Vh. \tag{1.1.18}$$

Taking the Neumann trace leads to the alternative direct formulation

$$Wv = \frac{h}{2} + K'h. \tag{1.1.19}$$

Using the single layer and double layer potential ansatz leads as before to the indirect formulations

$$\frac{\phi}{2} - K'\phi = -h \tag{1.1.20}$$

and

$$Ww = h, \tag{1.1.21}$$

where ϕ and w are unknown density functions. Note that for the case of an absorbing scatterer with boundary conditions (1.1.3) similar boundary integral formulations can be obtained (cf. [12]). In Chapter 2 we will derive explicit representations of exact solutions for the problems (1.1.14)-(1.1.21) on the sphere.

We will focus in this thesis mainly on Dirichlet problems based on the indirect formulation (1.1.16) involving the single layer potential. Here, the unknown density function ϕ occurs

as the trace difference of the solution of the exterior and the solution of the interior wave equation. Since the solution of the interior problem is governed by the reflections of the waves inside the scatterer, the density function ϕ usually admits an oscillatory, non-decaying shape. In some cases the direct formulation (1.1.14) or (1.1.15) might therefore be easier to solve than the indirect problem. Note however, that in the case of non-convex scatterers oscillations might occur also for the exterior problem so that the difficulty to compute a solution with the direct formulation becomes comparable to the indirect formulation.
Existence and uniqueness results for the boundary integral equation (1.1.16) were proved in [1, 17, 12].

1.2 Discretization in Time

One of the key questions for a successful numerical handling of time-domain boundary integral equations arising in acoustics or electromagnetics is how to discretize these equations in time. The choice of the discretization scheme has a major impact on the accuracy, stability and implementational difficulties of the overall numerical method. A large number of methods use collocation schemes for the time discretization. Unfortunately this approach tends to exhibit numerical instabilities (cf. [14, 5]). Although several stabilization techniques such as averaging over the last few timesteps (cf. [10, 20]) or implicit time-stepping (cf. [6]) were proposed a general proof for the stability of these methods is not yet available. In this thesis we will concentrate on discretization schemes based on space-time variational formulations as well as methods based on convolution quadrature. For both approaches the stability of the resulting methods can be proved. In the following we briefly recall some important properties of these techniques.

1.2.1 Galerkin Methods based on Space-Time Variational Formulations

For the discretization of the TDBIEs above by a Galerkin method in space and time suitable space-time variational formulations are necessary. In 1986 A. Bamberger and T. Ha-Duong (cf. [1]) developed an approach which led to a continuous and coercive variational formulation of problem (1.1.16), where instead of a finite time interval $[0,T]$ the whole positive real line $\mathbb{R}_+$ was considered. They showed the existence and uniqueness of a weak solution as well as unconditional stability of conforming Galerkin approximations by boundary element methods. The essential idea of obtaining such results is to transform the time-dependent boundary integral equation (1.1.16) into frequency domain using a Laplace transformation. The transformed equation is a Helmholtz problem with complex frequency which is uniquely solvable in appropriate Sobolev spaces. Furthermore a variational formulation can be derived and analyzed for this problem. By applying an inverse Laplace transform the results in the frequency domain can then be used to show the corresponding properties in the time-domain using the Paley-Wiener and Parseval's theorem.

Remark 1.2.1. *This approach of proving properties of TDBIEs and obtaining suitable variational formulations can be applied to several problems, including the Dirichlet problem* (1.1.17)*, the Neumann problems* (1.1.20) *and* (1.1.21) *as well as problems with absorbing boundary conditions (cf. [12]). Furthermore also TDBIEs arising in electromagnetic scattering can be analyzed in this way (cf. [19, 22, 23, 8]).*

Ha-Duong extended in [12] the results of [1] to finite time intervals. Let us define the spaces

$$H^{1/2,1/2}(\Gamma \times [0,T]) := L^2(0,T;H^{1/2}(\Gamma)) \cap H^{1/2}(0,T;L^2(\Gamma)) \tag{1.2.1}$$

and

$$H^{-1/2,-1/2}(\Gamma \times [0,T]) := L^2(0,T;H^{-1/2}(\Gamma)) + H^{-1/2}(0,T;L^2(\Gamma)). \tag{1.2.2}$$

Now we consider the variational formulation: Find $\phi \in \left\{ \phi \,|\, \dot{\phi} \in H^{-1/2,-1/2}(\Gamma \times [0,T]) \right\}$ such that

$$\int_0^T \int_\Gamma V\dot{\phi}(x,t)\zeta(x,t)dt = \int_0^T \int_\Gamma \dot{g}(x,t)\zeta(x,t)dt \tag{1.2.3}$$

for all test functions $\zeta \in H^{-1/2,-1/2}(\Gamma \times [0,T])$. Then, the following theorem holds:

Theorem 1.2.2. *Let the right-hand side g in* (1.1.16) *be given such that $\dot{g} \in H^{1/2,1/2}(\Gamma \times [0,T])$ and null conditions at $t = 0$. Then, the variational formulation* (1.2.3) *admits a unique solution ϕ satisfying the stability estimate*

$$\|\phi\|_{H^{-1/2,-1/2}(\Gamma\times[0,T])} \leq C\|\dot{g}\|_{H^{1/2,1/2}(\Gamma\times[0,T])}.$$

Furthermore ϕ is a solution of the boundary integral equation (1.1.16).

The conforming Galerkin approach now consists of replacing the ansatz and test space $H^{-1/2,-1/2}(\Gamma \times [0,T])$ by a finite dimensional subspace V_G. The discretized problem then reads: Find ϕ_G such that $\dot{\phi}_G \in V_G$ and

$$\int_0^T \int_\Gamma V\dot{\phi}_G(x,t)\zeta_G(x,t)dt = \int_0^T \int_\Gamma \dot{g}(x,t)\zeta_G(x,t)dt$$

for all test functions $\zeta_G \in V_G$. The stability of conforming Galerkin solutions is an immediate consequence of Theorem 1.2.2.

1.2.2 Methods based on Convolution Quadrature

An alternative approach to discretize TDBIEs in time is based on convolution quadrature. It was developed by C. Lubich in [15, 16] and has since then been applied to numerous problems. We refer the interested reader to the review papers [18, 4] and the references therein. In Chapter 5 we briefly recall the method and apply it to time-domain boundary integral equations arising in electromagnetics.

An important advantage of convolution quadrature is that only the Laplace transform of time-domain fundamental solution is required. This feature makes the method applicable to a large class of problems, including many applications in engineering, where often only the Laplace domain kernel functions are known explicitly. Methods like the Galerkin approach above, which compute entirely in the time domain, are only of limited use for many of these problems since the distributional fundamental solutions are too complicated to handle numerically, if they exist at all.

Another important property of convolution quadrature is its unconditional stability which is due to the A-stability of the underlying discretization scheme. Here, classically linear multistep methods were used to approximate the ordinary differential equation which arises in the construction of the method. However, the fact that by Dahlquist's barrier the order of an A-stable linear multistep method cannot be greater than 2, led recently to an increased

interest in Runge-Kutta methods to solve these equations numerically. The ability to obtain higher order methods in time as well as the promising numerical and theoretical results (cf. e.g. [2, 3]) seem to underline the importance of Runge-Kutta convolution quadrature for the discretization of time-domain boundary integral equations.

References

[1] A. Bamberger and T. Ha Duong. Formulation Variationnelle Espace-Temps pur le Calcul par Potientiel Retardé de la Diffraction d'une Onde Acoustique. *Math. Meth. in the Appl. Sci.*, 8:405–435, 1986.

[2] L. Banjai. Multistep and multistage convolution quadrature for the wave equation: Algorithms and experiments. *SIAM J. Sci. Comput.*, 32(5):2964–2994, 2010.

[3] L. Banjai, J. Melenk, and C. Lubich. Runge-Kutta convolution quadrature for operators arising in wave propagation. *Numer. Math.*, 119(1):1–20, 2011.

[4] L. Banjai and M. Schanz. Wave Propagation Problems treated with Convolution Quadrature and BEM. Preprint 60/2010, MPI Leipzig.

[5] B. Birgisson, E. Siebrits, and A. Peirce. Elastodynamic Direct Boundary Element Methods with Enhanced Numerical Stability Properties. *Int. J. Num. Meth. Eng.*, 46:871–888, 1999.

[6] M. J. Bluck and S. P. Walker. Analysis of three dimensional transient acoustic wave propagation using the boundary integral equation method. *Int. J. Num. Meth. Eng.*, 39:1419–1431, 1996.

[7] M. Cessenat. *Mathematical Methods in Electromagnetism.* World Scietific Publishing, 1996.

[8] Q. Chen, P. Monk, X. Wang, and D. Weile. Analysis of Convolution Quadrature Applied to the Time-Domain Electric Field Integral Equation. *Submitted.*

[9] M. Costabel. Time-dependent problems with the boundary integral equation method. *Encyclopedia of Computational Mechanics*, pages 1–28, 2004.

[10] P. J. Davies and D. B. Duncan. Averaging techniques for time-marching schemes for retarded potential integral equations. *Appl. Numer. Math.*, 23:291–310, May 1997.

[11] A. Geranmayeh. *Time Domain Boundary Integral Equations Analysis.* PhD thesis, Institut Theorie Elektromagnetischer Felder (TEMF), Januar 2011.

[12] T. Ha-Duong. On retarded potential boundary integral equations and their discretisation. In *Topics in Computational Wave Propagation: Direct and Iverse Problems*, volume 31 of *Lect. Notes Comput. Sci. Eng.*, pages 301–336. Springer, Berlin, 2003.

[13] T. Ha-Duong, B. Ludwig, and I. Terrasse. A Galerkin BEM for transient acoustic scattering by an absorbing obstacle. *International Journal for Numerical Methods in Engineering*, 57:1845–1882, 2003.

[14] D. Jones. *Methods in Electromagnetic Wave Propagation.* Clarendon Press, Oxford, second ed., 1994.

[15] C. Lubich. Convolution Quadrature and Discretized Operational Calculus I. *Numerische Mathematik*, 52:129–145, 1988.

[16] C. Lubich. Convolution Quadrature and Discretized Operational Calculus II. *Numerische Mathematik*, 52:413–425, 1988.

[17] C. Lubich. On the multistep time discretization of linear initial-boundary value problems and their boundary integral equations. *Numerische Mathematik*, 67(3):365–389, 1994.

[18] C. Lubich. Convolution quadrature revisited. *BIT Numerical Mathematics*, 44:503–514, 2004.

[19] A. Pujols. Time Dependent Integral Method for Maxwell Equations. *Rapport CESTA/SI A. P. 6589*, 1991.

[20] B. P. Rynne and P. D. Smith. Stability of Time Marching Algorithms for the Electric Field Integral Equation. *J. Electromagnetic Waves and Appl.*, 4:1181–1205, 1990.

[21] J. Stratton. *Electromagnetic Theory.* McGraw-Hill, 1941.

[22] I. Terrasse. *Résolution mathématique et numérique des équations de Maxwell instationnaires par une méthode de potentiels retardés.* PhD thesis, Ecole polytechnique, 1993.

[23] A. Veit. Convolution quadrature for time-dependent Maxwell equations. Master's thesis, University of Zurich, 2009.

2

Exact Solutions for Dirichlet and Neumann Problems in Acoustic Scattering

In Section 1.1 we introduced various retarded boundary integral equations in order to solve Dirichlet and Neumann problems in acoustic scattering. In the literature there exist different approaches to solve these equations numerically, examples being collocation schemes, methods based on bandlimited interpolation and extrapolation, convolution quadrature as well as methods using space-time integral equations.
The development of efficient and accurate numerical methods for time-domain boundary integral equations requires a careful implementation and a systematic testing of the schemes with respect to various parameters. These tasks are not trivial, especially for general situations like curved scatterers or nonuniform time grids. The availability of exact solutions of the underlying integral equations for some special cases is hence very useful.
In this chapter we will derive exact solutions of acoustic scattering problems in the case where the scatterer is the unit ball in $\mathbb{R}^3$. We consider direct and indirect formulations for both Dirichlet and Neumann problems and therefore seek solutions for the problems (1.1.14)-(1.1.21) involving the single layer operator V, the double layer operator K, the adjoint double layer operator K' and the hypersingular operator W. As we will see in the next section we will make extensive use of Laplace transformations. This allows us to transfer the time-dependent boundary integral equations to univariate problems in time which can be solved analytically. The obtained formulas lead to exact solutions of the full scattering problem on the sphere. They are easy to implement and can therefore serve as reference solutions for numerical approximations schemes.
The results in this chapter were partially published in [9], where we considered solutions for the Dirichlet problem (1.1.16). An easy to use MATLAB script that implements the obtained formulas for this case is available at `https://www.math.uzh.ch/compmath/?exactsolutions`. (cf. [10])

2.1 General Framework

In this section we want to show how the retarded boundary integral equations (1.1.14)-(1.1.21) can be solved analytically on the sphere assuming that the boundary data admits a special structure. In general each of these problems can be written in the form

$$R_1\varphi = R_2\eta \tag{2.1.1}$$

with unknown density function φ, boundary data η and boundary integral operators $R_1, R_2 \in \operatorname{span}\{I, V, K, K', W\}$, where I denotes the identity. In order to solve equations of type (2.1.1) we will use Laplace transformations. Recall the definition of the Laplace transform

$$\hat{\phi}(s) := (\mathcal{L}\phi)(s) = \int_0^\infty \phi(t)\,\mathrm{e}^{-st}\,dt$$

with inverse

$$(\mathcal{L}^{-1}\hat{\phi})(s) = \frac{1}{2\pi i}\int_{\sigma-\mathrm{i}\infty}^{\sigma+\mathrm{i}\infty} \hat{\phi}(s)\,\mathrm{e}^{st}\,ds.$$

Furthermore, we will need properties of the involved boundary integral operators in the Laplace domain. Therefore we consider the Helmholtz equation

$$\Delta U - s^2 U = 0.$$

With the Laplace transform of the time-domain fundamental solution k (cf. (1.1.6)), which reads

$$\hat{k}(s,z) = (\mathcal{L}k)(s,z) = \frac{\mathrm{e}^{-s\|z\|}}{4\pi\|z\|},$$

we can define the single layer potential $\hat{V}$, the double layer potential $\hat{K}$, the adjoint double layer potential $\hat{K}'$, and the hypersingular potential $\hat{W}$ for the Helmholtz operator on the surface Γ by (cf. [8]):

$$\begin{aligned}
(\hat{V}(s)\phi)(x) &:= \int_\Gamma \hat{k}(s, x-y)\phi(y)d\Gamma_y,\\
(\hat{K}(s)\phi)(x) &:= \int_\Gamma \partial_{n_y}\hat{k}(s, x-y)\phi(y)d\Gamma_y,\\
(\hat{K}'(s)\phi)(x) &:= \int_\Gamma \partial_{n_x}\hat{k}(s, x-y)\phi(y)d\Gamma_y,\\
(\hat{W}(s)\phi)(x) &:= \text{p.f.}\int_\Gamma \partial_{n_x}\partial_{n_y}\hat{k}(s, x-y)\phi(y)d\Gamma_y,
\end{aligned}$$

where we write the last integral formally as an improper integral. Note that $\hat{V}$, $\hat{K}$, $\hat{K}'$ and $\hat{W}$ are just the Laplace transforms of the corresponding operators in the time domain and satisfy

$$\widehat{L\phi}(s,z) = (\hat{L}(s)\hat{\phi}(\cdot,s))(x), \tag{2.1.2}$$

where $L \in \{V, K, K', W\}$. This is a consequence of the fact that the Laplace transform of a convolution in the time domain corresponds to a multiplication in the frequency domain. Important properties of these frequency domain operators on the sphere are stated in the next theorem.

Theorem 2.1.1. *Let $\Gamma = \mathbb{S}^2$ be the unit sphere and define*

$$\phi_n^m := \int_{\mathbb{S}^2} \phi(\theta,\varphi)\overline{Y_n^m}(\theta,\varphi)$$

for a function ϕ, where Y_n^m are spherical harmonics of degree n and order m in spherical coordinates (θ,φ) with normalization convention $\left(Y_n^m, Y_{n'}^{m'}\right)_{L^2(\mathbb{S}^2)} = \delta_{n,n'}\delta_{m,m'}$. Then, the operators $\hat{V}, \hat{K}, \hat{K}'$ and $\hat{W}$ admit the following expansions:

$$\begin{aligned}
\hat{V}(s)\phi &= \sum_{n=0}^{\infty}\sum_{m=-n}^{n} -sj_n(\mathrm{i}s)h_n^{(1)}(\mathrm{i}s)\phi_n^m Y_n^m(\theta,\varphi),\\
\hat{K}(s)\phi = \hat{K}'(s)\phi &= \sum_{n=0}^{\infty}\sum_{m=-n}^{n} \left(-\mathrm{i}s^2 j_n(\mathrm{i}s)\,\partial h_n^{(1)}(\mathrm{i}s) + \frac{1}{2}\right)\phi_n^m Y_n^m(\theta,\varphi),\\
\hat{W}(s)\phi &= \sum_{n=0}^{\infty}\sum_{m=-n}^{n} s^3\partial j_n(\mathrm{i}s)\,\partial h_n^{(1)}(\mathrm{i}s)\phi_n^m Y_n^m(\theta,\varphi),
\end{aligned}$$

where j_n are spherical Bessel functions, i.e.,

$$j_n(x) = (-x)^n\left(\frac{1}{x}\frac{d}{dx}\right)^n\frac{\sin(x)}{x}$$

and $h_n^{(1)}$ are spherical Hankel functions of the first kind, i.e.,

$$h_n^{(1)}(x) = (-\mathrm{i})^{n+1}\frac{\mathrm{e}^{\mathrm{i}x}}{x}\sum_{m=0}^{n}\frac{\mathrm{i}^m}{m!(2x)^m}\frac{(n+m)!}{(n-m)!}.$$

Proof. See [7, 1, 8]. □

Corollary 2.1.2. *The spherical harmonics Y_n^m are eigenfunctions of the operators V, K, K' and W. It holds*

$$\hat{V}(s)Y_n^m = \lambda_n^{(\hat{V})}(s)Y_n^m \qquad \textit{with} \qquad \lambda_n^{(\hat{V})}(s) := -sj_n(\mathrm{i}s)h_n^{(1)}(\mathrm{i}s), \tag{2.1.3}$$

$$\hat{K}(s)Y_n^m = \lambda_n^{(\hat{K})}(s)Y_n^m \qquad \textit{with} \qquad \lambda_n^{(\hat{K})}(s) := -\mathrm{i}s^2 j_n(\mathrm{i}s)\,\partial h_n^{(1)}(\mathrm{i}s) + \frac{1}{2}, \tag{2.1.4}$$

$$\hat{K}'(s)Y_n^m = \lambda_n^{(\hat{K}')}(s)Y_n^m \qquad \textit{with} \qquad \lambda_n^{(\hat{K}')}(s) := \lambda_n^{(\hat{K})}(s), \tag{2.1.5}$$

$$\hat{W}(s)Y_n^m = \lambda_n^{(\hat{W})}(s)Y_n^m \qquad \textit{with} \qquad \lambda_n^{(\hat{W})}(s) := s^3\partial j_n(\mathrm{i}s)\,\partial h_n^{(1)}(\mathrm{i}s). \tag{2.1.6}$$

Let us now consider again problem (2.1.1). We assume from now on that the scatterer is the unit ball in $\mathbb{R}^3$, i.e., $\Gamma = \mathbb{S}^2$. Since $R_1, R_2 \in \operatorname{span}\{I, V, K, K', W\}$, these operators satisfy property (2.1.2). Furthermore the spherical harmonics Y_n^m are eigenfunctions of the corresponding operators $\hat{R}_1, \hat{R}_2$ in the Laplace domain with

$$\hat{R}_1(s)Y_n^m = \lambda_n^{(\hat{R}_1)}(s)Y_n^m \qquad \text{and} \qquad \hat{R}_2(s)Y_n^m = \lambda_n^{(\hat{R}_2)}(s)Y_n^m.$$

In order to solve (2.1.1) we reduce the equation to a univariate problem in time. We therefore adopt the setting in [2]. For the right-hand side η we assume causality i.e. $\eta(x,t) = 0 \quad \text{for } t \leq$

0 and furthermore that at least the first time derivative of η vanishes at $t = 0$. Moreover, η is supposed to be of the form

$$\eta(x,t) = \eta(t)Y_n^m.$$

For the solution φ we make the same ansatz $\varphi(x,t) = \varphi(t)Y_n^m$ with unknown function $\varphi(t)$. Then, problem (2.1.1) decouples and leads to a one dimensional problem in time, since

$$\begin{aligned} & R_1\left(\varphi(t)Y_n^m\right) = R_2\left(\eta(t)Y_n^m\right) \\ \Leftrightarrow \quad & \hat{R}_1(s)\left(\hat{\varphi}(s)Y_n^m\right) = \hat{R}_2(s)\left(\hat{\eta}(s)Y_n^m\right) \\ \Leftrightarrow \quad & \lambda_n^{(\hat{R}_1)}(s)\,\hat{\varphi}(s) = \lambda_n^{(\hat{R}_2)}(s)\,\hat{\eta}(s). \end{aligned}$$

Rearranging terms and applying an inverse Laplace transformation finally leads to an expression for φ:

$$\varphi(t) = \int_0^t \eta(\tau)\mathcal{L}^{-1}\left(\frac{\lambda_n^{(\hat{R}_2)}}{\lambda_n^{(\hat{R}_1)}}\right)(t-\tau)d\tau. \tag{2.1.7}$$

Note that $\varphi(t)Y_n^m$ with $\varphi(t)$ as above is a solution of the full problem (2.1.1) in the case where $\Gamma = \mathbb{S}^2$ and $\eta(x,t) = \eta(t)Y_n^m$. In the following sections we will compute exact solutions of the Dirichlet and Neumann problems (1.1.14)-(1.1.21) with formula (2.1.7) and the appropriate choice of R_1 and R_2. Note that therefore the Laplace inversion of the quotient of the eigenvalues of these operators is the crucial step. Unless otherwise stated we will use the formulas in [3] for these inversions.

Before we proceed with the computation of (2.1.7) for the different cases, note that with the above formulas it is also possible to find an expression for the solution $\varphi(x,t)$ in (2.1.1) for more general right-hand sides.

Theorem 2.1.3. *Let η in (2.1.1) be causal and assume that $\partial_t \eta(x,0) = 0, \forall x \in \mathbb{S}^2$. Let η be of the form*

$$\eta(x,t) = \sum_{n=0}^{\infty}\sum_{m=-n}^{n} \eta_{n,m}(t)Y_n^m.$$

Then, the solution φ has the form

$$\varphi(x,t) = \sum_{n=0}^{\infty}\sum_{m=-n}^{n} \varphi_{n,m}(t)Y_n^m,$$

where

$$\varphi_{n,m} = \int_0^t \eta_{n,m}(\tau)\,\mathcal{L}^{-1}\left(\frac{\lambda_n^{(\hat{R}_2)}}{\lambda_n^{(\hat{R}_1)}}\right)(t-\tau)\,d\tau.$$

Note that the expressions in Theorem 2.1.3 are considered as formal series. However, in the case of a Dirichlet problem with $R_1 = V$ and $R_2 = I$, which will be in the main focus in this thesis, the existence and uniqueness results in [5] imply that for given right-hand side η with $\dot{\eta} \in H^{1/2,1/2}(\Gamma \times [0,T])$, where sufficiently many time derivatives vanish at $t = 0$ the solution φ exists in $H^{-1/2,-1/2}(\Gamma \times [0,T])$.
If only finitely many Fourier coefficients of η are non-zero, then, the expansion of φ and the existence in the classical pointwise sense is obvious.

2.2 Solutions of the Dirichlet problem $V\phi = g$

In this section we will derive exact solutions and some analytic properties of these solutions for Dirichlet problem (1.1.16). As in the last section we assume that the boundary of the scatterer Γ is the unit sphere in $\mathbb{R}^3$. As shown above a right hand side of the form $g(x,t) = g(t)Y_n^m$ leads to a solution of the form $\phi(x,t) = \phi(t)Y_n^m$, where

$$\phi(t) = \int_0^t g(\tau)\mathcal{L}^{-1}\left(\frac{1}{\lambda_n^{(\hat{V})}}\right)(t-\tau)d\tau. \tag{2.2.1}$$

In order to find an explicit representation for $\phi(t)$, it is necessary to find the inverse Laplace transform of $1/\lambda_n^{(\hat{V})}(s)$. With the formulas [4, Sec. 8.467 and 8.468] we get:

$$\lambda_n^{(\hat{V})}(s) = I_{n+\frac{1}{2}}(s)K_{n+\frac{1}{2}}(s) = \frac{y_n(-\frac{1}{s})y_n(\frac{1}{s}) + (-1)^{n+1}y_n^2(\frac{1}{s})\,\mathrm{e}^{-2s}}{2s}, \tag{2.2.2a}$$

where

$$y_n(s) := \sum_{k=0}^{n}(n,k)s^k \quad \text{and } (n,k) := \frac{(n+k)!}{2^k k!(n-k)!} \tag{2.2.2b}$$

are the Bessel polynomials (see [6, Sec. 4.10]). This is equivalent to

$$\lambda_n^{(\hat{V})}(s) = (-1)^n\frac{\theta_n(s)}{2s^{2n+1}}\left(\theta_n(-s) - \theta_n(s)\,\mathrm{e}^{-2s}\right),$$

where θ_n are the reversed Bessel polynomials

$$\theta_n(s) := \sum_{k=0}^{n}(n,k)s^{n-k}.$$

After some manipulations we therefore get for the inverse Laplace transform

$$\mathcal{L}^{-1}\left(\frac{1}{\lambda_n^{(\hat{V})}}\right) = 2\delta' + (-1)^n 2\,\partial_t\mathcal{L}^{-1}\left(\frac{\tilde{\theta}_{2n-2}(s) + (-1)^n\theta_n(s)^2\,\mathrm{e}^{-2s}}{\theta_n(-s)\theta_n(s) - \theta_n(s)^2\,\mathrm{e}^{-2s}}\right), \tag{2.2.3}$$

where

$$\mathbb{P}_{\max(0,2n-2)} \ni \tilde{\theta}_{2n-2}(s) = s^{2n} - (-1)^n\,\theta_n(-s)\theta_n(s).$$

We expand the term in the brackets in the right-hand side of (2.2.3) with respect to $\varepsilon = \mathrm{e}^{-2s}$ about 0 and obtain

$$\begin{aligned}\frac{\tilde{\theta}_{2n-2}(s) + (-1)^n\theta_n(s)^2\,\mathrm{e}^{-2s}}{\theta_n(-s)\theta_n(s) - \theta_n(s)^2\,\mathrm{e}^{-2s}} &= \underbrace{\frac{\tilde{\theta}_{2n-2}(s)}{\theta_n(-s)\theta_n(s)}}_{R_n^{(1)}} \\ &\quad + \sum_{k=1}^{\infty}\left\{(-1)^n\underbrace{\frac{\theta_n(s)^k}{\theta_n(-s)^k}\,\mathrm{e}^{-2ks}}_{R_{n,k}^{(2)}} + \underbrace{\frac{\tilde{\theta}_{2n-2}(s)\theta_n(s)^{k-1}}{\theta_n(-s)^{k+1}}\,\mathrm{e}^{-2ks}}_{R_{n,k}^{(3)}}\right\}.\end{aligned} \tag{2.2.4}$$

The computation of the inverse Laplace transforms of $R_n^{(1)}, R_{n,k}^{(2)}$ and $R_{n,k}^{(3)}$ boils down to the inversion of rational functions. This is done with the formulas in [3, Sec. 5.2]. Note that $\theta_n(s)$ is a polynomial of degree n and has exactly n complex-valued, simple zeros (cf. [6]). Let

$$\theta_n(\alpha_i) = 0 \quad \text{for } i = 1 \dots n, \quad \text{where } \alpha_i = \alpha_i^{\mathrm{re}} + \mathrm{i}\,\alpha_i^{\mathrm{im}} \text{ with } \alpha_i^{\mathrm{re}}, \alpha_i^{\mathrm{im}} \in \mathbb{R}.$$

It follows that the zeros of $\theta_n(-s)$ are $-\alpha_1, \dots, -\alpha_n$. Thus we get

$$\mathcal{L}^{-1}\left(R_n^{(1)}\right)(t) = \sum_{j=1}^{n} c_{n,j}^{(1)}\, \mathrm{e}^{\alpha_j t} + \tilde{c}_{n,j}^{(1)}\, \mathrm{e}^{-\alpha_j t}.$$

Since the solution ϕ is real, we may restrict our consideration to the real part of $\mathcal{L}^{-1}(R_n^{(1)})$. We denote the real part of $c_{n,j}^{(1)}$ by $c_{n,j}^{(1),\mathrm{re}}$ and its imaginary part by $c_{n,j}^{(1),\mathrm{im}}$. The notations for $\tilde{c}_{n,j}^{(1)}$ are chosen accordingly. We obtain

$$\begin{aligned}\mathcal{L}_{\mathrm{re}}^{-1}\left(R_n^{(1)}\right)(t) = \sum_{j=1}^{n} & c_{n,j}^{(1),\mathrm{re}}\, \mathrm{e}^{\alpha_j^{\mathrm{re}} t} \cos(\alpha_j^{\mathrm{im}} t) - c_{n,j}^{(1),\mathrm{im}}\, \mathrm{e}^{\alpha_j^{\mathrm{re}} t} \sin(\alpha_j^{\mathrm{im}} t) \\ & + \tilde{c}_{n,j}^{(1),\mathrm{re}}\, \mathrm{e}^{-\alpha_j^{\mathrm{re}} t} \cos(-a_j^{\mathrm{im}} t) - \tilde{c}_{n,j}^{(1),\mathrm{im}}\, \mathrm{e}^{-\alpha_j^{\mathrm{re}} t} \sin(-\alpha_j^{\mathrm{im}} t).\end{aligned}$$

Remark 2.2.1. *In Section 2.2.1 and 2.2.2 we will state explicit representations of ϕ for $n = 0, 1$. In this case the above formula simplifies considerably. It holds*

$$\mathcal{L}_{\mathrm{re}}^{-1}\left(R_0^{(1)}\right)(t) = 0$$

and

$$\mathcal{L}_{\mathrm{re}}^{-1}\left(R_1^{(1)}\right)(t) = \frac{1}{2}\left(\mathrm{e}^{-t} - \mathrm{e}^{t}\right) = -\sinh(t). \tag{2.2.5}$$

For larger n the arising coefficients from the inversions can be easily computed with computer algebra systems.

For the computation of $\mathcal{L}^{-1}\left(R_{n,k}^{(2)}\right)$ we use the time shifting property of the Laplace transformation. We employ the Heaviside step function

$$H(t) = \begin{cases} 0 & t \le 0, \\ 1 & t > 0, \end{cases}$$

to obtain

$$\begin{aligned}\mathcal{L}^{-1}\left(R_{n,k}^{(2)}\right)(t) &= \mathcal{L}^{-1}\left(\frac{\theta_n(s)^k}{\theta_n(-s)^k}\, \mathrm{e}^{-2ks}\right)(t) = H(t-2k)\, \mathcal{L}^{-1}\left(\frac{\theta_n(s)^k}{\theta_n(-s)^k}\right)(t-2k) \\ &= (-1)^{nk}\delta(t-2k)H(t-2k) + \sum_{i=1}^{n}\sum_{j=1}^{k} c_{n,k,j,i}^{(2)}\, H(t-2k)(t-2k)^{j-1}\, \mathrm{e}^{-\alpha_i(t-2k)}\end{aligned}$$

with some complex coefficients $c_{n,k,j,i}^{(2)} = c_{n,k,j,i}^{(2),\mathrm{re}} + \mathrm{i}\, c_{n,k,j,i}^{(2),\mathrm{im}}$. For the real part of $\mathcal{L}^{-1}\left(R_{n,k}^{(2)}\right)$ we

get:

$$\begin{aligned}\mathcal{L}_{\mathrm{re}}^{-1}\left(R_{n,k}^{(2)}\right)(t) &= (-1)^{nk}\delta(t-2k)H(t-2k) \\ &+ \sum_{i=1}^{n}\sum_{j=1}^{k} c_{n,k,j,i}^{(2),\mathrm{re}}\, H(t-2k)(t-2k)^{j-1}\,\mathrm{e}^{-\alpha_i^{\mathrm{re}}(t-2k)}\cos\left(-\alpha_i^{\mathrm{im}}(t-2k)\right) \\ &- \sum_{i=1}^{n}\sum_{j=1}^{k} c_{n,k,j,i}^{(2),\mathrm{im}}\, H(t-2k)(t-2k)^{j-1}\,\mathrm{e}^{-\alpha_i^{\mathrm{re}}(t-2k)}\sin\left(-\alpha_i^{\mathrm{im}}(t-2k)\right).\end{aligned} \tag{2.2.6}$$

For the inverse Laplace transform of $R_{n,k}^{(3)}$ we use again the shift property and get

$$\begin{aligned}\mathcal{L}^{-1}\left(R_{n,k}^{(3)}\right)(t) &= \mathcal{L}^{-1}\left(\frac{\tilde{\theta}_{2n-1}(s)\theta_n(s)^{k-1}}{\theta_n(-s)^{k+1}}\,\mathrm{e}^{-2ks}\right)(t) \\ &= H(t-2k)\mathcal{L}^{-1}\left(\frac{\tilde{\theta}_{2n-1}(s)\theta_n(s)^{k-1}}{\theta_n(-s)^{k+1}}\right)(t-2k) \\ &= H(t-2k)\left[\sum_{i=1}^{n}\sum_{j=1}^{k} c_{n,k,j,i}^{(3)}(t-2k)^j\,\mathrm{e}^{-\alpha_i(t-2k)}\right].\end{aligned}$$

The real part of $\mathcal{L}^{-1}\left(R_{n,k}^{(2)}\right)$ can therefore be written as

$$\begin{aligned}\mathcal{L}_{\mathrm{re}}^{-1}\left(R_{n,k}^{(3)}\right)(t) &= \sum_{i=1}^{n}\sum_{j=1}^{k} c_{n,k,j,i}^{(3),\mathrm{re}}\, H(t-2k)(t-2k)^{j}\,\mathrm{e}^{-\alpha_i^{\mathrm{re}}(t-2k)}\cos\left(-\alpha_i^{\mathrm{im}}(t-2k)\right) \\ &- \sum_{i=1}^{n}\sum_{j=1}^{k} c_{n,k,j,i}^{(3),\mathrm{im}}\, H(t-2k)(t-2k)^{j}\,\mathrm{e}^{-\alpha_i^{\mathrm{re}}(t-2k)}\sin\left(-\alpha_i^{\mathrm{im}}(t-2k)\right).\end{aligned} \tag{2.2.7}$$

With these formulas for $\mathcal{L}_{\mathrm{re}}^{-1}\left(R_n^{(1)}\right), \mathcal{L}_{\mathrm{re}}^{-1}\left(R_{n,k}^{(2)}\right)$ and $\mathcal{L}_{\mathrm{re}}^{-1}\left(R_{n,k}^{(3)}\right)$ it is now possible to invert the remaining term in (2.2.3). Inserting this in (2.2.1) leads to explicit formulas for the exact solution $\phi(t)$.

Note that the complex zeros of $\theta_n(s)$ are located in left half plane of $\mathbb{R}^2$, i.e., $-\alpha_i^{\mathrm{re}} > 0$ for any i and n (cf. Figure 2.1, [6]). The representations of $\phi(t)$ that we will derive, have therefore to be handled with care when being evaluated numerically because they contain exponentially increasing functions which cancel each other and the behaviour of the final solution typically is bounded and oscillatory.

2.2.1 The case $n = 0$

For $n = 0$ the eigenfunctions of V are constant. We are therefore in the case where

$$g(x,t) := 2\sqrt{\pi}Y_0^0\, g(t) = g(t)$$

is purely time-dependent. This case was already treated in [2] and an explicit representation of $\phi(t)$ in (2.2.1) was given for $t \in [0, 2[$. We generalize this to $t \geq 0$. Therefore note that the associated eigenvalue in this case is given by

$$\lambda_0(s) = \frac{1 - e^{-2s}}{2s}$$

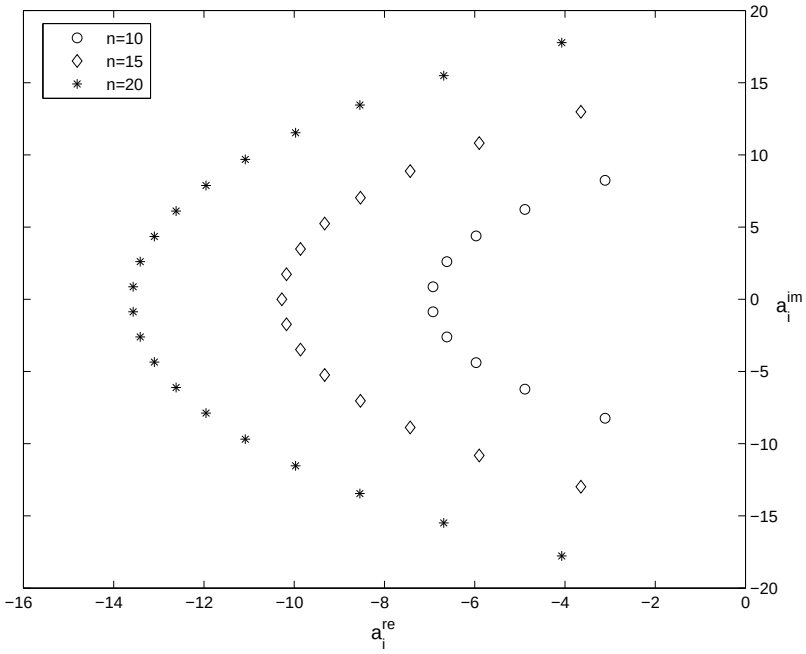

Figure 2.1: *Complex zeros of* $\theta_{10}(s), \theta_{15}(s)$ *and* $\theta_{20}(s)$.

and from the above computations we can see that

$$\mathcal{L}\left(\frac{1}{\lambda_0}\right)(t) = 2\delta'(t) + 2\partial_t\left(\sum_{k=1}^{\infty}\delta(t-2k)H(t-2k)\right).$$

Therefore the exact solution in this simple case is given by

$$\begin{aligned}
\phi(t) &= \int_0^t g(t-\tau)\left[2\delta'(\tau) + 2\partial_\tau\left(\sum_{k=1}^{\infty}\delta(\tau-2k)H(\tau-2k)\right)\right]d\tau \\
&= 2g'(t) + 2\sum_{k=1}^{\infty}\int_0^t g(t-\tau)\partial_t\left(\delta(\tau-2k)H(\tau-2k)\right)d\tau \\
&= 2g'(t) + 2\sum_{k=1}^{\infty} g'(t-2k) \\
&= 2\sum_{k=0}^{\lfloor t/2\rfloor} g'(t-2k) \qquad (2.2.8)
\end{aligned}$$

due to the causality of g. Figure 2.2 shows a typical behaviour of $\phi(t)$ (cf. [10]). Note the oscillatory, non-decaying shape of the solution for larger times t. This is due to the fact that in indirect methods $\phi(t)$ is the trace difference of the solution of the exterior and the solution of the interior wave equation. The latter is determined by the many reflections inside the sphere and therefore causes the oscillations in the solution.

A closer look at Figure 2.2 suggests that $\phi(t)$ becomes a very regular function for large times. Indeed it can be shown that $\phi(t)$ tends to a periodic function for sufficiently fast

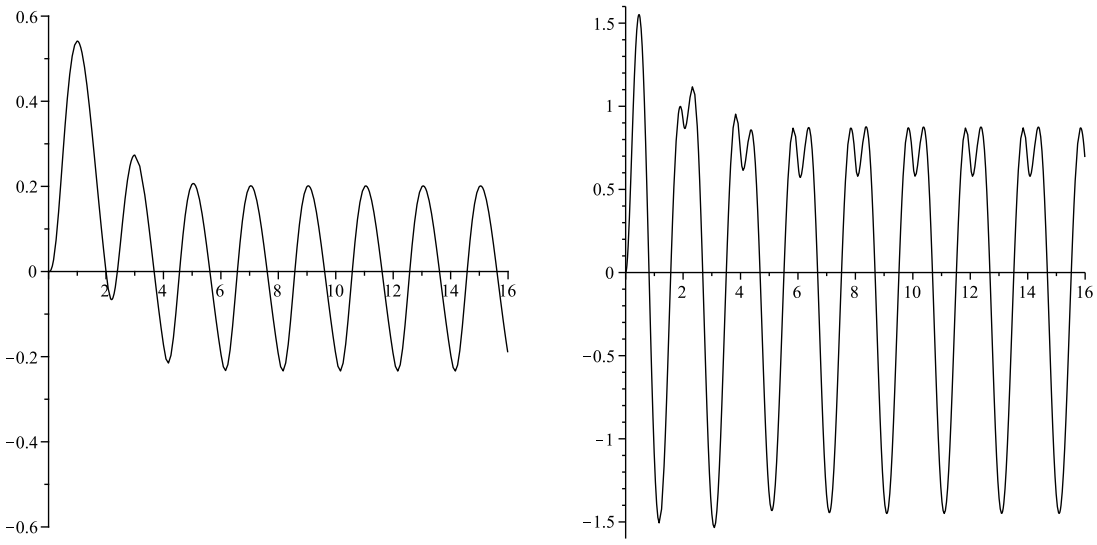

Figure 2.2: *Exact solution $\phi(t)$ with $n = 0$ for $g(t) = t^4 e^{-2t}$ and $g(t) = \sin(2t)^2 t e^{-t}$.*

decaying right-hand sides $g(t)$. In order to see that we set

$$t = 2l + \tau, \qquad \text{with } \tau \in [0, 2[,\ l \in \mathbb{N}_0$$

and get

$$\phi(2l + \tau) = 2 \sum_{k=0}^{l} g'(2k + \tau).$$

Suppose that $g(t)$ satisfies

$$g(0) = g'(0) = 0, \tag{2.2.9}$$

$$|g'(t)| \leq C\, t^{-\alpha}, \tag{2.2.10}$$

for $t > 0$ with $\alpha > 1$ and a positive constant C . With these assumptions, the following lemma holds.

Lemma 2.2.2. *Let* (2.2.9) *and* (2.2.10) *be satisfied. Then the sequence of functions* $\{\phi(2l + \tau)\}_{l \in \mathbb{N}_0}$ *converges uniformly to a function* $f(\tau) : [0, 2[\to \mathbb{R}$.

Proof. Let $\varepsilon > 0$. Since $\alpha > 1$, we find $N \in \mathbb{N}$ such that

$$\sum_{k=l+1}^{m} (2k + 2)^{-\alpha} < \frac{\varepsilon}{2C}$$

for all $m > l > N$. Thus,

$$\begin{aligned} |\phi(2m + \tau) - \phi(2l + \tau)| &\leq 2 \sum_{k=l+1}^{m} |g'(2k + \tau)| \leq 2C \sum_{k=l+1}^{m} (2k + \tau)^{-\alpha} \\ &\leq 2C \sum_{k=l+1}^{m} (2k + 2)^{-\alpha} \leq \varepsilon \end{aligned}$$

for all $m > l > N$ and therefore the uniform convergence. □

Corollary 2.2.3. *The limit function $f(\tau)$ is continuous and satisfies*

$$f(0) = \lim_{\tau \to 2} f(\tau).$$

The solution of the scattering problem therefore tends to a periodic function for large times for every right hand side satisfying (2.2.9) and (2.2.10).

Proof. $f(\tau)$ is continuous since the uniform limit of continuous functions is continuous. Furthermore,

$$\lim_{\tau \to 2} f(\tau) = \lim_{\tau \to 2} \lim_{n \to \infty} \phi(2n + \tau) = \lim_{n \to \infty} \lim_{\tau \to 2} \phi(2n + \tau) = \lim_{n \to \infty} \phi(2n + 2) = f(0)$$

again due to the continuity of ϕ. □

Let us suppose now that $g(t)$ is of the form

$$g(t) = v(t)\,\mathrm{e}^{-\alpha t} \quad \text{with} \quad v(t) = t^2 p(t), \tag{2.2.11}$$

where $p \in \mathbb{P}_q$ is a polynomial of degree q. In this case we can compute the limit function $f(\tau)$ explicitly. Let the constant c_m be defined as

$$c_m := \frac{v^{(m+1)}(0) - \alpha v^{(m)}(0)}{m!}.$$

Expanding $v(t)$ and $v'(t)$ about 0 leads to

$$\begin{aligned}
\phi(2l + \tau) &= 2 \sum_{k=0}^{l} \left[v'(2k + \tau) - \alpha v(2k + \tau) \right] \mathrm{e}^{-\alpha\tau - 2\alpha k} \\
&= 2 \sum_{k=0}^{l} \left[\sum_{m=1}^{q} c_m (2k + \tau)^m \right] \mathrm{e}^{-\alpha\tau - 2\alpha k} \\
&= 2\,\mathrm{e}^{-\alpha\tau} \sum_{m=1}^{q} \sum_{k=0}^{l} c_m (2k + \tau)^m\, \mathrm{e}^{-2\alpha k} \\
&= 2\,\mathrm{e}^{-\alpha\tau} \sum_{m=1}^{q} \sum_{k=0}^{l} c_m \left(\sum_{j=0}^{m} \binom{m}{j} \tau^{m-j} (2k)^j \right) \mathrm{e}^{-2\alpha k} \\
&= 2\,\mathrm{e}^{-\alpha\tau} \sum_{m=1}^{q} \sum_{j=0}^{m} 2^j \binom{m}{j} c_m \tau^{m-j} \underbrace{\sum_{k=0}^{l} k^j\, \mathrm{e}^{-2\alpha k}}_{=: R_{l,j,\alpha}}.
\end{aligned}$$

We are interested in $\phi(t)$ for large times t. Therefore we need an expression for $R_{l,j,\alpha}$ when l tends to infinity.

Lemma 2.2.4. *Let $j \in \mathbb{N}$ and $\alpha \in \mathbb{R}_{>0}$ be fixed. Then*

$$\sum_{k=0}^{\infty} k^j\, \mathrm{e}^{-2\alpha k} = \sum_{m=0}^{j} \sum_{q=0}^{m} \frac{(-1)^{m-q}\, q^j \binom{j+1}{m-q}\, \mathrm{e}^{2\alpha(j-m+1)}}{(\mathrm{e}^{2\alpha} - 1)^{j+1}}.$$

Proof. Since we want to compute $\lim_{l\to\infty} R_{l,j,\alpha}$, we assume that $l \geq j$. We get

$$\begin{aligned}\left[\sum_{k=0}^{l} k^j \,\mathrm{e}^{-2\alpha k}\right](\mathrm{e}^{2\alpha}-1)^{j+1} &= \sum_{k=0}^{l}\sum_{q=0}^{j+1}(-1)^{j-q+1}k^j\binom{j+1}{q}\mathrm{e}^{-2\alpha(k-q)}\\ &= \sum_{m=-(j+1)}^{-1}\sum_{q=-m}^{j+1}(-1)^{j+1-q}(q+m)^j\binom{j+1}{q}\mathrm{e}^{-2\alpha m}\\ &+ \sum_{m=0}^{l-j-1}\sum_{q=0}^{j+1}(-1)^{j+1-q}(q+m)^j\binom{j+1}{q}\mathrm{e}^{-2\alpha m}\\ &+ \sum_{m=l-j}^{l}\sum_{q=0}^{l-m}(-1)^{j+1-q}(q+m)^j\binom{j+1}{q}\mathrm{e}^{-2\alpha m}.\end{aligned}$$

The second double sum in the last term is zero since for any polynomial p of degree less than j the equation

$$\sum_{q=0}^{j}(-1)^q p(q)\binom{j}{q} = 0$$

holds. Therefore

$$\begin{aligned}\left[\sum_{k=0}^{l} k^j \,\mathrm{e}^{-2\alpha k}\right](\mathrm{e}^{2\alpha}-1)^{j+1} &= \sum_{m=-(j+1)}^{-1}\sum_{q=-m}^{j+1}(-1)^{j+1-q}(q+m)^j\binom{j+1}{q}\mathrm{e}^{-2\alpha m}\\ &+ \sum_{m=-j}^{0}\sum_{q=0}^{-m}(-1)^{j+1-q}(q+l+m)^j\binom{j+1}{q}\mathrm{e}^{-2\alpha(l+m)}.\end{aligned}$$

Now we can pass to the limit for $l \to \infty$ where the second double sum vanishs. After a reordering of the terms we get

$$\left[\sum_{k=0}^{\infty} k^j \,\mathrm{e}^{-2\alpha k}\right](\mathrm{e}^{2\alpha}-1)^{j+1} = \sum_{m=0}^{j}\sum_{q=0}^{m}(-1)^{m-q}q^j\binom{j+1}{m-q}\mathrm{e}^{2\alpha(j-m+1)}.$$

Dividing by $(\mathrm{e}^{2\alpha}-1)^{j+1}$ leads to the desired result. □

If we assume a right-hand side of the form (2.2.11) we get by Lemma 2.2.4 that

$$\phi(2l+\tau) \underset{l\to\infty}{\longrightarrow} f(\tau) \qquad \tau \in [0,2[, \tag{2.2.12}$$

where f is given by

$$f(\tau) = 2\,\mathrm{e}^{-\alpha\tau}\sum_{m=1}^{q}\sum_{j=0}^{m}\tilde{c}_{m,j,\alpha}\tau^{m-j} \tag{2.2.13}$$

and

$$\tilde{c}_{m,j,\alpha} = c_m\sum_{k=0}^{j}\sum_{q=0}^{k}(-1)^{k-q}(2q)^j\binom{m}{j}\binom{j+1}{k-q}\mathrm{e}^{2\alpha(j-k+1)}(\mathrm{e}^{2\alpha}-1)^{-j-1}.$$

With Lemma 2.2.4 it is also possible to show that the convergence in (2.2.12) is exponentially fast in l up to a polynomial factor if $g(t)$ is decaying exponentially.

Lemma 2.2.5. *Suppose that $g(t)$ is of the form*

$$g(t) = v(t)\,\mathrm{e}^{-\alpha t} \tag{2.2.14}$$

with $\alpha > 0$, where $v(t)$ is a continuous function satisfying

$$\begin{aligned} v(0) = v'(0) &= 0, \\ |v(t)| &\le C_1\, t^{p_1}, \\ |v'(t)| &\le C_2\, t^{p_2}, \end{aligned}$$

for some $p_1, p_2 \in \mathbb{N}$ and positive constants C_1 and C_2. For $l \ge \max\{p_1, p_2\}$ we have

$$\sup_{\tau\in[0,2[} |f(\tau) - \phi(2l+\tau)| \le p(l+1)\,\mathrm{e}^{-2\alpha(l+1)},$$

where p is a polynomial of degree $\max\{p_1, p_2\}$ and f is as in Lemma 2.2.2.

Proof. From the proof of Lemma 2.2.4 it follows

$$\sum_{k=l+1}^{\infty} k^j\,\mathrm{e}^{-2\alpha k} \le l^j\,\mathrm{e}^{-2\alpha l} \underbrace{\sum_{m=-j}^{0}\sum_{i=0}^{-m} \frac{\binom{j+1}{i}\,\mathrm{e}^{-2\alpha m}}{(\mathrm{e}^{2\alpha}-1)^{j+1}}}_{=:c_{\alpha,j}}$$

for $l \ge j$. Then we get

$$\begin{aligned} |f(\tau) - \phi(2l+\tau)| &\le 2\sum_{k=l+1}^{\infty} |g'(2k+\tau)| \\ &= 2\sum_{k=l+1}^{\infty} |u'(2k+\tau) - \alpha u(2k+\tau)|\,\mathrm{e}^{-\alpha\tau-2\alpha k} \\ &\le 2\,\mathrm{e}^{-\alpha\tau}\left(\sum_{k=l+1}^{\infty} |u'(2k+\tau)|\,\mathrm{e}^{-2\alpha k} + \sum_{k=l+1}^{\infty} \alpha|u(2k+\tau)|\,\mathrm{e}^{-2\alpha k}\right) \\ &\le 2\,\mathrm{e}^{-\alpha\tau}\left(\sum_{k=l+1}^{\infty} C_2\,(2k+\tau)^{p_2}\,\mathrm{e}^{-2\alpha k} + \sum_{k=l+1}^{\infty} \alpha C_1\,(2k+\tau)^{p_1}\,\mathrm{e}^{-2\alpha k}\right) \\ &\le C_2 2^{p_2+1}\sum_{k=l+1}^{\infty} (k+1)^{p_2}\,\mathrm{e}^{-2\alpha k} + \alpha C_1 2^{p_1+1}\sum_{k=l+1}^{\infty} (k+1)^{p_1}\,\mathrm{e}^{-2\alpha k} \\ &= C_2 2^{p_2+1}\,\mathrm{e}^{2\alpha}\sum_{k=l+2}^{\infty} k^{p_2}\,\mathrm{e}^{-2\alpha k} + \alpha C_1 2^{p_1+1}\,\mathrm{e}^{2\alpha}\sum_{k=l+2}^{\infty} k^{p_1}\,\mathrm{e}^{-2\alpha k} \\ &\le \left[C_2 2^{p_2+1} c_{\alpha,p_2}(l+1)^{p_2} + \alpha C_1 2^{p_1+1} c_{\alpha,p_1}(l+1)^{p_1}\right]\mathrm{e}^{-2\alpha(l+1)} \end{aligned}$$

for arbitrary $\tau \in [0, 2[$. □

2.2.2 The case $n = 1$

In the case of linear eigenfunctions Y_1^m of V the representation of the solution $\phi(t)$ becomes more complicated than in the previous case. For $n = 1$ the eigenvalue is given by

$$\lambda_1(s) = \frac{-\theta_1(-s)\theta_1(s) + \theta_1^2(s)\,\mathrm{e}^{-2s}}{2s^3},$$

where

$$\theta_1(s) = s + 1.$$

which has one real zero namely $\alpha_1 = -1$. With the above computations we get

$$\begin{aligned}
&\mathcal{L}^{-1}\left(\frac{\tilde{\theta}_0(s) - \theta_1(s)^2\,\mathrm{e}^{-2s}}{\theta_1(-s)\theta_1(s) - \theta_1(s)^2\,\mathrm{e}^{-2s}}\right)(t)\\
&\overset{(2.2.4)}{=} \mathcal{L}^{-1}\left(R_1^{(1)}\right)(t) + \sum_{k=1}^{\infty}\left(-\mathcal{L}^{-1}\left(R_{1,k}^{(2)}\right)(t) + \mathcal{L}^{-1}\left(R_{1,k}^{(3)}\right)(t)\right)\\
&\overset{(2.2.5)}{=} -\sinh(t)\\
&\quad\overset{(2.2.6)}{-} \sum_{k=1}^{\infty}(-1)^k\delta(t-2k)H(t-2k) - \sum_{k=1}^{\infty}\sum_{j=1}^{k} c_{1,k,j,1}^{(2),\mathrm{re}}\,H(t-2k)(t-2k)^{j-1}\,\mathrm{e}^{t-2k}\\
&\quad\overset{(2.2.7)}{+} \sum_{k=1}^{\infty}\sum_{j=1}^{k} c_{1,k,j,1}^{(3),\mathrm{re}}\,H(t-2k)(t-2k)^{j}\,\mathrm{e}^{t-2k}\\
&= -\sinh(t) + \sum_{k=1}^{\infty}(-1)^{k+1}\delta(t-2k)H(t-2k)\\
&\quad + \sum_{k=1}^{\infty}\left[\sum_{j=1}^{k}\left(c_{k,j}^{(2)} + c_{k,j}^{(3)}t - c_{k,j}^{(3)}2k\right)(t-2k)^{j-1}\,\mathrm{e}^{t-2k}\right]H(t-2k),
\end{aligned}$$

where

$$c_{k,j}^{(2)} := c_{1,k,j,1}^{(2),\mathrm{re}} \quad \text{and} \quad c_{k,j}^{(3)} := c_{1,k,j,1}^{(3),\mathrm{re}}.$$

With the formulas in [3, Sec 5.2] we obtain the following explicit expressions for these constants:

$$\begin{aligned}
c_{k,j}^{(2)} &= (-1)^{k+1}\sum_{m=0}^{j-1}\frac{(1-(-1)^{j-m})k!}{(j-1)!m!(k-j)!(j-m)!} \quad \text{and}\\
c_{k,j}^{(3)} &= (-1)^{k+1}\frac{2^{j-1}(k-1)!}{(j-1)!j!(k-j)!},
\end{aligned}$$

where we used

$$\frac{(1+s)^k}{(1-s)^k} = (-1)^k + \frac{\sum_{i=0}^{k-1}\binom{k}{i}(-1)^k(1-(-1)^{k-i})s^i}{(s-1)^k}$$

in order to compute $c_{k,j}^{(2)}$. With (2.2.3) and (2.2.1) we therefore get for the solution

$$\begin{aligned}
\phi(t) &= \int_0^t g(t-\tau)\mathcal{L}^{-1}\left(\frac{1}{\lambda_1}\right)(\tau)d\tau\\
&= 2g'(t) - 2\int_0^t\Bigg(-\sinh(\tau) + \sum_{k=1}^{\infty}(-1)^{k+1}\delta(\tau-2k)H(\tau-2k)\\
&\quad + \sum_{k=1}^{\infty}\sum_{j=1}^{k}(c_{k,j}^{(2)} + c_{k,j}^{(3)}\tau - c_{k,j}^{(3)}2k)(\tau-2k)^{j-1}\,\mathrm{e}^{\tau-2k}\,H(\tau-2k)\Bigg)\,g'(t-\tau)d\tau
\end{aligned}$$

$$
\begin{aligned}
&= 2g'(t) + 2\sum_{k=1}^{\lfloor t/2\rfloor}(-1)^k g'(t-2k) + 2\int_0^t \sinh(\tau)g'(t-\tau)d\tau \\
&- 2\sum_{k=1}^{\infty}\sum_{j=1}^{k}\int_0^t (c_{k,j}^{(2)} + c_{k,j}^{(3)}\tau - c_{k,j}^{(3)}2k)(\tau-2k)^{j-1}\,\mathrm{e}^{\tau-2k}\,H(\tau-2k)g'(t-\tau)d\tau \\
&= 2\sum_{k=0}^{\lfloor t/2\rfloor}(-1)^k g'(t-2k) + 2\int_0^t \sinh(\tau)g'(t-\tau)d\tau \\
&- 2\sum_{k=1}^{\lfloor t/2\rfloor}\sum_{j=1}^{k}\int_{2k}^t (c_{k,j}^{(2)} + c_{k,j}^{(3)}\tau - c_{k,j}^{(3)}2k)(\tau-2k)^{j-1}\,\mathrm{e}^{\tau-2k}\,g'(t-\tau)d\tau. \qquad (2.2.15)
\end{aligned}
$$

Figure 2.3 shows solutions for different right-hand sides $g(t)$ (cf. [10]). As for the case $n = 0$ we have an oscillatory behaviour for larger times t which is again due to shape of the solution of the interior wave problem. Similar properties of these solutions as before could not be observed i.e. in general $\phi(t)$ does not seem to adopt a simple periodic pattern as time evolves.

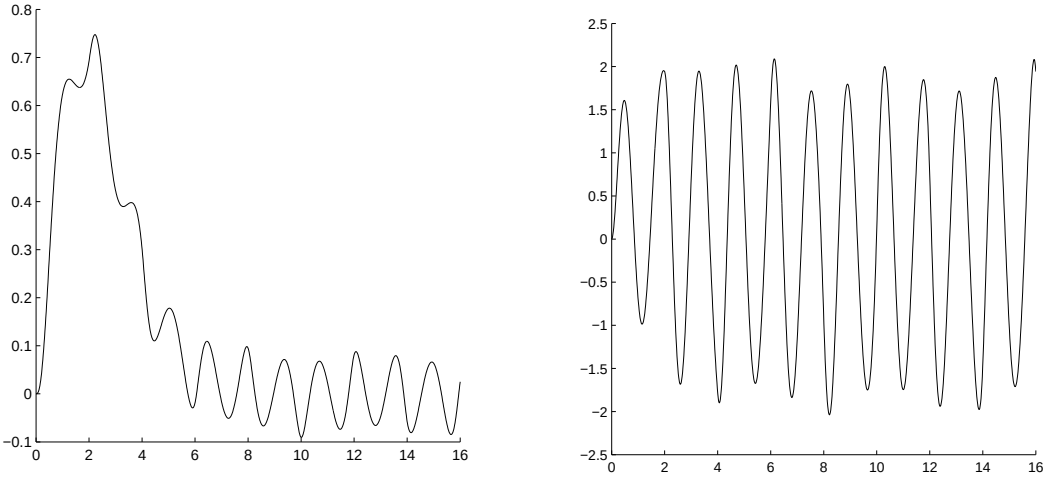

Figure 2.3: *Exact solution $\phi(t)$ with $n = 0$ for $g(t) = t^4e^{-2t}$ and $g(t) = \sin(2t)^2te^{-t}$.*

2.3 Solutions of the Dirichlet problem $w/2 + Kw = g$

In this section we will derive exact solutions of the Dirichlet problem (1.1.17) which is based on an indirect formulation involving the double layer potential. In this case the involved boundary integral operators are $R_1 = I/2 + K$ and $R_2 = I$ such that the problem on the sphere with the boundary data $g(x,t) = g(t)Y_n^m$ has the solution

$$
w(x,t) = w(t)Y_n^m, \qquad \text{with} \qquad w(t) = \int_0^t g(\tau)\mathcal{L}^{-1}\left(\frac{1}{\lambda_n^{(\hat{R}_1)}}\right)(t-\tau)d\tau. \qquad (2.3.1)
$$

With Corollary 2.1.2 we get that

$$
\lambda_n^{(\hat{R}_1)}(s) = -\mathrm{i}s^2 j_n(\mathrm{i}s)\,\partial h_n^{(1)}(\mathrm{i}s) + 1.
$$

In the following we compute the solutions for the cases $n = 0$ and $n = 1$.

2.3.1 The case $n = 0$

As in the previous section we assume for $n = 0$ a purely time-dependent right-hand side

$$g(x,t) := 2\sqrt{\pi}Y_0^0\, g(t) = g(t).$$

In this case we have

$$j_0(x) = \frac{\sin(x)}{x} \qquad \text{and} \qquad \frac{\partial}{\partial x} h_0^{(1)}(x) = \frac{(x+\mathrm{i})\,\mathrm{e}^{\mathrm{i}x}}{x^2},$$

and thus

$$\frac{1}{\lambda_0^{(\hat{R}_1)}(s)} = \frac{2s}{s-1+(s+1)\,\mathrm{e}^{-2s}}.$$

A formal Taylor expansion with respect to $\varepsilon = \mathrm{e}^{-2s}$ about 0 leads to

$$\frac{1}{\lambda_0^{(\hat{R}_1)}(s)} = \sum_{k=0}^{\infty}(-1)^k \frac{2s(s+1)^k}{(s-1)^{k+1}}\,\mathrm{e}^{-2ks}.$$

The inverse Laplace transform can now be written as

$$\mathcal{L}^{-1}\left(\frac{1}{\lambda_0^{(\hat{R}_1)}}\right)(t) = 2\sum_{k=0}^{\infty}(-1)^k H(t-2k)\,\partial_t \mathcal{L}^{-1}\left(\frac{(s+1)^k}{(s-1)^{k+1}}\right)(t-2k).$$

Here, only the Laplace inversion of a rational function is left. With the same formulas as in the previous section we get

$$\mathcal{L}^{-1}\left(\frac{(s+1)^k}{(s-1)^{k+1}}\right)(t) = \sum_{l=1}^{k+1} c_{k,l}\, t^{k-l+1}\mathrm{e}^t$$

with

$$c_{k,l} := \binom{k}{l-1}\frac{2^{k-l+1}}{(k-l+1)!}.$$

For the solution w of the scattering problem we therefore obtain with (2.3.1)

$$\begin{aligned}
w(t) &= \int_0^t g(t-\tau)\mathcal{L}^{-1}\left(\frac{1}{\lambda_0^{(\hat{R}_1)}}\right)(\tau)d\tau \\
&= \int_0^t g'(t-\tau)\left(2\sum_{k=0}^{\infty}(-1)^k H(\tau-2k)\sum_{l=1}^{k+1} c_{k,l}\,(\tau-2k)^{k-l+1}\,\mathrm{e}^{\tau-2k}\right)d\tau \\
&= 2\sum_{k=0}^{\infty}\sum_{l=1}^{k+1}(-1)^k \int_0^t g'(t-\tau)\left(H(\tau-2k)c_{k,l}\,(\tau-2k)^{k-l+1}\,\mathrm{e}^{\tau-2k}\right)d\tau \\
&= 2\sum_{k=0}^{\lfloor t/2\rfloor}\sum_{l=1}^{k+1}(-1)^k \int_{2k}^t c_{k,l}\,(\tau-2k)^{k-l+1}\,\mathrm{e}^{\tau-2k}\,g'(t-\tau)d\tau.
\end{aligned}$$

An example of such a solution is shown in Figure 2.4. Note that this solution, in contrast to the shape of the solutions before, is not bounded but increases in a linear manner.

2.3.2 The case $n = 1$

For $n = 1$ we have to invert the term

$$\frac{1}{\lambda_1^{(\hat{R}_1)}(s)} = \frac{2s^3}{s^3 - s^2 + 2 - (s^3 + 3s^2 + 4s + 2)\,\mathrm{e}^{-2s}}.$$

A Taylor expansion with respect to $\varepsilon = \mathrm{e}^{-2s}$ about 0 leads to

$$\frac{1}{\lambda_1^{(\hat{R}_1)}(s)} = \sum_{k=0}^{\infty} \frac{2s^3(s^3 + 3s^2 + 4s + 2)^k}{(s^3 - s^2 + 2)^{k+1}}\,\mathrm{e}^{-2ks}.$$

In order to obtain an explicit representation of w in (2.3.1) in an interval $[0, 2l[, l \in \mathbb{N}_{>0}$, it is necessary to invert l terms of the expansion above. For simplicity we compute the solution of this problem only in the interval $t \in [0, 2[$, i.e., we consider only the first term in the expansion. Since

$$\mathcal{L}^{-1}\left(\frac{2s^3}{s^3 - s^2 + 2}\right)(t) = 2\delta(t) - \frac{2}{5}\mathrm{e}^{-t} + \frac{4}{5}\mathrm{e}^{t}(3\cos(t) - \sin(t)),$$

we get the solution

$$w(t) = 2g(t) + \int_0^t g(t-\tau)\left(-\frac{2}{5}\mathrm{e}^{-\tau} + \frac{4}{5}\mathrm{e}^{\tau}(3\cos(\tau) - \sin(\tau))\right)\,d\tau$$

for $t \in [0, 2[$. In contrast to the case $n = 0$ these solutions behave again as in the section before; in all the tested examples they were bounded and oscillatory (cf. Figure 2.4).

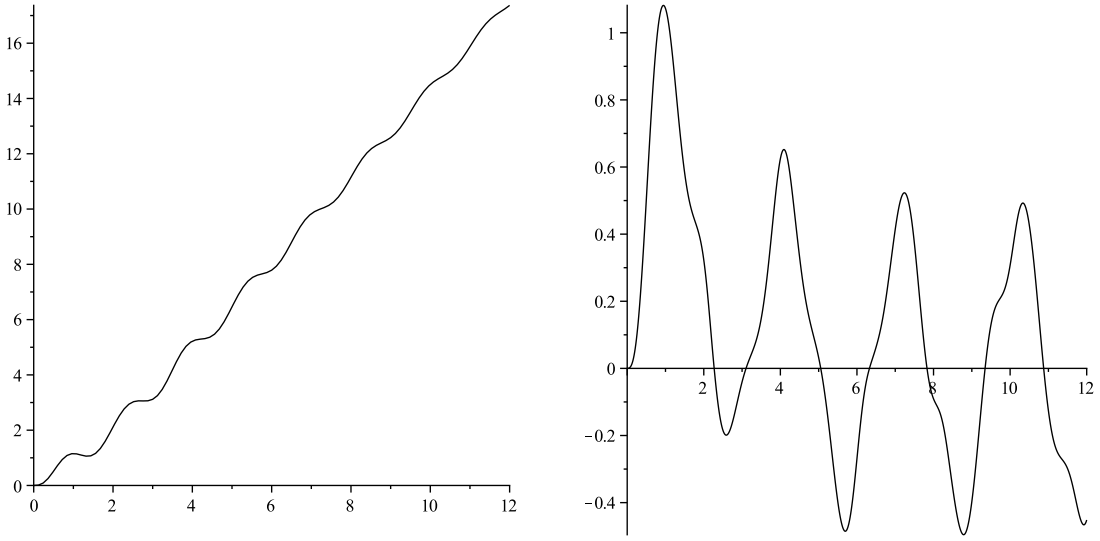

Figure 2.4: *Left: Exact solution $w(t)$ for $n = 0$ and $g(t) = \sin(2t)^2 te^{-t}$. Right: Exact solution $w(t)$ for $n = 1$ and $g(t) = \sin(2t)^2 te^{-t}$.*

2.4 Solutions of the Dirichlet problems $V\psi = -g/2 + Kg$ and $\psi/2 + K'\psi = Wg$

In this section we derive exact solutions of the Dirichlet problems (1.1.14) and (1.1.15). Both formulas can be obtained by taking the traces of the representation formula (1.1.5) and can be considered therefore as direct formulations of the problem. Since the solutions of these two equations coincide, we only consider the case (1.1.14). The involved boundary integral operators then are $R_1 = V$ and $R_2 = -I/2 + K$ such that the problem on the sphere with the boundary data $g(x,t) = g(t)Y_n^m$ has the solution

$$\psi(x,t) = \psi(t)Y_n^m, \qquad \text{with} \qquad \psi(t) = \int_0^t g(\tau)\mathcal{L}^{-1}\left(\frac{\lambda_n^{(\hat{R}_2)}}{\lambda_n^{(\hat{R}_1)}}\right)(t-\tau)d\tau. \tag{2.4.1}$$

With Corollary 2.1.2 we get that

$$\lambda_n^{(\hat{R}_1)}(s) = -sj_n(\mathrm{i}s)h_n^{(1)}(\mathrm{i}s) \qquad \text{and} \qquad \lambda_n^{(\hat{R}_2)}(s) = -\mathrm{i}s^2 j_n(\mathrm{i}s)\,\partial h_n^{(1)}(\mathrm{i}s).$$

In the following we compute the solutions in the cases $n = 0$ and $n = 1$.

2.4.1 The case $n = 0$

For $n = 0$ the expression we have to invert is

$$\frac{\lambda_0^{(\hat{R}_2)}}{\lambda_0^{(\hat{R}_1)}} = \frac{\mathrm{i}s\,\partial h_0^{(1)}(\mathrm{i}s)}{h_0^{(1)}(\mathrm{i}s)} = -s - 1.$$

The solution is therefore simply given by

$$\psi(t) = -g'(t) - g(t).$$

An example of such a solution is shown in Figure 2.5. Since we solve here the exterior problem directly, the solution tends to 0 for large t and is not oscillatory like for indirect formulations of the problem.

2.4.2 The case $n = 1$

For $n = 1$ we have

$$\frac{\lambda_1^{(\hat{R}_2)}}{\lambda_1^{(\hat{R}_1)}} = \frac{\mathrm{i}s\,\partial h_1^{(1)}(\mathrm{i}s)}{h_1^{(1)}(\mathrm{i}s)} = -\frac{s^2+2s+2}{s+1}.$$

Since

$$\mathcal{L}^{-1}\left(-\frac{s^2+2s+2}{s+1}\right)(t) = -\delta'(t) - \delta(t) - \mathrm{e}^{-t},$$

the solution in this case is given by

$$\psi(t) = -g'(t) - g(t) - \int_0^t g(t-\tau)\,\mathrm{e}^{-\tau}\,d\tau.$$

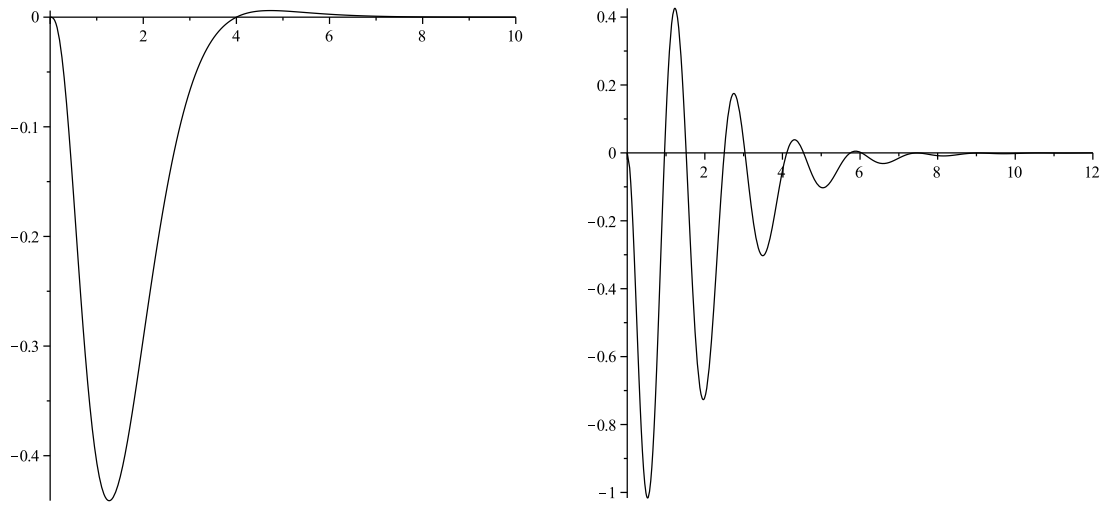

Figure 2.5: *Left: Exact solution $\psi(t)$ for $n = 0$ and $g(t) = t^4 e^{-2t}$. Right: Exact solution $\psi(t)$ for $n = 1$ and $g(t) = \sin(2t)^2 t e^{-t}$.*

2.5 Solutions of the Neumann problem $\phi/2 - K'\phi = -h$

Here we derive exact solutions of the Neumann problem (1.1.20). The involved boundary integral operators then are $R_1 = K' - I/2$ and $R_2 = I$ such that the problem on the sphere with the boundary data $h(x,t) = h(t)Y_n^m$ has the solution

$$\phi(x,t) = \phi(t)Y_n^m, \qquad \text{with} \qquad \phi(t) = \int_0^t h(\tau)\mathcal{L}^{-1}\left(\frac{1}{\lambda_n^{(\hat{R}_1)}}\right)(t-\tau)d\tau. \tag{2.5.1}$$

With Corollary 2.1.2 we get that

$$\lambda_n^{(\hat{R}_1)}(s) = -\mathrm{i}s^2 j_n(\mathrm{i}s)\,\partial h_n^{(1)}(\mathrm{i}s).$$

In the following we compute the solutions in the cases $n = 0$ and $n = 1$.

2.5.1 The case $n = 0$

For $n = 0$ the expression we have to invert is

$$\frac{1}{\lambda_0^{(\hat{R}_1)}(s)} = \frac{1}{-\mathrm{i}s^2 j_0(\mathrm{i}s)\,\partial h_0^{(1)}(\mathrm{i}s)} = -\frac{s}{\sinh(s)(s+1)\,\mathrm{e}^{-s}} = -\frac{2s}{s+1}\sum_{k=0}^{\infty}\mathrm{e}^{-2ks}.$$

For the inverse Laplace transform we get therefore

$$\mathcal{L}^{-1}\left(\frac{1}{\lambda_0^{(\hat{R}_1)}}\right)(t) = -2\sum_{k=1}^{\infty}\delta(t-2k) + 2\sum_{k=0}^{\infty}H(t-2k)\,\mathrm{e}^{-(t-2k)}.$$

For the solution ϕ we obtain

$$\phi(t) = -2\sum_{k=0}^{\lfloor t/2\rfloor}h(t-2k) + 2\sum_{k=0}^{\lfloor t/2\rfloor}\int_{2k}^{t}\mathrm{e}^{-(\tau-2k)}\,h(t-\tau)d\tau.$$

An example of such a solution is shown in Figure 2.6. This boundary integral equation was derived by taking the normal derivative of the single layer potential. As numerical experiments indicate the derived solutions in this case share properties with the solutions in Section 2.2.1 where we solved the Dirichlet problem using the the single layer potential. As before also the solutions for this Neumann problem seem to adopt a simple 2-periodic pattern for large times. We will not prove this here.

2.5.2 The case $n = 1$

In the case $n = 1$ we have

$$\begin{aligned}\frac{1}{\lambda_0^{(\hat{R}_1)}(s)} &= -\frac{2s^3}{s^2+2s+2}\cdot\frac{1}{s-1+(s+1)\,\mathrm{e}^{-2s}} \\ &= -\frac{2s^3}{s^2+2s+2}\sum_{k=0}^{\infty}(-1)^k\frac{(s+1)^k}{(s-1)^{k+1}}\,\mathrm{e}^{-2ks}\,.\end{aligned}$$

In order to keep the presentation short we compute the exact solution in this case only in the interval $t \in [0, 2[$. Thus, we consider only the first term (i.e. $k = 0$) in the expansion above. Since

$$\mathcal{L}^{-1}\left(-\frac{2s^3}{(s^2+2s+2)(s-1)}\right) = -2\,\delta(t) - \frac{2}{5}\,\mathrm{e}^{t} + \frac{4}{5}\,\mathrm{e}^{-t}\left(3\,\cos(t) + \sin(t)\right),$$

we get the exact solution

$$\phi(t) = -2h(t) + \int_0^t h(t-\tau)\left(-\frac{2}{5}\,\mathrm{e}^{\tau} + \frac{4}{5}\,\mathrm{e}^{-\tau}\left(3\,\cos(\tau) + \sin(\tau)\right)\right)d\tau$$

for $t \in [0, 2[$.

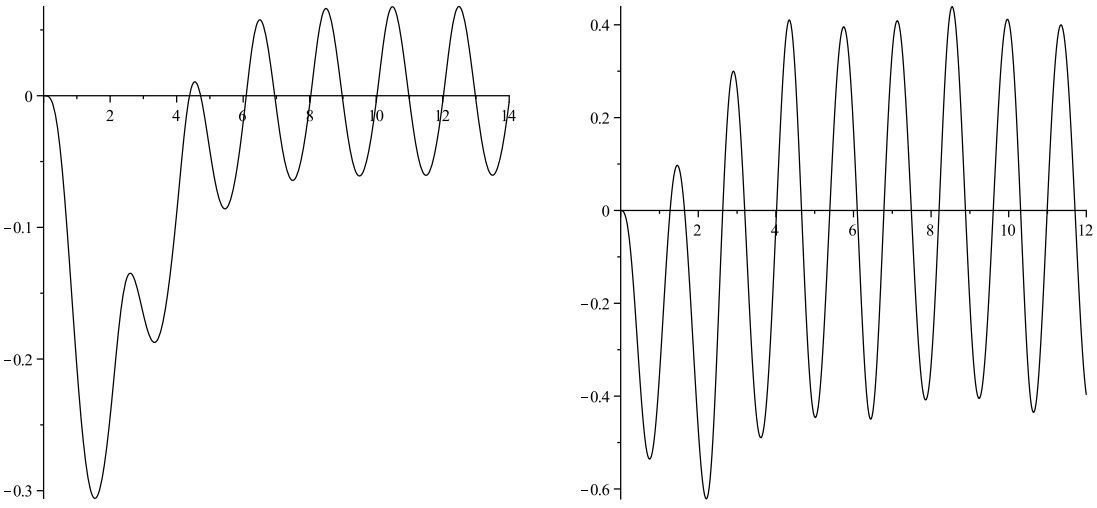

Figure 2.6: *Left: Exact solution $\phi(t)$ for $n = 0$ and $h(t) = t^4e^{-2t}$. Right: Exact solution $\phi(t)$ for $n = 1$ and $h(t) = \sin(2t)^2te^{-t}$.*

2.6 Solutions of the Neumann problem $Ww = h$

In this section we derive exact solutions of the Neumann problem (1.1.21). The involved boundary integral operators then are $R_1 = W$ and $R_2 = I$ such that the problem on the sphere with the boundary data $h(x,t) = h(t)Y_n^m$ has the solution

$$w(x,t) = w(t)Y_n^m, \qquad \text{with} \qquad w(t) = \int_0^t h(\tau)\mathcal{L}^{-1}\left(\frac{1}{\lambda_n^{(\hat{R}_1)}}\right)(t-\tau)d\tau. \tag{2.6.1}$$

With Corollary 2.1.2 we get that

$$\lambda_n^{(\hat{R}_1)}(s) = s^3 \partial j_n(\mathrm{i}s)\, \partial h_n^{(1)}(\mathrm{i}s).$$

In the following we compute the solutions in the cases $n = 0$ and $n = 1$.

2.6.1 The case $n = 0$

In the case of a purely time-dependent right-hand side we have to Laplace invert the term

$$\begin{aligned}\frac{1}{\lambda_0^{(\hat{R}_1)}(s)} &= -\frac{2s}{s^2 - 1 + (s+1)^2\mathrm{e}^{-2s}} = -\sum_{k=0}^{\infty}(-1)^k \frac{2s(s+1)^{2k}}{(s^2-1)^{k+1}}\mathrm{e}^{-2ks} \\ &= -\frac{2s}{s^2-1} + \sum_{k=1}^{\infty}(-1)^{k+1}\frac{2s(s+1)^{k-1}}{(s-1)^{k+1}}\mathrm{e}^{-2ks}.\end{aligned}$$

Now the inversion is similar to the case in Section 2.3.1. Since

$$\mathcal{L}^{-1}\left(\frac{1}{\lambda_0^{(\hat{R}_1)}}\right)(t) = -2\cosh(t) + 2\sum_{k=1}^{\infty}(-1)^{k+1}H(t-2k)\,\partial_t\mathcal{L}^{-1}\left(\frac{(s+1)^{k-1}}{(s-1)^{k+1}}\right)(t-2k)$$

and

$$\mathcal{L}^{-1}\left(\frac{(s+1)^{k-1}}{(s-1)^{k+1}}\right)(t) = \sum_{l=1}^{k} c_{k,l}\, t^{k-l+1}\mathrm{e}^t$$

with

$$c_{k,l} := \binom{k-1}{l-1}\frac{2^{k-l}}{(k-l+1)!},$$

we obtain for the solution w of the scattering problem (2.6.1)

$$\begin{aligned}w(t) &= -2\int_0^t h(t-\tau)\cosh(\tau)d\tau \\ &\quad + \int_0^t h'(t-\tau)\left(2\sum_{k=1}^{\infty}(-1)^{k+1}H(\tau-2k)\sum_{l=1}^{k} c_{k,l}\,(\tau-2k)^{k-l+1}\,\mathrm{e}^{\tau-2k}\right)d\tau \\ &= -2\int_0^t h(t-\tau)\cosh(\tau)d\tau + 2\sum_{k=1}^{\lfloor t/2\rfloor}\sum_{l=1}^{k}(-1)^{k+1}\int_{2k}^{t} c_{k,l}\,(\tau-2k)^{k-l+1}\mathrm{e}^{\tau-2k}h'(t-\tau)d\tau.\end{aligned}$$

An example of such a solution is shown in Figure 2.7. Note that the solutions in this case exhibit a similar behavior as the solutions in Section 2.3.1, where we solved a Dirichlet problem using the double layer potential.

2.6.2 The case $n = 1$

In the case $n = 1$ we have to invert

$$\frac{1}{\lambda_0^{(\hat{R}_1)}(s)} = \frac{2s^3}{s^2+2s+2} \cdot \frac{1}{-s^2+2s-2+(s^2+2s+2)\mathrm{e}^{-2s}}$$
$$= \frac{2s^3}{s^2+2s+2} \sum_{k=0}^{\infty} (-1)^k \frac{(s^2+2s+2)^k}{(-s^2+2s-2)^{k+1}} \mathrm{e}^{-2ks}.$$

In order to obtain the solution of (2.6.1) in the interval $[0, 2[$ we consider the first term of the expansion above. Since

$$\mathcal{L}^{-1}\left(\frac{2s^3}{(s^2+2s+2)(-s^2+2s-2)}\right)(t) = -2\cosh(t)\cos(t),$$

we get the solution

$$w(t) = -2\int_0^t h(t-\tau)\cosh(\tau)\cos(\tau)d\tau.$$

for $t \in [0, 2[$.

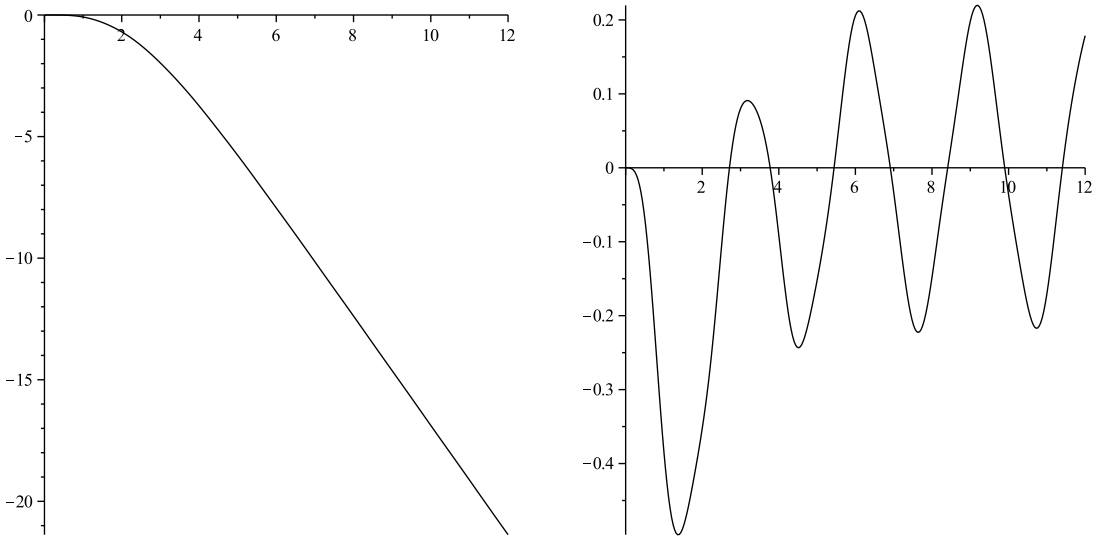

Figure 2.7: *Left: Exact solution $w(t)$ for $n = 0$ and $g(t) = t^4 e^{-2t}$. Right: Exact solution $w(t)$ for $n = 1$ and $g(t) = \sin(2t)^2 t e^{-t}$.*

2.7 Solutions of the Neumann problems $v/2 - Kv = -Vh$ and $Wv = h/2 + K'h$

Here we derive exact solutions of the Neumann problems (1.1.18) and (1.1.19). These boundary integral equations are based on a direct formulation of the problem and the necessary computations in order to obtain solutions on the sphere are very similar to the cases in Section 2.4. Let us consider the case (1.1.18). The involved boundary integral operators then

are $R_1 = -I/2 + K$ and $R_2 = V$ such that the problem on the sphere with the boundary data $h(x,t) = h(t)Y_n^m$ has the solution

$$v(x,t) = v(t)Y_n^m, \qquad \text{with} \qquad v(t) = \int_0^t h(\tau)\mathcal{L}^{-1}\left(\frac{\lambda_n^{(\hat{R}_2)}}{\lambda_n^{(\hat{R}_1)}}\right)(t-\tau)d\tau. \tag{2.7.1}$$

and

$$\lambda_n^{(\hat{R}_1)}(s) = -\mathrm{i}s^2 j_n(\mathrm{i}s)\,\partial h_n^{(1)}(\mathrm{i}s) \qquad \text{and} \qquad \lambda_n^{(\hat{R}_2)}(s) = -sj_n(\mathrm{i}s)h_n^{(1)}(\mathrm{i}s)$$

In the following we compute the solutions in the cases $n = 0$ and $n = 1$.

2.7.1 The case $n = 0$

With the computations in Section 2.4 we get

$$\mathcal{L}^{-1}\left(\frac{\lambda_0^{(\hat{R}_2)}}{\lambda_0^{(\hat{R}_1)}}\right)(t) = -\mathrm{e}^{-\mathrm{t}}.$$

The solution in this case is therefore given by

$$v(t) = -\int_0^t h(t-\tau)\mathrm{e}^{-\tau}\mathrm{d}\tau.$$

An example of such a solution is shown in Figure 2.8.

2.7.2 The case $n = 1$

For $n = 1$ we have

$$\mathcal{L}^{-1}\left(\frac{\lambda_1^{(\hat{R}_2)}}{\lambda_1^{(\hat{R}_1)}}\right)(t) = \mathcal{L}^{-1}\left(-\frac{s+1}{s^2+2s+2}\right)(t) = -\mathrm{e}^{-\mathrm{t}}\cos(\mathrm{t}),$$

and therefore the solution

$$v(t) = -\int_0^t h(t-\tau)\,\mathrm{e}^{-\tau}\cos(\tau)d\tau.$$

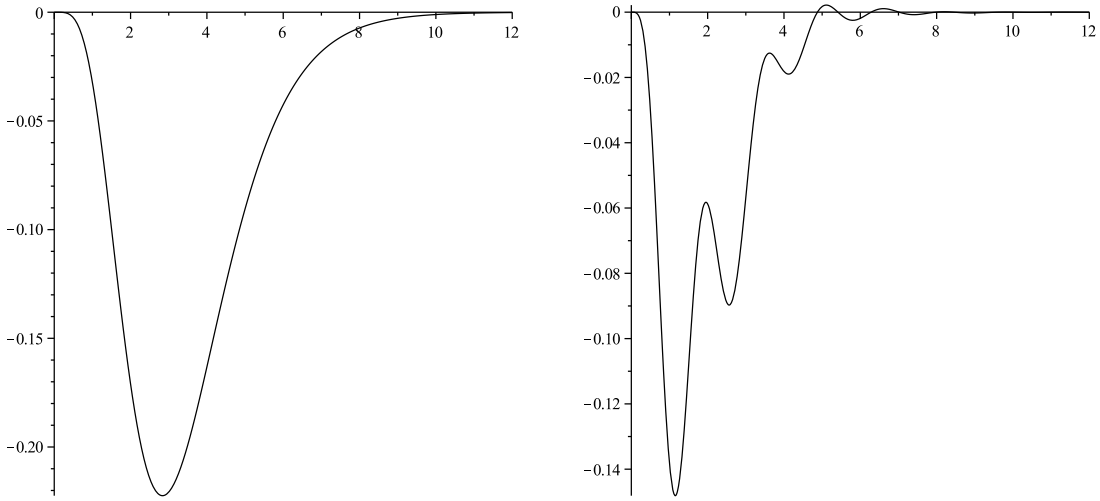

Figure 2.8: *Left: Exact solution $v(t)$ for $n = 0$ and $h(t) = t^4 e^{-2t}$. Right: Exact solution $v(t)$ for $n = 1$ and $h(t) = \sin(2t)^2 t e^{-t}$.*

References

[1] L. Banjai and S. Sauter. A refined Galerkin error and stability analysis for highly indefinite variational problems. *SIAM J. Numer. Anal.*, 45:37–53, 2007.

[2] L. Banjai and S. Sauter. Rapid solution of the wave equation in unbounded domains. *SIAM Journal on Numerical Analysis*, 47:227–249, 2008.

[3] A. Erdélyi, W. Magnus, F. Oberhettinger, and F. G. Tricomi. *Tables of Integral Transforms.* McGraw-Hill Book Company, Inc., 1954.

[4] I. Gradshteyn and I. Ryzhik. *Table of Integrals, Series, and Products.* Academic Press, 1965.

[5] T. Ha-Duong. On retarded potential boundary integral equations and their discretisation. In *Topics in Computational Wave Propagation: Direct and Iverse Problems*, volume 31 of *Lect. Notes Comput. Sci. Eng.*, pages 301–336. Springer, Berlin, 2003.

[6] M. Ismail. *Classical and quantum orthogonal polynomials in one variable*, volume 98. Cambridge University Press, Cambridge, 2009.

[7] R. Kress. Minimizing the condition number of boundary integral operators in acoustic and electromagnetic scattering. *The Quarterly Journal of Mechanics and Applied Mathematics*, 38(2):323–341, 1985.

[8] J. C. Nédélec. *Acoustic and Electromagnetic Equations.* Springer-Verlag, 2001.

[9] S. Sauter and A. Veit. Exact Solutions of Retarded Boundary Integral Equations. Preprint 03-2011, Universität Zürich.

[10] A. Veit. A MATLAB code for computing exact solutions of retarded potential equations for a spherical scatterer. 2011. Available via: `https://www.math.uzh.ch/compmath/?exactsolutions`.

3

[Preprint 04-2011, Institute of Mathematics, University of Zurich]

Adaptive Time Discretization for Retarded Potentials

S. Sauter* A. Veit† ‡

Abstract

We consider retarded boundary integral formulations of the three-dimensional wave equation in unbounded domains. Our goal is to apply a Galerkin method in space and time in order to solve these problems numerically. In this approach the computation of the system matrix entries is the major bottleneck. We will propose new types of finite-dimensional spaces for the time discretization. They allow variable time-stepping, variable order of approximation and simplify the quadrature problem arising in the generation of the system matrix substantially. The reason is that the basis functions of these spaces are globally smooth and compactly supported.

In order to perform numerical tests concerning our new basis functions we consider the special case that the boundary of the scattering problem is the unit sphere. In this case explicit solutions of the problem are available which will serve as reference solutions for the numerical experiments.

AMS subject classifications: 35L05, 65N38, 65R20

Key words: retarded potentials, acoustic scattering, boundary integral equations, partition of unity method, Galerkin approach, variable timesteps.

3.1 Introduction

Mathematical modeling of acoustic and electromagnetic wave propagation and its efficient and accurate numerical simulation is a key technology for numerous engineering applications

*Institut für Mathematik, Universität Zürich, Winterthurerstrasse 190, CH-8057 Zürich, Switzerland, e-mail: stas@math.uzh.ch

†Institut für Mathematik, Universität Zürich, Winterthurerstrasse 190, CH-8057 Zürich, Switzerland, e-mail: alexander.veit@math.uzh.ch

‡The second author gratefully acknowledges the support given by SNF, No. PDFMP2_127437/1

as, e.g., in detection (nondestructive testing, radar), communication (optoelectronic and wireless) and medicine (sonic imaging, tomography). An adequate model problem for the development of efficient numerical methods for such types of physical applications is the three-dimensional wave equation in unbounded exterior domains. In this setting the method of integral equations is an elegant approach since it reduces the problem in the unbounded domain to an integral equation on the bounded surface of the scatterer.
In this paper we apply a Galerkin method for the discretization of these retarded boundary integral equations (cf. [3, 13, 17, 18]). This approach allows variable time stepping and spatially curved scatterers. Until now, a severe drawback of this method was, however, that the domain for the spatial integration is the intersection of (possibly curved) pairs of surface panels with the discrete light cone which is very complicated to handle numerically. Quadrature schemes tailored to this problem were derived for example in [15, 21, 24]. These methods are restricted to polyhedral scatterers and their implementation is difficult.
Other approaches for the numerical discretization of retarded boundary integral equations use collocation schemes (cf. [8, 9, 11, 14, 22]). Although they play an important role in practice, the mathematical analysis of these methods is challenging. In more than two dimensions stability and convergence of collocation schemes can only be shown for special geometries (cf. [12]). Furthermore the application of these techniques to curved scatterers is difficult. More recent approaches include methods based on bandlimited interpolation and extrapolation (cf. [30, 29, 31, 32]) and convolution quadrature (cf. [4, 5, 6, 7, 10, 19, 20, 28]). The latter enjoys nice stability properties and allows to apply many techniques known from frequency domain problems. However the stepsize for the time discretization must be constant in these methods and a generalization to non-uniform time meshes is not straightforward.
In our paper we will present a new time discretization method for the retarded potential equations which circumvents the numerical integration over intersections of the light cone with the spatial surface mesh. For this purpose, we will introduce infinitely smooth and compactly supported basis functions in time. These functions are constructed by using the Partition of Unity Method (cf. [2]).
In order to test the choice of the new basis functions numerically we consider the wave equation on the sphere with Dirichlet boundary conditions. For the resulting problems explicit representations of the exact solutions are available (cf. [23]). We apply a Galerkin method using our basis functions to these problems and perform numerical experiments.

3.2 Integral Formulation of the Wave Equation

Let $\Omega \subset \mathbb{R}^3$ be a Lipschitz domain with boundary Γ. We consider the homogeneous wave equation

$$\partial_t^2 u - \Delta u = 0 \quad \text{in } \Omega \times [0,T] \tag{3.2.1a}$$

with initial conditions

$$u(\cdot,0) = \partial_t u(\cdot,0) = 0 \quad \text{in } \Omega \tag{3.2.1b}$$

and Dirichlet boundary conditions

$$u = g \quad \text{on } \Gamma \times [0,T] \tag{3.2.1c}$$

on a time interval $[0,T]$ for $T > 0$. In applications, Ω is often the unbounded exterior of a bounded domain. For such problems, the method of boundary integral equations is an elegant

tool where this partial differential equation is transformed to an equation on the bounded surface Γ. We employ an ansatz as a *single layer potential* for the solution u,

$$u(x,t) := S\phi(x,t) := \int_\Gamma \frac{\phi(y, t - \|x-y\|)}{4\pi\|x-y\|} d\Gamma_y, \quad (x,t) \in \Omega \times [0,T] \tag{3.2.2}$$

with unknown density function ϕ. S is also referred to as *retarded single layer potential* due to the retarded time argument $t - \|x-y\|$ which connects time and space variables.

The ansatz (3.2.2) satisfies the wave equation (3.2.1a) and the initial conditions (3.2.1b). Since the single layer potential can be extended continuously to the boundary Γ, the unknown density function ϕ is determined such that the boundary conditions (3.2.1c) are satisfied. This results in the boundary integral equation for ϕ,

$$\int_\Gamma \frac{\phi(y, t - \|x-y\|)}{4\pi\|x-y\|} d\Gamma_y = g(x,t) \quad \forall (x,t) \in \Gamma \times [0,T]\,. \tag{3.2.3}$$

In order to solve this boundary integral equation numerically we introduce the following space-time variational formulation (cf. [3, 17]): Find ϕ such that

$$\int_0^T \int_\Gamma \int_\Gamma \frac{\dot\phi(y, t - \|x-y\|)\zeta(x,t)}{4\pi\|x-y\|} d\Gamma_y d\Gamma_x dt = \int_0^T \int_\Gamma \dot g(x,t)\zeta(x,t) d\Gamma_x dt \tag{3.2.4}$$

for all ζ, where we denote by $\dot\phi$ the derivative with respect to time.

3.3 Numerical Discretization

We turn our attention to the discretization of (3.2.4). In order to find an approximate solution we apply a Galerkin method in space and time. The variational formulation (3.2.4) is coercive in

$$H^{-1/2,-1/2}(\Gamma \times [0,T]) := L^2(0,T; H^{-1/2}(\Gamma)) + H^{-1/2}(0,T; L^2(\Gamma)) \tag{3.3.1}$$

(cf. [17]) and is uniquely solvable in this Sobolev space. Furthermore this ensures existence and uniqueness of the solution of a conforming Galerkin discretization.

Let V_{Galerkin} be a finite dimensional subspace of (3.3.1) being spanned by N basis functions $\{b_i\}_{i=1}^N$ in time and M basis functions $\{\varphi_i\}_{i=1}^N$ in space. This leads to the ansatz

$$\phi_{\text{Galerkin}}(x,t) = \sum_{i=1}^N \sum_{j=1}^M \alpha_i^j \varphi_j(x) b_i(t), \quad (x,t) \in \Gamma \times [0,T]\,, \tag{3.3.2}$$

where α_i^j are the unknown coefficients. Plugging the ansatz (3.3.2) into the variational formulation leads to the Galerkin discretization: Find $\alpha_i^j, i = 1,\dots,N, j = 1,\dots,M$ such that

$$\int_0^T \int_\Gamma \int_\Gamma \sum_{i=1}^N \sum_{j=1}^M \frac{\alpha_i^j \varphi_j(y) \dot b_i(t - \|x-y\|) \varphi_l(x) b_k(t)}{4\pi\|x-y\|} d\Gamma_y d\Gamma_x dt$$
$$= \int_0^T \int_\Gamma \dot g(x,t)\, \varphi_l(x)\, b_k(t) d\Gamma_x dt$$

for $k = 1, \ldots, N$ and $l = 1, \ldots, M$. Rearranging terms shows that this is equivalent to: Find α_i^j for $i = 1 \ldots, N$ and $j = 1, \ldots, M$ such that

$$\sum_{i=1}^{N} \sum_{j=1}^{M} A_{j,l}^{i,k} \alpha_i^j = g_l^k \qquad \forall 1 \leq k \leq N \quad \forall 1 \leq l \leq M, \tag{3.3.3}$$

where

$$g_l^k := \int_0^T \int_\Gamma \dot{g}(x,t)\, \varphi_l(x)\, b_k(t) d\Gamma_x dt$$

and

$$\begin{aligned} A_{j,l}^{i,k} &:= \int_\Gamma \int_\Gamma \varphi_j(y)\, \varphi_l(x)\, \psi_{i,k}(\|x-y\|) d\Gamma_y d\Gamma_x \\ &= \int_{\mathrm{supp}(\varphi_l)} \int_{\mathrm{supp}(\varphi_j)} \varphi_j(y)\, \varphi_l(x)\, \psi_{i,k}(\|x-y\|) d\Gamma_y d\Gamma_x \end{aligned} \tag{3.3.4}$$

with

$$\psi_{i,k}(r) := \int_0^T \frac{\dot{b}_i(t-r) b_k(t)}{4\pi r} dt,$$

where $r \in \mathbb{R}_{>0}$. The computation of a Galerkin solution via (3.3.3) leads to large linear system with NM unknowns. The corresponding boundary element matrix consists of $N \times N$ blocks of size $M \times M$. Each matrix block is symmetric and furthermore sparse if the basis functions in space and time have compact support. This is due to the fact that $\psi_{i,k}$ has compact support in this case and therefore only those combinations of j and l lead to nonzero matrix entries for which

$$\{\|x-y\|, x \in \mathrm{supp}(\varphi_l), y \in \mathrm{supp}(\varphi_j)\} \cap \mathrm{supp}(\psi_{i,k}) \neq \emptyset.$$

The numerical realization of the Galerkin method requires the efficient and accurate approximation of the matrix entries $A_{j,l}^{i,k}$ which is a major challenge. In the literature (cf. [17, 18, 24]) piecewise polynomial basis functions in time are employed while, then, $\psi_{i,k}(\|x-y\|)$ in general is only a *piecewise* analytic function in $x \in \mathrm{supp}(\varphi_l)$ and $y \in \mathrm{supp}(\varphi_j)$ (even if $\mathrm{supp}(\varphi_l)$ and $\mathrm{supp}(\varphi_j)$ are properly separated). Consequently, high order Gauss rules are converging only at a suboptimal rate. To obtain a sufficiently high accuracy, the integration is carried out on the intersections of the surface panels with the discrete light cone, i.e., with the support of $\psi_{i,k}(\|x-y\|)$. The stable handling of these intersections and the implementation of these quadrature rules is difficult and especially complicated for curved surface patches.

In this paper, we will introduce infinitely smooth and compactly supported basis functions in time. This will simplify the problem of computing the matrix entries $A_{j,l}^{i,k}$ considerably while maintaining the sparsity of the system matrix. Since the integrand will be smooth in this case we can apply standard quadrature rules to the double integral in (3.3.4). Furthermore the discretization with curved surface panels is straightforward since the numerical handling of the complicated geometry of the intersection of panels with the discrete light cone is circumvented.

The construction of the aforementioned basis functions in time is in the spirit of the Partition of Unity Method (PUM) (cf. [2]). Before we define and construct the finite element space in time we recall some basic definitions of the PUM.

Definition 3.3.1. *Let $\Theta := [0,T]$ be the time interval and $\{\Theta_i\}$ be a closed cover of Θ satisfying the overlap condition*

$$\exists L \in \mathbb{N} \quad s.t \quad \forall t \in \Theta, \quad \#\{i | t \in \Theta_i\} \leq L.$$

Let $\{\varphi_i\} \subset C^m(\mathbb{R}), m \in \mathbb{N}_0$ be a partition of unity subordinate to the cover $\{\Theta_i\}$ with

$$\begin{array}{ll} \operatorname{supp} \varphi_i \subset \Theta_i, & \sum_i \varphi_i \equiv 1 \text{ on } \Theta, \\ \|\varphi_i\|_{L^\infty(\mathbb{R})} \leq C_\infty, & \|\varphi_i'\|_{L^\infty(\mathbb{R})} \leq \frac{C_G}{|\Theta_i|}, \end{array}$$

for all i where C_∞ and C_G are constants and $|\Theta_i|$ denotes the length of the interval Θ_i. Then $\{\varphi_i\}$ is called a (L, C_∞, C_G) partition of unity of degree m subordinate to the cover $\{\Theta_i\}$.

Multiplying such a partition of unity with localized finite dimensional spaces S_i consisting of functions with support in Θ_i leads to PUM spaces on $[0,T]$.

Definition 3.3.2. *Let Θ and $\{\Theta_i\}$ be as in Definition 3.3.1 and let $\{\varphi_i\}$ be a (L, C_∞, C_G) partition of unity subordinate to $\{\Theta_i\}$. Let $S_i \subset \left\{w \in L^2(\Theta) : \operatorname{supp} w \in \Theta_i\right\}$ be given. Then the space*

$$S := \sum_i \varphi_i S_i := \left\{ \sum_i \varphi_i v_i \mid v_i \in S_i \right\} \subset L^2(\Theta)$$

is called the PUM space. The spaces S_i are the local approximation spaces.

In Definition 3.3.2, S is a subspace of $L^2(\Theta)$. We can easily obtain smoother spaces by choosing an appropriate partition of unity and smooth local approximation spaces. As mentioned above our goal is to define a PUM space $S \subset C^\infty(\mathbb{R})$ with smooth and compactly supported basis functions. Therefore we will first construct a partition of unity of infinite degree. Consider the function

$$f(t) := \begin{cases} \operatorname{erf}(2 \operatorname{arctanh}(t)), & \text{for } |t| < 1, \\ -1, & \text{for } t \leq -1, \\ 1, & \text{for } t \geq 1. \end{cases} \tag{3.3.5}$$

Lemma 3.3.3. *The function f as defined in (3.3.5) belongs to $C^\infty(\mathbb{R})$.*

Proof. It can be proved by induction that the m-th derivative of f in the interval $(-1,1)$ can be written as

$$f^{(m)}(t) = C\, \mathrm{e}^{-4 \operatorname{arctanh}^2(t)} (t^2-1)^{-m} \sum_{i=0}^{m-1} \alpha_i \operatorname{arctanh}^i(t)\, t^{m-i-1}$$

for constants C and α_i. Therefore

$$\lim_{|t| \to 1} f^{(m)}(t) = 0$$

for arbitrary $m \in \mathbb{N}$. □

Let $a < b$ be two real numbers. We make a change of variable and define

$$h_{a,b}(t) := \frac{1}{2} f\left(2\frac{t-a}{b-a} - 1\right) + \frac{1}{2}.$$

Then $h_{a,b} : \mathbb{R} \to [0,1]$ is a C^∞-function such that

$$h_{a,b}(t) = \begin{cases} 0, & \text{for } t \le a, \\ 1, & \text{for } t \ge b. \end{cases}$$

Now we can define a C^∞-bump function $\rho_{a,b,c}$ for real numbers $a < b < c$ by

$$\rho_{a,b,c}(t) := \begin{cases} h_{a,b}(t), & \text{for } t \le b, \\ 1 - h_{b,c}(t), & \text{for } t \ge b. \end{cases}$$

Due to the above properties, $\rho_{a,b,c}$ satisfies $\rho_{a,b,c} \ge 0$ in $\mathbb{R}$ and

$$\rho_{a,b,c}(t) = \begin{cases} 0, & \text{for } t \le a \text{ and } t \ge c, \\ 1, & \text{for } t = b. \end{cases}$$

Let us now consider the closed interval $\Theta = [0,T]$ and N (not necessarily equidistant) timesteps t_i such that $0 = t_0 < t_1 < t_2 < \ldots < t_{N-2} < t_{N-1} = T$. We define $\tau_i := [t_{i-1}, t_i]$ for $i = 1, \ldots, N-1$. Then a closed cover $\{\Theta_i\}$ of Θ, satisfying the pointwise overlap condition in Definition 3.3.1 with $L = 2$, is given by

$$\begin{aligned} \Theta_1 &:= \tau_1, \\ \Theta_i &:= \tau_{i-1} \cup \tau_i \quad \text{for} \quad i = 2, \ldots, N-1, \\ \Theta_N &:= \tau_{N-1}. \end{aligned}$$

Next we define

$$\begin{aligned} \varphi_1(t) &:= 1 - h_{t_0,t_1}(t), \\ \varphi_i(t) &:= \rho_{t_{i-2},t_{i-1},t_i}(t) \quad \text{for} \quad i = 2, \ldots, N-1, \\ \varphi_N(t) &:= h_{t_{N-2},t_{N-1}}(t). \end{aligned}$$

Then $\{\varphi_i\}$ is a smooth partition of unity subordinate to the cover $\{\Theta_i\}$. Figure 3.1 shows an example of such a set of functions.

We want a more detailed characterization of this partition of unity in the sense of Definition 3.3.1 in order to get error estimates for the PUM. Therefore we assume that the partition is locally quasiuniform:

$$1 \le \frac{|\Theta_i|}{\min\{|\tau_{i-1}|, |\tau_i|\}} \le c_{\max} \quad \text{for } i = 2, \ldots, N-1$$

with a moderate constant $c_{\max}$. By taking into account

$$\|h'_{a,b}\|_{L^\infty(\mathbb{R})} = \left|h'_{a,b}\left(\frac{a+b}{2}\right)\right| = \frac{4\pi^{-1/2}}{b-a}$$

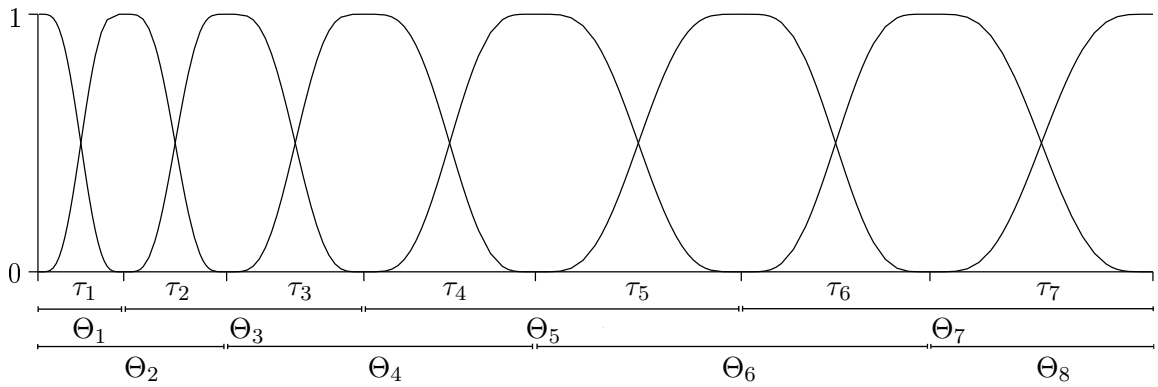

Figure 3.1: *Partition of unity $\{\varphi_i\}$ subordinate to the cover $\{\Theta_i\}$ for $N = 4$.*

we get

$$\begin{aligned}
\|\varphi_1'\|_{L^\infty([0,T])} &= \frac{4\pi^{-1/2}}{|\Theta_1|}, \\
\|\varphi_i'\|_{L^\infty([0,T])} &= \frac{4\pi^{-1/2}}{\min\{|\tau_{i-1}|, |\tau_i|\}} \leq \frac{4\pi^{-1/2}\, c_{\max}}{|\Theta_i|} \quad \text{for} \quad i = 2, \ldots, N-1, \\
\|\varphi_N'\|_{L^\infty([0,T])} &= \frac{4\pi^{-1/2}}{|\Theta_N|}.
\end{aligned}$$

Since $\|\varphi_i\|_{L^\infty([0,T])} = 1$ for $i = 1, \ldots, N$ we get that $\{\varphi_i\}$ is a $(2, 1, 4\pi^{-1/2} c_{\max})$ partition of unity of infinite degree subordinate to the cover $\{\Theta_i\}$.

With this construction of a smooth and compactly supported partition of unity we will define the global finite element space according to Definition 3.3.2. By taking into account that the exact solution of (3.2.1) and its derivative vanish at $t = 0$ we define, for given polynomial degree $p \in \mathbb{N}$, the spaces

$$\begin{aligned}
S_1 &:= t^2 \mathbb{P}_{p-2} \quad \text{on } \Theta_1, \\
S_i &:= \mathbb{P}_p \quad \text{on } \Theta_i, \;\; i = 2, \ldots, N,
\end{aligned}$$

where $\mathbb{P}_p$ denotes the space of polynomials of degree p and, formally, we set $\mathbb{P}_{-2} := \mathbb{P}_{-1} := \mathbb{P}_0$.

Remark 3.3.4. *The definition of the spaces S_i could be generalized by choosing local polynomial degrees p_i depending on the local patches Θ_i in the spirit of adaptive hp methods. We do not elaborate on this aspect here.*

The global PUM space S contains linear combinations of products of polynomials and functions of the partition of unity $\{\varphi_i\}$. To derive error estimates for the PUM we remark that the spaces S_i meet the following approximation property: Let $u \in H^k(\Theta), k \geq 1$. Then, for each patch Θ_i, $1 \leq i \leq N$, there exists $u_{S_i} \in S_i$ such that

$$\begin{aligned}
\|u - u_{S_i}\|_{L^2(\Theta_i)} &\leq C_1 |\Theta_i|^{\min(k-1,p)+1} \|u\|_{H^k(\Theta_i)}, \\
\|u' - u_{S_i}'\|_{L^2(\Theta_i)} &\leq C_2 |\Theta_i|^{\min(k-1,p)} \|u\|_{H^k(\Theta_i)},
\end{aligned}$$

where C_1 and C_2 depend on k, p and $c_{\max}$. From [2, Theorem 1] we conclude that the global approximation

$$u_S = \sum_{i=1}^{N} \varphi_i u_{S_i} \in S \subset H^1(\Theta)$$

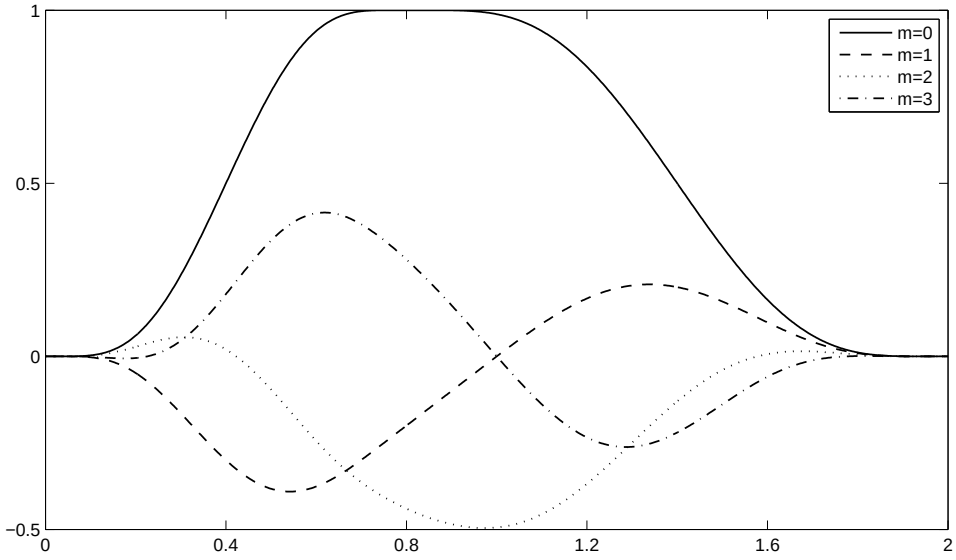

Figure 3.2: *Basis function of S for $t_0 = 0$,$t_1 = 0.8$ and $t_2 = 2$*

satisfies the error bounds

$$\begin{aligned} \|u - u_S\|_{L^2(\Theta)} &\leq 2C_1 \tilde{\Theta}^{\min(k-1,p)+1} \|u\|_{H^k(\Theta)}, \\ \|u' - u_S'\|_{L^2(\Theta)} &\leq 2C_2 \sqrt{8\pi^{-1/2} c_{\max} + 2}\; \tilde{\Theta}^{\min(k-1,p)} \|u\|_{H^k(\Theta)}. \end{aligned} \tag{3.3.6}$$

where $\tilde{\Theta} := \max_{1 \leq i \leq N} |\Theta_i|$. For the implementation of this method we need a basis of the PUM space. It can be determined by multiplying the basis elements of the local approximation spaces with the appropriate partition of unity function. An $L^2(-1,1)$-orthogonal basis of $\mathbb{P}_p$ is given by the Legendre polynomials $\{P_m\}_{m=0}^p$. An appropriate scaling results in a basis of the PUM space S:

$$\begin{aligned} b_{1,m}(t) &:= \varphi_1(t)\, t^2 P_{m-2}\left(\frac{2}{t_1}t - 1\right) && m = 2, \ldots, \max(2,p), \\ b_{i,m}(t) &:= \varphi_i(t) P_m\left(2\frac{t - t_{i-2}}{t_i - t_{i-2}} - 1\right) && m = 0, \ldots, p,\ i = 2, \ldots, N-1, \\ b_{N,m}(t) &:= \varphi_N(t) P_m\left(2\frac{t - t_{N-2}}{t_{N-1} - t_{N-2}} - 1\right) && m = 0, \ldots, p. \end{aligned} \tag{3.3.7}$$

Figure 3.2 shows the shape of these basis functions for some different values of m on a nonuniform time grid. For $m = 0$ the basis functions are simply the shape functions of the partition of unity. For higher m this function is multiplied by the appropriate Legendre polynomial.

3.4 Application to a problem on the sphere

In this section we apply a Galerkin method using our new basis functions in time to the integral equation (3.2.3) in the case where the boundary Γ is the unit sphere $\mathbb{S}^2$. Furthermore

we assume that the right-hand side g is causal i.e. $g(x,t) = 0$ for $t \leq 0$ and that at least the first time derivative of g vanishes at $t = 0$. Moreover, g is supposed to be of the form

$$g(x,t) = g(t)Y_n^m,$$

where Y_n^m denotes a spherical harmonic of degree n and order m. This setting was already used in [6] and allows to reduce the boundary integral equation (3.2.3) to a univariate problem in time. To see this note that an equivalent formulation of the retarded single layer potential (3.2.2) is given by

$$S\phi(x,t) = \int_0^t \int_\Gamma k(x-y, t-\tau)\phi(y,\tau)d\Gamma_y d\tau, \quad (x,t) \in \Omega \times [0,T]\,, \tag{3.4.1}$$

where $k(z,t)$ is the fundamental solution of the wave equation,

$$k(z,t) = \frac{\delta(t - \|z\|)}{4\pi\|z\|},$$

$\delta(t)$ being the Dirac delta distribution. Furthermore we introduce the single layer potential for the Helmholtz operator $\Delta U - s^2 U = 0$ which is given by

$$(V(s)\varphi)(x) := \int_\Gamma K(s, x-y)\varphi(y,\tau)d\Gamma_y,$$

where

$$K(s,z) := \frac{\mathrm{e}^{-s\|z\|}}{4\pi\|z\|}$$

is the fundamental solution of the Helmholtz equation in three dimensions. An important property of the single layer potential $V(s)$ is that

$$V(s)Y_n^m = \lambda_n(s)Y_n^m, \tag{3.4.2}$$

i.e., the spherical harmonics Y_n^m are eigenfunctions of this operator with eigenvalues $\lambda_n(s)$. The latter can be expressed in terms of modified Bessel functions I_κ and K_κ (see [1])

$$\lambda_n(s) = I_{n+\frac{1}{2}}(s)K_{n+\frac{1}{2}}(s). \tag{3.4.3}$$

Next, we will transform equation (3.2.3) into frequency domain using Laplace transformations. Property (3.4.2) and a back transformation then leads to a univariate problem in time. Recall the definition of the Laplace transform

$$\hat{\phi}(s) := (\mathcal{L}\phi)(s) = \int_0^\infty \phi(t)\,\mathrm{e}^{-st}\,dt$$

with inverse

$$(\mathcal{L}^{-1}\hat{\phi})(s) = \frac{1}{2\pi i}\int_{\sigma-i\infty}^{\sigma+i\infty} \hat{\phi}(s)\,\mathrm{e}^{st}\,ds.$$

Note that the fundamental solution of the Helmholtz equation is the Laplace transform of the fundamental solution of the wave equation. Using the representation (3.4.1) for S and

expressing k in terms of its Laplace transform leads to the integral equation

$$\begin{aligned} g(t)Y_n^m &= \int_0^t \int_\Gamma k(t-\tau, \|x-y\|)\phi(y,\tau)d\Gamma_y d\tau \\ &= \frac{1}{2\pi i}\int_{\sigma-i\infty}^{\sigma+i\infty} \int_0^t \mathrm{e}^{s\tau} \int_\Gamma K(s, \|x-y\|)\phi(y,t-\tau)d\Gamma_y d\tau ds \\ &= \frac{1}{2\pi i}\int_{\sigma-i\infty}^{\sigma+i\infty} \int_0^t \mathrm{e}^{s\tau}(V(s)\phi(\cdot,t-\tau))(x)d\tau ds. \end{aligned}$$

Inserting the ansatz $\phi(x,t) = \phi(t)Y_n^m$ and using (3.4.2) leads to the one dimensional problem: Find $\phi(t)$ such that

$$\int_0^t \mathcal{L}^{-1}(\lambda_n)(\tau)\phi(t-\tau)d\tau = g(t), \quad t \in [0,T]. \tag{3.4.4}$$

Note that $\phi(t)Y_n^m$ where $\phi(t)$ satisfies (3.4.4) is a solution of the full problem (3.2.1) in the case where $\Gamma = \mathbb{S}^2$ and $g(x,t) = g(t)Y_n^m$. In order to analyse our new approach for the temporal discretization we choose (3.4.4) as our model problem.

Example. *Explicit representations of the exact solutions of* (3.4.4) *were computed in [23, 27].*

(a) For $n = 0$ the solution is given by

$$\phi(t) = 2\sum_{k=0}^{\lfloor t/2 \rfloor} g'(t-2k). \tag{3.4.5}$$

(b) For $n = 1$ we have

$$\begin{aligned} \phi(t) &= 2\sum_{k=0}^{\lfloor t/2 \rfloor}(-1)^k g'(t-2k) + 2\int_0^t \sinh(\tau)g'(t-\tau)d\tau \\ &\quad - 2\sum_{k=1}^{\lfloor t/2 \rfloor}\sum_{j=1}^{k}\int_{2k}^t (c_{k,j}^{(2)} + c_{k,j}^{(3)}\tau - c_{k,j}^{(3)}2k)(\tau-2k)^{j-1}\,\mathrm{e}^{\tau-2k}\,g'(t-\tau)d\tau. \end{aligned} \tag{3.4.6}$$

where

$$\begin{aligned} c_{k,j}^{(2)} &= (-1)^{k+1}\sum_{m=0}^{j-1}\frac{(1-(-1)^{j-m})k!}{(j-1)!m!(k-j)!(j-m)!} \quad \textit{and} \\ c_{k,j}^{(3)} &= (-1)^{k+1}\frac{2^{j-1}(k-1)!}{(j-1)!j!(k-j)!}. \end{aligned}$$

These formulas will serve as reference solutions for our numerical experiments.

In order to apply a Galerkin method to (3.4.4) we need a suitable variational formulation. If we choose V_{Galerkin} in (3.3.2) by $V_{\text{Galerkin}} = Y_n^m S$, the space-time Galerkin discretization decouples and reduces to the purely temporal problem:

$$\text{Find } \phi_S \in S: \quad \int_0^T\int_0^t \mathcal{L}^{-1}(\lambda_n)(\tau)\dot{\phi}_S(t-\tau)\zeta(t)d\tau dt = \int_0^T \dot{g}(t)\zeta(t)dt \qquad \forall \zeta \in S. \tag{3.4.7}$$

For the numerical solution of this equation we employ the representation with respect to the PUM basis (cf. (3.3.7)) and define the index set

$$\mathcal{P}_i := \begin{cases} \{2,3,\dots \max\{2,p\}\} & i=1, \\ \{0,1,\dots,p\} & 2 \le i \le N. \end{cases}$$

Then, inserting the ansatz

$$\phi_S(t) = \sum_{i=1}^{N} \sum_{m\in\mathcal{P}_i} \alpha_{i,m} b_{i,m}(t)$$

leads to the discrete problem: Find $\alpha_{i,m}$ such that

$$\sum_{i=1}^{N} \sum_{m\in\mathcal{P}_i} \alpha_{i,m} \int_0^T \int_0^t \mathcal{L}^{-1}(\lambda_n)(t-\tau)\dot{b}_{i,m}(\tau) b_{j,k}(t) d\tau dt = \int_0^T \dot{g}(t) b_{j,k}(t) dt \tag{3.4.8}$$

for $j = 1,2,\dots,N$ and $k \in \mathcal{P}_j$. In order to find the solution of (3.4.8) we have to compute $\mathcal{L}^{-1}(\lambda_n)(t)$. After some algebraic manipulations (cf. [23]) we obtain from (3.4.3)

$$\lambda_n(s) = \sum_{l=0}^{2n} \frac{c_{n,l}^{\mathrm{I}}}{s^{l+1}} + \mathrm{e}^{-2s} \sum_{l=0}^{2n} \frac{c_{n,l}^{\mathrm{II}}}{s^{l+1}},$$

where

$$c_{n,l}^{\mathrm{I}} := \begin{cases} \sum_{j=0}^{l} \frac{1}{2}(-1)^{l-j}(n,l-j)(n,j), & \text{for } l \le n, \\ \sum_{j=l-n}^{n} \frac{1}{2}(-1)^{l-j}(n,l-j)(n,j), & \text{for } n < l \le 2n, \end{cases}$$

and

$$c_{n,l}^{\mathrm{II}} := \begin{cases} \sum_{j=0}^{l} \frac{1}{2}(-1)^{n+1}(n,l-j)(n,j), & \text{for } l \le n, \\ \sum_{j=l-n}^{n} \frac{1}{2}(-1)^{n+1}(n,l-j)(n,j), & \text{for } n < l \le 2n \end{cases}$$

with $(n,k) := \frac{(n+k)!}{2^k k!(n-k)!}$. The inverse Laplace transform of $\lambda_n(s)$ is therefore given by

$$\mathcal{L}^{-1}(\lambda_n)(t) = \sum_{l=0}^{2n} \frac{c_{n,l}^{\mathrm{I}}}{l!} t^l H(t) + \sum_{l=0}^{2n} \frac{c_{n,l}^{\mathrm{II}}}{l!} (t-2)^l H(t-2),$$

where

$$H(t) = \begin{cases} 0 & t \le 0, \\ 1 & t > 0 \end{cases}$$

denotes the Heaviside step function. This shows that the discrete problem (3.4.8) is equivalent to: Find $\alpha_{i,m}$ such that

$$\sum_{i=1}^{N} \sum_{m\in\mathcal{P}_i} \alpha_{i,m} \left[\int_0^T \int_0^t q_n^{\mathrm{I}}(t-\tau) b_{i,m}(\tau) \dot{b}_{j,k}(t) d\tau dt \right.$$
$$\left. + \int_0^T \int_0^t q_n^{\mathrm{II}}(t-\tau-2) H(t-\tau-2) b_{i,m}(\tau) \dot{b}_{j,k}(t) d\tau dt \right] = \int_0^T g(t) \dot{b}_{j,k}(t) dt \tag{3.4.9}$$

for $j = 1,\dots,N$, $k \in \mathcal{P}_j$, where

$$q_n^{\mathrm{I}}(t) := \sum_{l=0}^{2n} \frac{c_{n,l}^{\mathrm{I}}}{l!} t^l \quad \text{and} \quad q_n^{\mathrm{II}}(t) := \sum_{l=0}^{2n} \frac{c_{n,l}^{\mathrm{II}}}{l!} t^l.$$

We now turn our attention to the numerical computation of the double integral

$$\int_0^T \int_0^t q_n^{\mathrm{I}}(t-\tau) b_{i,m}(\tau) \dot{b}_{j,k}(t) d\tau dt \tag{3.4.10}$$

arising in (3.4.9). Therefore let

$$\operatorname{supp} b_{i,m} = \Theta_i = [m_i, M_i] \quad \text{and}$$
$$\operatorname{supp} b_{j,k} = \Theta_j = [m_j, M_j].$$

We write "..." short for "$q_n^{\mathrm{I}}(t-\tau) b_{i,m}(\tau) \dot{b}_{j,k}(t) d\tau dt$" and distinguish between the following six cases (see Figure 3.3):

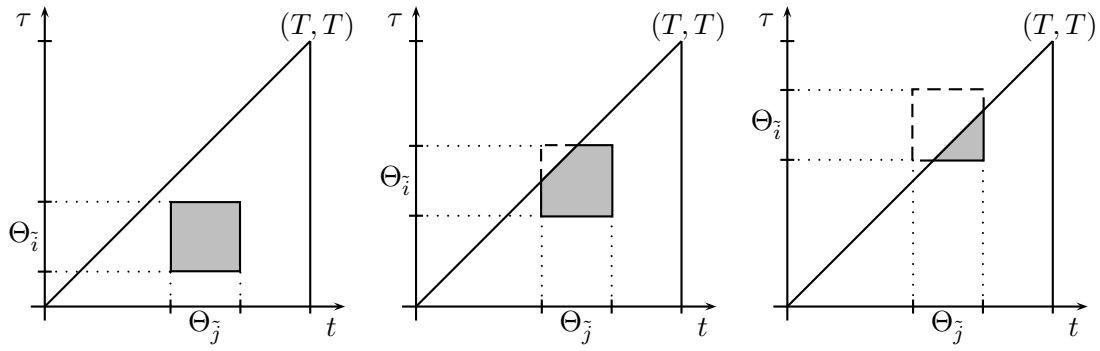

(a) Domain of integration case (i)

(b) Domain of integration case (ii)

(c) Domain of integration case (iii)

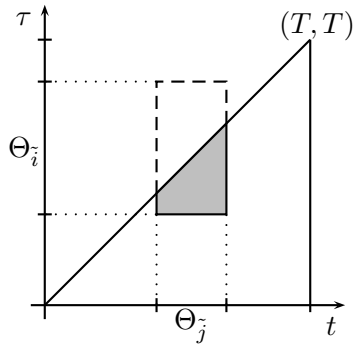

(d) Domain of integration case (iv)

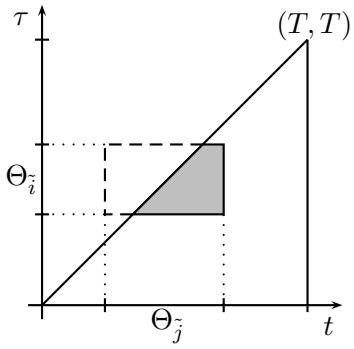

(e) Domain of integration case (v)

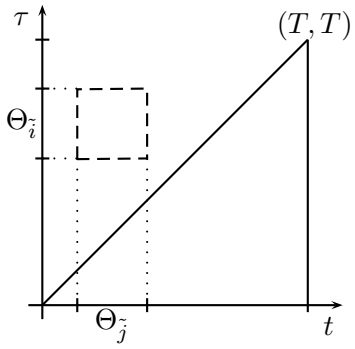

(f) Domain of integration case (vi)

Figure 3.3: *Different domains of integration for integral (3.4.10)*

(i) $m_i \le M_i \le m_j \le M_j$. Then,

$$\int_0^T \int_0^t \ldots = \int_{\Theta_j} \int_{\Theta_i} \ldots$$

(ii) $m_i \le m_j \le M_i \le M_j$. Then,

$$\int_0^T \int_0^t \ldots = \int_{m_j}^{M_i} \int_{m_i}^{t} \ldots + \int_{M_i}^{M_j} \int_{\Theta_i} \ldots$$

(iii) $m_j \leq m_i \leq M_j \leq M_i$. Then,

$$\int_0^T \int_0^t \ldots = \int_{m_i}^{M_j} \int_{m_i}^t \ldots$$

(iv) $m_i \leq m_j \leq M_j \leq M_i$. Then,

$$\int_0^T \int_0^t \ldots = \int_{\Theta_j} \int_{m_i}^t \ldots$$

(v) $m_j \leq m_i \leq M_i \leq M_j$. Then,

$$\int_0^T \int_0^t \ldots = \int_{\Theta_i} \int_{m_i}^t \ldots + \int_{M_i}^{M_j} \int_{\Theta_i} \ldots$$

(vi) $m_j \leq M_j \leq m_i \leq M_i$. Then,

$$\int_0^T \int_0^t \ldots = 0.$$

The computation of the second double integral

$$\int_0^T \int_0^t q_n^{\mathrm{II}}(t-\tau-2)H(t-\tau-2)b_{i,m}(\tau)\dot{b}_{j,k}(t)d\tau dt$$

in (3.4.9) is similar. Note that this integral vanishes for $T \leq 2$. For $T > 2$ we have to distinguish between six cases as for the integrals in (3.4.10). We do not detail this here.

Remark 3.4.1. *The resulting integration domains in the cases (i)-(vi) are either rectangles or triangles. Because simplex coordinates transform triangles to squares, we can restrict to rectangular integration domains and apply properly scaled n-point tensor Gauss-Legendre quadrature rules for the numerical approximation of the arising integrals.*

3.5 Quadrature Error Analysis

In this section we analyse the error that arises from approximating integrals of the form

$$\mathcal{I}\rho_{a,b,c} := \int_a^c \rho_{a,b,c}(t)\, dt \tag{3.5.1}$$

by a n-point Gauss-Legendre quadrature rule in the interval $[a,c]$, denoted by $Q_n\rho_{a,b,c}$. For given $a < b < c \in \mathbb{R}$, the functions $\rho_{a,b,c}(t)$ are the C^∞-bump functions defined in Section 3.3 with $\operatorname{supp}\rho_{a,b,c} = [a,c]$. It is well known that Gauss-Legendre quadrature converges exponentially for integrands that are analytic in a sufficiently large (complex) neighborhood of the integration domain. Since the functions $\rho_{a,b,c}(t)$ are smooth but not analytic in the points a, b and c, these classical estimates for the quadrature error

$$\mathcal{E}_n\rho_{a,b,c} := |\mathcal{I}\rho_{a,b,c} - Q_n\rho_{a,b,c}|$$

do not hold. We define the linear scaling functions

$$\zeta_{r,s} : [r,s] \to [-1,1],\ t \mapsto 2\frac{t-r}{s-r} - 1 \quad \text{and its inverse}$$

$$\xi_{r,s} : [-1,1] \to [r,s],\ t \mapsto \frac{1}{2}(s-r)(t+1) + r.$$

In order to find bounds for $\mathcal{E}_n\rho_{a,b,c}$ we need the following Lemma.

Lemma 3.5.1. *Let $n \in \mathbb{N}$ and $1 \le k \le 2n$. Then we have for $g \in C^{k+1}([a,b])$,*

$$|\mathcal{I}g - Q_n g| \le \frac{32}{15\pi}\left(\frac{b-a}{2}\right)^{k+1} \frac{1}{k(2n+1-k)^k} \int_a^b \frac{|g^{(k+1)}(t)|}{\sqrt{1-\zeta_{a,b}(t)^2}} dt.$$

Proof. For the interval $[a,b] = [-1,1]$, Theorem 4.5 in [26] gives

$$|\mathcal{I}g - Q_n g| \le \frac{32}{15\pi} \frac{1}{k(2n+1-k)^k} \int_{-1}^1 \frac{|g^{(k+1)}(t)|}{\sqrt{1-t^2}} dt$$

for $k \in \{1,\dots,2n\}$. For general $[a,b]$, a linear change of variable leads to

$$|\mathcal{I}g - Q_n g| \le \frac{32}{15\pi}\left(\frac{b-a}{2}\right)^{k+2} \frac{1}{k(2n+1-k)^k} \int_{-1}^1 \frac{|g^{(k+1)}(\xi_{a,b}(t))|}{\sqrt{1-t^2}} dt.$$

The substitution $t = \zeta_{a,b}(t)$ leads to the desired result. □

In our case Lemma 3.5.1 reads

$$\mathcal{E}_n \rho_{a,b,c} \le \frac{32}{15\pi}\left(\frac{c-a}{2}\right)^{k+1} \frac{1}{k(2n+1-k)^k} \int_a^c \frac{\left|\rho_{a,b,c}^{(k+1)}(t)\right|}{\sqrt{1-\zeta_{a,c}(t)^2}} dt.$$

The definition of $\rho_{a,b,c}(t)$ leads to

$$\mathcal{E}_n \rho_{a,b,c} \le \frac{32}{15\pi}\left(\frac{c-a}{2}\right)^{k+1} \frac{1}{k(2n+1-k)^k} \left(\int_a^b \frac{\left|h_{a,b}^{(k+1)}(t)\right|}{\sqrt{1-\zeta_{a,c}(t)^2}} dt + \int_b^c \frac{\left|h_{b,c}^{(k+1)}(t)\right|}{\sqrt{1-\zeta_{a,c}(t)^2}} dt \right). \tag{3.5.2}$$

The formula above shows that we have to estimate the derivatives of the cutoff functions $h_{a,b}$ and $h_{b,c}$.

Lemma 3.5.2. *The cutoff function $h_{a,b}$ satisfies the estimate*

$$\left|h_{a,b}^{(k+1)}(t)\right| \le \frac{C_2}{b-a}\left(\frac{2C_1}{b-a}\right)^k k! \left| \frac{\mathrm{e}^{-2\operatorname{arctanh}^2(\zeta_{a,b}(t))}}{(1-\zeta_{a,b}(t)^2)^{k+1}} \right| q^k(\zeta_{a,b}(t))$$

for $k \ge 1$ with $q(t) := \ln \frac{4}{1-t^2}$, $C_1 := 6\sqrt{2}\,\mathrm{e}$ and $C_2 = \frac{10\kappa}{\sqrt{\pi}} \frac{C_1 \ln(4)}{C_1 \ln(4) - 2}$ where $\kappa \approx 1.086435$.

Proof. Use Theorem 3.A.4 and the chain rule. □

Further estimation of the bound in Lemma 3.5.2 leads to:

Lemma 3.5.3. *Let $q(t), C_1$ and C_2 be as in Lemma 3.5.2. Then we have*

$$\left\|h_{a,b}^{(k+1)}\right\|_\infty \le \frac{C_2}{b-a}\left(\frac{2\lambda 4^{1/\lambda} C_1}{b-a}\right)^k k!\, \mathrm{e}^{\sigma_{(1+1/\lambda)k+1}}$$

for $k \ge 1$ and $\lambda > 0$, where

$$\sigma_\alpha := \frac{1}{4}\alpha^2 + \frac{1}{2} - \ln\left(\frac{1}{2}\alpha + \frac{1}{2}\sqrt{\alpha^2-4}\right)$$

for $\alpha \geq 2$.

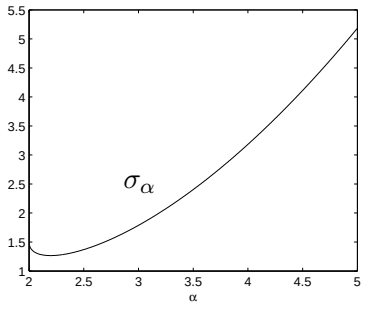

Proof. Since

$$q^k(t) = \left(\ln \frac{4}{1-t^2}\right)^k \leq \left(4^{1/\lambda}\lambda\right)^k \left(\frac{1}{1-t^2}\right)^{k/\lambda}$$

for $\lambda > 0$, the result follows from Lemma 3.5.2 and Lemma 3.A.5. □

Corollary 3.5.4. *The bump function* $\rho_{a,b,c}$ *satisfies the estimate*

$$\|\rho_{a,b,c}^{(k+1)}\|_\infty \leq \|h_{a,b}^{(k+1)}\|_\infty \quad \textit{in the case} \quad b-a \leq c-b,$$
$$\|\rho_{a,b,c}^{(k+1)}\|_\infty \leq \|h_{b,c}^{(k+1)}\|_\infty \quad \textit{in the case} \quad c-b \leq b-a.$$

In order to estimate $\mathcal{E}_n\rho_{a,b,c}$, we assume that $b-a \leq c-b$, the other case being treated analogously. Furthermore we assume $c-a \leq c_{\max}(b-a)$, which corresponds to the local quasiuniformity of a given time mesh. With

$$\frac{1}{\sqrt{1-\zeta_{a,c}(t)^2}} \leq \frac{c_{\max}}{\sqrt{1-\zeta_{a,b}(t)^2}}, \quad t \in (a,b),$$

Lemma 3.5.2, Lemma 3.A.5, and Lemma 3.A.6 we get

$$\begin{aligned}
\int_a^b \frac{\left|h_{a,b}^{(k+1)}(t)\right|}{\sqrt{1-\zeta_{a,c}(t)^2}}dt &\leq \frac{C_2}{b-a}\left(\frac{2C_1}{b-a}\right)^k k! \int_a^b \frac{\left|\mathrm{e}^{-2\operatorname{arctanh}^2(\zeta_{a,b}(t))}\right| q^k(\zeta_{a,b}(t))}{\left|(1-\zeta_{a,b}(t)^2)^{k+1}\right| \sqrt{1-\zeta_{a,c}(t)^2}}dt \\
&\leq \frac{C_2 c_{\max}}{b-a}\left(\frac{2C_1}{b-a}\right)^k k! \int_a^b \frac{\left|\mathrm{e}^{-2\operatorname{arctanh}^2(\zeta_{a,b}(t))}\right| q^k(\zeta_{a,b}(t))}{\left|(1-\zeta_{a,b}(t)^2)^{k+3/2}\right|}dt \\
&\leq \frac{C_2 c_{\max}}{b-a}\left(\frac{2C_1}{b-a}\right)^k k!\, \mathrm{e}^{\sigma_{k+3/2}} \int_a^b q^k(\zeta_{a,b}(t))dt \\
&\leq \frac{C_2 c_{\max}}{2}\left(\frac{2C_1}{b-a}\right)^k k!\, \mathrm{e}^{\sigma_{k+3/2}} \int_{-1}^1 q^k(t)dt \\
&\leq 8C_2 c_{\max}\left(\frac{2C_1}{b-a}\right)^k (k!)^2\, \mathrm{e}^{\sigma_{k+3/2}},
\end{aligned}$$

where $\sigma_{k+3/2}$ is as in Lemma 3.5.3. Similar arguments show that also

$$\int_b^c \frac{\left|h_{b,c}^{(k+1)}(t)\right|}{\sqrt{1-\zeta_{a,c}(t)^2}}dt \leq 8C_2 c_{\max}\left(\frac{2C_1}{b-a}\right)^k (k!)^2\, \mathrm{e}^{\sigma_{k+3/2}}$$

holds. With (3.5.2) the quadrature error can be estimated by

$$\mathcal{E}_n\rho_{a,b,c} \leq \frac{256\, C_2\, c_{\max}\,(c-a)}{15\pi} \frac{1}{k(2n+1-k)^k} \left(C_1 c_{\max}\right)^k (k!)^2\, \mathrm{e}^{\sigma_{k+3/2}}$$

for $k \in \{1, \dots, 2n\}$. Finally, Stirling's estimate $k! \leq 1.1\sqrt{2\pi k}\, k^k \, \mathrm{e}^{-k}$ yields

$$\mathcal{E}_n \rho_{a,b,c} \leq 41.5\, C_2\, c_{\max}\, (c-a) \left(\frac{C_1 c_{\max} k^2}{(2n+1-k)\, \mathrm{e}^2} \right)^k \mathrm{e}^{\sigma_{k+3/2}}$$

for $k \in \{1, \dots, 2n\}$. It remains to choose k such that the right-hand side in the above inequality becomes small. We define

$$E_{c_{\max}}(n,k) := \left(\frac{C_1 c_{\max} k^2}{(2n+1-k)\, \mathrm{e}^2} \right)^k \mathrm{e}^{\sigma_{k+3/2}}$$

for $k \in \{1, \dots, 2n\}$. The next Lemma shows that $E_{c_{\max}}(n,k)$ decays superalgebraically for an appropriate choice of k.

Lemma 3.5.5. *Let $\gamma \in \left(0, \frac{3}{4}\right)$ and $a, b, c \in \mathbb{R}$ with $c - a \leq c_{\max}(b-a)$ be given. If $n \in \mathbb{N}_{\geq 3}$ satisfies the condition*

$$(\ln n)^2 n^{-3/4+\gamma} \leq \frac{2 - \mathrm{e}^{-2}}{C_1 c_{\max}\, \mathrm{e}^{-1/4}}, \tag{3.5.3}$$

the error bound

$$\mathcal{E}_n \rho_{a,b,c} \leq \hat{C} n^{-\gamma \ln(n)}$$

holds, with $\hat{C} := 41.5\, C_2\, c_{\max}\, (c-a) \left(2 - \mathrm{e}^{-2}\right) \mathrm{e}^{17/16}$.

Proof. Since

$$\sigma_{k+3/2} \leq \frac{1}{4} k^2 + \frac{3}{4} k + \frac{17}{16},$$

we have

$$E_{c_{\max}}(n,k) \leq \mathrm{e}^{17/16} \left(\tilde{C} \right)^k k^{2k} (2n+1-k)^{-k}\, \mathrm{e}^{k^2/4}$$

where $\tilde{C} := C_1 c_{\max}\, \mathrm{e}^{-5/4}$. We set $k = \lfloor \ln(n) \rfloor$ and get

$$\begin{aligned} E_{c_{\max}}(n, \lfloor \ln(n) \rfloor) &\leq \mathrm{e}^{17/16} \left(\tilde{C} \right)^{\lfloor \ln(n) \rfloor} \lfloor \ln(n) \rfloor^{2\lfloor \ln(n) \rfloor} (2n + 1 - \lfloor \ln(n) \rfloor)^{-\lfloor \ln(n) \rfloor}\, \mathrm{e}^{\lfloor \ln(n) \rfloor^2/4} \\ &\leq \mathrm{e}^{17/16} \left(\tilde{C} \right)^{\ln(n)} \ln(n)^{2\ln(n)} (2n + 1 - \ln(n))^{-\ln(n)+1}\, \mathrm{e}^{(\ln n)^2/4}. \end{aligned}$$

Simple calculus shows

$$1 - \ln(n) \geq -\mathrm{e}^{-2} n \quad \text{for } n \in \mathbb{N},$$

so that the error can be estimated by

$$E_{c_{\max}}(n, \lfloor \ln(n) \rfloor) \leq \left(2 - \mathrm{e}^{-2}\right) \mathrm{e}^{17/16} \left(\frac{\tilde{C}}{2 - \mathrm{e}^{-2}} \right)^{\ln(n)} (\ln n)^{2\ln(n)} n^{-\ln(n)+1}\, \mathrm{e}^{\ln(n)^2/4}.$$

Applying the logarithm on both sides yields

$$\begin{aligned} \ln\left(E_{c_{\max}}(n, \lfloor \ln(n) \rfloor)\right) &\leq \ln\left(\left(2 - \mathrm{e}^{-2}\right) \mathrm{e}^{17/16} \right) \\ &\quad + \ln(n) \left[\ln\left(\frac{\tilde{C}}{2 - \mathrm{e}^{-2}} \right) + 2\ln(\ln(n)) + 1 - \frac{3}{4} \ln(n) \right]. \end{aligned}$$

For given $\gamma \in \left(0, \frac{3}{4}\right)$, let n satisfy condition (3.5.3). Then we get

$$\ln\left(E_{c_{\max}}(n, \lfloor \ln(n) \rfloor)\right) \leq \ln\left(\left(2 - \mathrm{e}^{-2}\right) \mathrm{e}^{17/16} \right) - \gamma (\ln n)^2,$$

which leads to the desired result. ∎

Remark 3.5.6. *The asymptotic behaviour of the error bound in Lemma 3.5.5 is sharp in the sense that the choice* $k = \lfloor (\ln n)^\delta \rfloor$ *with* $\delta > 1$ *leads to the divergence of* $E_{c_{\max}}(n,k)$ *if* n *tends to infinity.*

Although Lemma 3.5.5 suggests that the error of Gauss-Legendre quadrature applied to integrals of the form (3.5.1) decreases superalgebraically but not exponentially, we want to show numerically that $E_{c_{\max}}(n,k)$ decays faster for certain ranges of n. In order to demonstrate this, an appropriate choice of k is crucial. Lemma 3.5.5 shows that k has to be chosen very small compared to n due to the fast growth of the derivatives of $\rho_{a,b,c}$. To illustrate this, Table 3.1 shows the optimal k, denoted by k_{opt}, such that $E_{c_{\max}}(n,k)$ is minimal for given n and different $c_{\max}$.

$c_{\max} = 2.0$	n	2-680	681-5929	5930-33776	33777-157999	158000-659277
	k_{opt}	1	2	3	4	5
$c_{\max} = 2.2$	n	2-748	749-6522	6523-37153	37154-173799	173800-725205
	k_{opt}	1	2	3	4	5
$c_{\max} = 2.4$	n	2-816	817-7115	7116-40531	40532-189598	189599-791132
	k_{opt}	1	2	3	4	5

Table 3.1: *k_{opt} for different ranges of n and different $c_{\max}$.*

Based on these observations we choose k optimal for every n and want to determine $r, \delta \in \mathbb{R}_{\geq 0}$ such that the estimate

$$E_{c_{\max}}(n, k_{\text{opt}}) \leq r\, \mathrm{e}^{-n^\delta}$$

holds for a preferably large range $n_{\min} \leq n \leq n_{\max}$.

$c_{\max}$	δ	r	$n_{\min}$	$n_{\max}$	$E_{c_{\max}}(n_{\max}, k_{\text{opt}})$
2.0	0.25	18	11	846975	$\approx 1.2 \cdot 10^{-12}$
	0.26	18	12	92231	$\approx 5.9 \cdot 10^{-8}$
2.2	0.25	20	11	649170	$\approx 9.4 \cdot 10^{-12}$
	0.26	20	12	67353	$\approx 3.0 \cdot 10^{-7}$
2.4	0.25	22	11	545048	$\approx 3.5 \cdot 10^{-11}$
	0.26	22	12	33776	$\approx 6.4 \cdot 10^{-6}$

Table 3.2: *Results for different choices of $c_{\max}$, δ and r.*

Table 3.2 shows the results of numerical experiments. It can be observed that $\mathcal{E}_n \rho_{a,b,c} = \mathcal{O}\left(\mathrm{e}^{-n^{1/4}}\right)$ for a large range of n in the case $c_{\max} \in \{2.0, 2.2, 2.4\}$.
Figure 3.4 shows the decay of the error in the case of the bump function $\rho_{0,\frac{10}{11},2}$ which corresponds to $c_{\max} = 2.2$. It can be observed that $\mathcal{E}_n \rho_{0,\frac{10}{11},2}$, which represents the relative error since $\mathcal{I}\rho_{0,\frac{10}{11},2} = 1$, decays even faster than predicted by theory at least for those accuracies that are of interest in practical computations.
The influence of $c_{\max}$ is rather small in practice. Numerical tests show that the error behaviour is similar to the one in Figure 3.4 for different (moderate) $c_{\max}$.

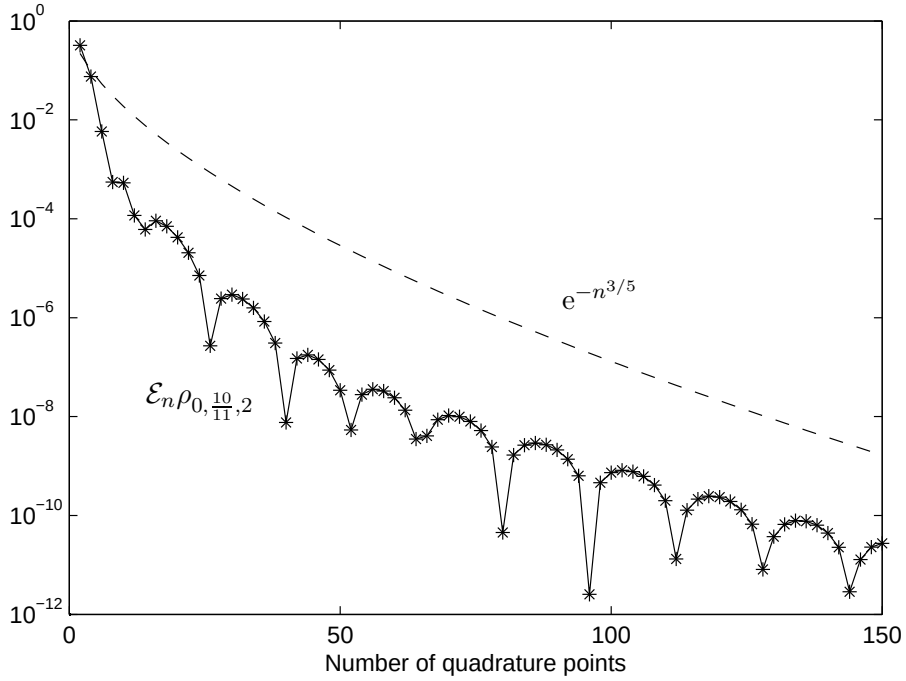

Figure 3.4: *Quadrature error for the case* $c_{\max} = 2.2$*, i.e., we consider the bump function* $\rho_{0,\frac{10}{11},2}$.

3.6 Numerical Experiments

In this section we present the results of numerical experiments. We solve the set of equations (3.4.9) in order to obtain a numerical solution of (3.4.4). The resulting error of the approximation, $\phi_S - \phi$, will be measured in the $L^2(0,T)$ norm. $L^2(0,T)$ is a suitable space for the solutions of (3.4.4) since it can be shown that if $\phi(t) \in L^2(0,T)$, then the corresponding solution of the full problem (3.2.3) satisfies $\phi(t)Y_n^m \in H^{-1/2,-1/2}(\Gamma \times [0,T])$. ϕ could also be considered in larger spaces than $L^2(0,T)$ but we expect analogous results of the numerical experiments in such spaces. We begin with the numerical tests and set

$$g(t) = \begin{cases} t^4 \,\mathrm{e}^{-2t} & t \geq 0, \\ 0 & t < 0. \end{cases}$$

In the following we check the sharpness of the convergence rates predicted by the theory in (3.3.6) for $n = 0$ and $n = 1$. We saw that the formulas for the exact solution of (3.4.4) involve derivatives of the right-hand side g (cf. (3.4.5) and (3.4.6)). Since $g \in H^4(\mathbb{R})$ we therefore have $\phi \in H^3(\mathbb{R})$. Thus we expect a convergence rate with respect to the L^2 error of h if we choose $p = 0$, i.e., if we approximate simply by the shape functions of the partition of unity. We expect a convergence rate of h^2 if we choose $p = 1$. These convergence rates could be confirmed by the numerical experiments (see Figure 3.5).

Next, we investigate the behaviour of the method for a right-hand side that is less smooth:

$$g(t) = \begin{cases} \sin^2(2t)\,\mathrm{e}^{-t} & t \geq 0, \\ 0 & t < 0. \end{cases}$$

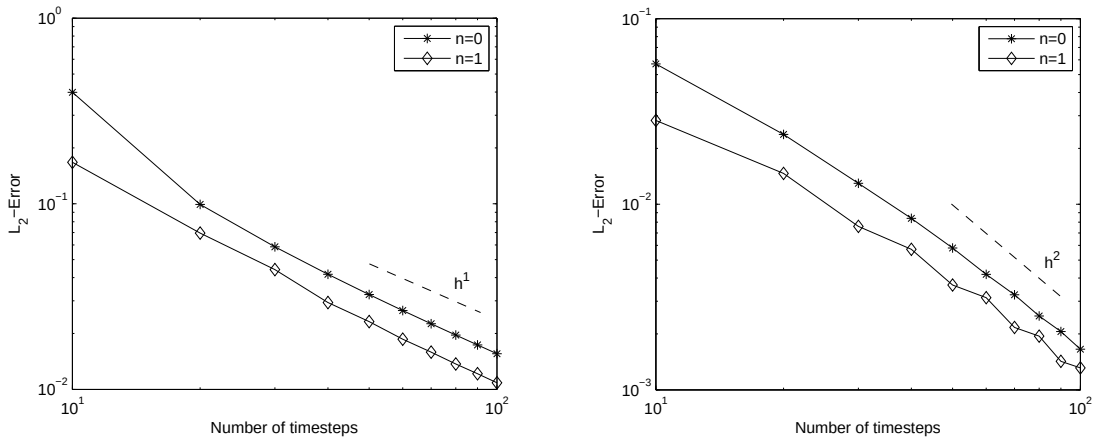

(a) local polynomial approximation spaces of degree $p = 0$

(b) local polynomial approximation spaces of degree $p = 1$

Figure 3.5: *Log-log scale plots of* $\|\phi_S - \phi\|_{L^2([0,T])}$ *for* $T = 6$, $g(t) = t^4 \mathrm{e}^{-2t}$ *and* n *as in (3.4.4).*

Note that $g \in H^2(\mathbb{R})$ and therefore $\phi \in H^1(\mathbb{R})$. Hence we expect a convergence rate of h in the case $p = 0$. Due to the lack of smoothness of the solution we do not expect that higher order PUM spaces lead to better convergence rates. Indeed Figure 3.6(b) indicates that in the case $p = 1$ a convergence rate of h^2 is not achieved.

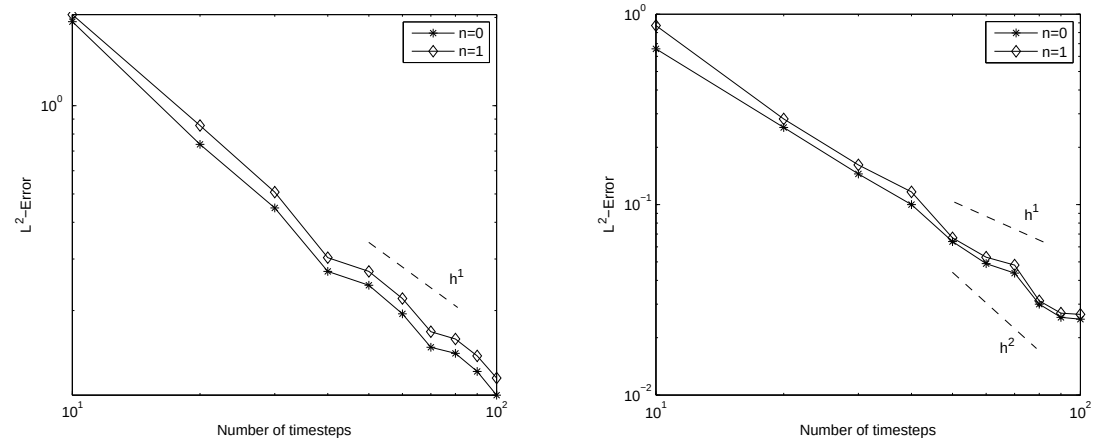

(a) local polynomial approximation spaces of degree $p = 0$

(b) local polynomial approximation spaces of degree $p = 1$

Figure 3.6: *Log-log scale plots of* $\|\phi_S - \phi\|_{L^2([0,T])}$ *for* $T = 6$, $g(t) = \sin^2(2t)\,\mathrm{e}^{-t}$ *and* n *as in (3.4.4).*

The PUM with smooth basis functions (3.3.7) allows variable time steps which can be adapted to the smoothness, e.g., of the right-hand side. In the following we illustrate the benefit of this feature by a numerical example. We choose the right-hand side by

$$g(t) = \begin{cases} -\sin(35t)t^3\,\mathrm{e}^{-12(4t-4)^2} & t \geq 0, \\ 0 & t < 0. \end{cases}$$

As we can see in Figure 3.7 this function has a sharp pulse in the interval $(1-\frac{1}{5}, 1+\frac{1}{5})$ and is almost zero otherwise. A similar behaviour can be observed for the corresponding solution ϕ for $n=0$. The 2-periodicity in (3.4.5) however implies that ϕ has peaks in small neighborhoods of all time points $t = 2l+1$, $l \in \mathbb{N}$ (cf. Figure 3.8). Therefore we will employ a time mesh which is graded towards the time points $t = 2l+1$ where the solution is highly oscillatory. We use a quadratic grading of the uniformly distributed mesh points towards the origin:

$$\pm\left(\frac{i}{m}\right)^2 \quad 0 \le i \le m.$$

We number these mesh points from left to right $-1 = \tilde{t}_0 < \ldots < \tilde{t}_{2m} = 1$. Translation of these points to the time intervals $[2l, 2l+2]$ leads to the time mesh in Figure 3.8.

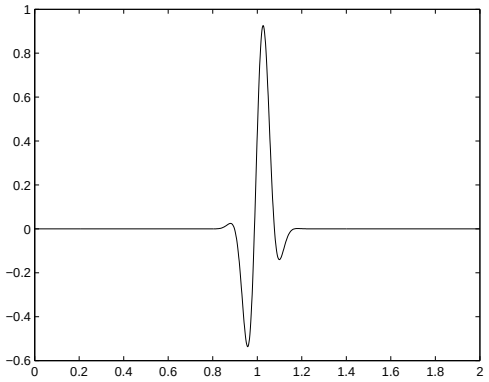

Figure 3.7: $g(t) = -\sin(35t)t^3\,\mathrm{e}^{-12(4t-4)^2}$.

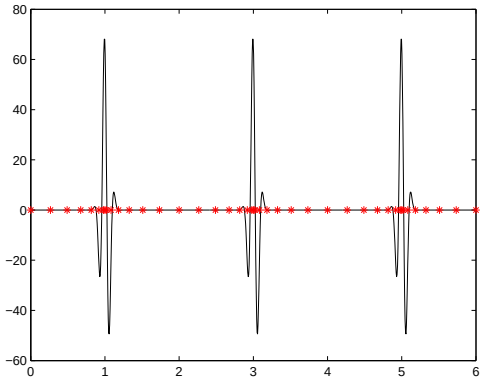

Figure 3.8: *Corresponding solution of (3.4.4) for $n = 0$ and a time grid with variable mesh-width.*

Figure 3.9 shows the error plots for this right-hand side for $n = 0$ and $p = 1, 2$. One can see that the error for the variable time mesh is considerably smaller than the error for the equidistant grid. Moreover the convergence starts earlier and the asymptotic convergence rate is already in the preasymptotic range. This shows that variable time stepping can improve the discretization substantially if knowledge about the solution is available. We expect similar benefits for the full problem.

Finally, we will show the performance of our method as a p-version for problems with smooth solutions, where we fix the number of timesteps and increase the polynomial degree of the local approximation spaces. Figure 3.10 shows two error plots for 5 and 10 timesteps, where we again set $g(t) = t^4\,\mathrm{e}^{-2t}$ for $t > 0$. Recall that $g \in H^4(\mathbb{R})$ and therefore $\phi \in H^3(\mathbb{R})$. Thus the following error estimate holds (cf. [2]):

$$\|\phi_S - \phi\|_{L^2([0,6])} \le Cp^{-2}\|\phi\|_{H^3([0,6])}.$$

3.7 Conclusion

We have introduced a new set of basis functions in time for the discretization of retarded boundary integral formulations of the wave equation. The obtained basis functions are

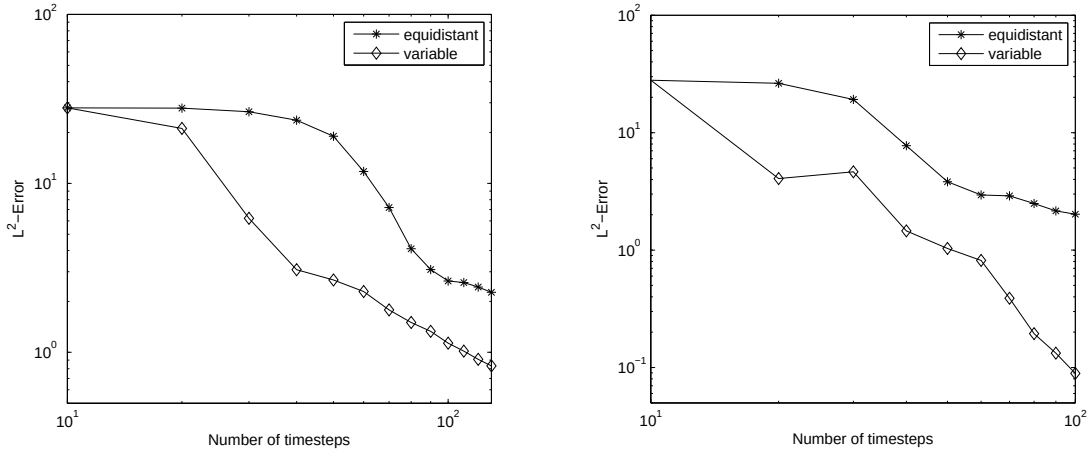

(a) local polynomial approximation spaces of degree $p = 1$

(b) local polynomial approximation spaces of degree $p = 2$

Figure 3.9: *Log-log scale plots of* $\|\phi_S - \phi\|_{L^2([0,T])}$ *for* $T = 6$, $g(t)$ *as in Figure 3.7 and* $n = 0$. *Comparison of equidistant and variable time meshes.*

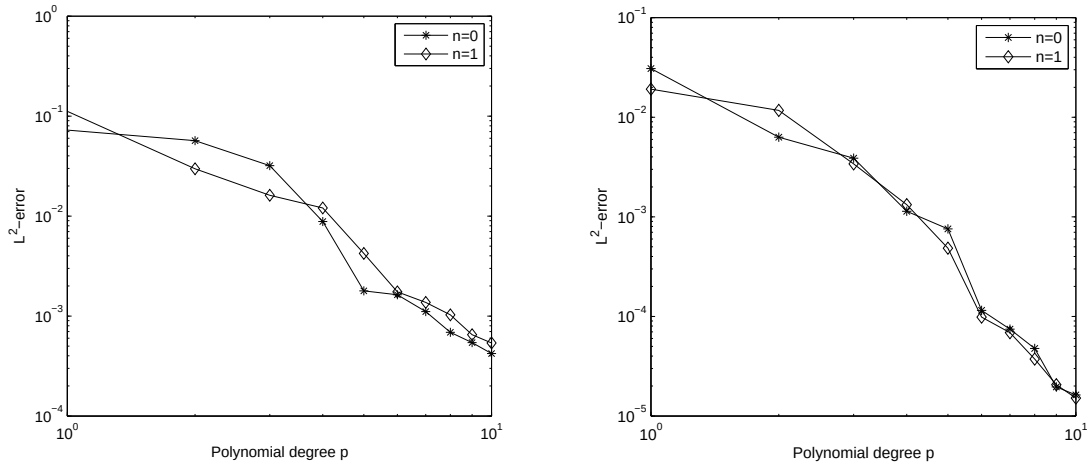

(a) Number of timesteps: 5

(b) Number of timesteps: 10

Figure 3.10: *Log-log scale plots of* $\|\phi_S - \phi\|_{L^2([0,T])}$ *for* $T = 6$, $g(t) = t^4 \, \mathrm{e}^{-2t}$.

smooth, compactly supported, allow variable order of approximation and can be easily defined on an arbitrary time grid. In order to test the approach we applied a Galerkin method to a special case of the wave equation on the sphere for which analytic solutions are available. These solutions were used as reference solutions for the numerical experiments. It could be shown that the use of variable stepsizes in time can improve the convergence of the Galerkin scheme considerably provided that information about the behaviour of the solution is known in advance.

In a forthcoming paper we will apply this approach to the full problem i.e. we will use a Galerkin method in space and time where we choose piecewise polynomial basis functions

in space and our smooth PUM space in time in order to discretize the problem. The global smoothness of the basis function in time will simplify the computation of the entries of the boundary element matrix considerably since the numerical handling of the complicated geometry of the discrete light cone with the surface panels becomes superfluous – the use of curved surface panels becomes straightforward. Furthermore the boundary element matrix will be sparse due to the compact support of the basis functions.

Acknowledgement. *Thanks are due to Christoph Schwab for fruitful discussions concerning the use of the PUM for the time discretization.*

3.A Technical estimates

In this section we want to estimate the n-th derivative of the function f as defined in (3.3.5). Therefore let

$$h(z) := \operatorname{erf}(z) \quad \text{and} \quad g(x) := \operatorname{arctanh} x = \frac{1}{2} \ln \frac{1+x}{1-x}$$

such that $f := h \circ 2g$. Note that [1, (7.1.19)] implies

$$h^{(n+1)}(z) = (-1)^n \frac{2}{\sqrt{\pi}} H_n(z) \, \mathrm{e}^{-z^2} \qquad n = 0, 1, 2, \ldots$$

where H_n are the Hermite polynomials. Hence,

$$\begin{aligned} f^{(n+1)}(x) &= \left(\frac{d}{dx}\right)^n \left(\frac{4}{\sqrt{\pi}\,(1-x^2)} \, \mathrm{e}^{-4g^2(x)}\right) \\ &= \frac{4}{\sqrt{\pi}} \sum_{\ell=0}^{n} \binom{n}{\ell} \left(\frac{1}{1-x^2}\right)^{(\ell)} \left(\mathrm{e}^{-4g^2(x)}\right)^{(n-\ell)}. \end{aligned} \tag{3.A.1}$$

Lemma 3.A.1 (Derivatives of g)**.** *It holds*

$$\left(\frac{1}{1-x^2}\right)^{(\ell)} = \frac{\ell! p_\ell(x)}{(1-x^2)^{\ell+1}} \qquad \forall x \in (-1,1),$$

where

$$p_\ell(x) := \frac{(x+1)^{\ell+1} - (x-1)^{\ell+1}}{2}.$$

Furthermore, we have

$$\left|g^{(\ell)}(x)\right| \leq \begin{cases} \frac{1}{2} \ln \dfrac{4}{1-x^2} & \ell = 0 \\ \dfrac{(\ell-1)! 2^{\ell-1}}{(1-x^2)^\ell} & \ell \in \mathbb{N}_{\geq 1} \end{cases} \qquad \forall x \in (-1,1), \tag{3.A.2}$$

as well as the more generous estimate

$$\left|g^{(\ell)}(x)\right| \leq q(x) \frac{\ell! 2^{\ell-1}}{(1-x^2)^\ell} \qquad \forall \ell \in \mathbb{N}_0 \tag{3.A.3}$$

with $q(x) = \ln \frac{4}{1-x^2}$.

Lemma 3.A.2 (Derivative of composite functions). *For $n \geq 1$ and $x \in (-1,1)$ we have*

$$\left(\mathrm{e}^{-4g^2(x)}\right)^{(n)} = \mathrm{e}^{-4g^2(x)} \sum_{k=1}^{n} A_{n,k}(x)\,(-1)^k\, H_k(2g(x)), \tag{3.A.4a}$$

where

$$A_{n,k}(x) = \frac{2^k}{k!} \sum_{\nu=1}^{k} (-1)^{k-\nu} \binom{k}{\nu} g^{k-\nu}(x)\,(g^{\nu})^{(n)}(x) \tag{3.A.4b}$$

and

$$(g^{\nu})^{(n)} = \sum_{\ell_{\nu-1}=0}^{n} \sum_{\ell_{\nu-2}=0}^{\ell_{\nu-1}} \cdots \sum_{\ell_1=0}^{\ell_2} \binom{n}{\ell_{\nu-1}} \binom{\ell_{\nu-1}}{\ell_{n-2}} \cdots \binom{\ell_2}{\ell_1} g^{(n-\ell_{\nu-1})} g^{(\ell_{\nu-1}-\ell_{\nu-2})} \cdots g^{(\ell_2-\ell_1)} g^{(\ell_1)}. \tag{3.A.5}$$

Proof. The representation (3.A.4) follows from [25, formulae (2), (7)], while (3.A.5) is proved by induction using Leibniz' product rule for differentiation. □

Lemma 3.A.3 (Estimate of derivatives of composite functions). *For $n \geq 1$ and $x \in (-1,1)$ we have*

$$\left|\left(\mathrm{e}^{-g^2(x)}\right)^{(n)}\right| \leq \frac{5}{2}\kappa n!\,\mathrm{e}^{-2g^2(x)} \left(\frac{C_1 q(x)}{1-x^2}\right)^n \tag{3.A.6}$$

with $\kappa \approx 1.086435$ and $C_1 = 6\sqrt{2}\,\mathrm{e}$.

Proof. From (3.A.3) and (3.A.5) we conclude for all $n \geq 1$, $\nu \geq 1$, and $x \in (-1,1)$

$$\begin{aligned}\left|(g^{\nu})^{(n)}(x)\right| &\leq n!2^{n-\nu} \frac{q^{\nu}(x)}{(1-x^2)^n} \sum_{\ell_{\nu-1}=0}^{n} \sum_{\ell_{\nu-2}=0}^{\ell_{\nu-1}} \cdots \sum_{\ell_1=0}^{\ell_2} 1 \\ &= n!2^{n-\nu} \frac{q^{\nu}(x)}{(1-x^2)^n} \binom{n+\nu-1}{\nu-1}.\end{aligned} \tag{3.A.7}$$

Thus, from (3.A.4b) we get that

$$\begin{aligned}|A_{n,k}(x)| &\leq \frac{2^k n!}{k!} \frac{q^k(x)}{(1-x^2)^n} \sum_{\nu=1}^{k} \binom{k}{\nu} 2^{n-\nu} \binom{n+\nu-1}{\nu-1} \\ &\leq \frac{2^n n!}{k!} \frac{q^k(x)}{(1-x^2)^n} \left(\frac{n+k}{k}\right)^k \sum_{\nu=1}^{k} \binom{k}{\nu} 2^{k-\nu} \\ &\leq \frac{2^n n!}{k!} \frac{1}{(1-x^2)^n} \left(\frac{3(n+k)\,q(x)}{k}\right)^k.\end{aligned} \tag{3.A.8}$$

From [1, (22.14.17)] we obtain

$$H_k(2g(x)) \leq \mathrm{e}^{2g^2(x)}\,\kappa 2^{k/2}\sqrt{k!}.$$

The combination of (3.A.4), (3.A.5), (3.A.7) and (3.A.8) results in the estimate for the n-th derivative of $\mathrm{e}^{-4g^2(x)}$:

$$\begin{aligned}\left|\left(\mathrm{e}^{-4g^2(x)}\right)^{(n)}\right| &\le \kappa 2^n n! \frac{\mathrm{e}^{-2g^2(x)}}{(1-x^2)^n}\sum_{k=1}^{n}\frac{1}{\sqrt{k!}}\left(\frac{3\sqrt{2}\,(n+k)\,q\,(x)}{k}\right)^k \\ &\le \kappa n!\,\mathrm{e}^{-2g^2(x)}\left(\frac{6\sqrt{2}q\,(x)}{1-x^2}\right)^n\sum_{k=1}^{n}\frac{1}{\sqrt{k!}}\left(\frac{n+k}{k}\right)^k \\ &\le \kappa n!\,\mathrm{e}^{-2g^2(x)}\left(\frac{6\sqrt{2}\,\mathrm{e}\,q\,(x)}{1-x^2}\right)^n\sum_{k=1}^{n}\frac{1}{\sqrt{k!}} \\ &\le \frac{5}{2}\kappa n!\,\mathrm{e}^{-2g^2(x)}\left(\frac{6\sqrt{2}\,\mathrm{e}\,q\,(x)}{1-x^2}\right)^n. \end{aligned}$$

□

Theorem 3.A.4 (Estimate of n-th derivative of f)**.** *We have*

$$|f^{(n+1)}\,(x)\,| \le C_2 C_1^n n! \frac{q(x)^n}{(1-x^2)^{n+1}}\,\mathrm{e}^{-2g^2(x)}$$

with $C_2 = \frac{10\kappa}{\sqrt{\pi}}\frac{C_1\ln(4)}{C_1\ln(4)-2}$.

Proof. From (3.A.1), (3.A.2) and (3.A.6) we get

$$\begin{aligned}|f^{(n+1)}\,(x)\,| &\le \frac{10\kappa}{\sqrt{\pi}}\sum_{l=0}^{n}\binom{n}{l}\frac{l!2^l}{(1-x^2)^{l+1}}(n-l)!\left(\frac{C_1 q(x)}{1-x^2}\right)^{n-l}\mathrm{e}^{-2g^2(x)} \\ &\le \frac{10\kappa}{\sqrt{\pi}}C_1^n n!\frac{q(x)^n}{(1-x^2)^{n+1}}\,\mathrm{e}^{-2g^2(x)}\sum_{l=0}^{n}\left(\frac{2}{C_1 q(x)}\right)^l \\ &\le \frac{10\kappa}{\sqrt{\pi}}\frac{C_1\ln(4)}{C_1\ln(4)-2}C_1^n n!\frac{q(x)^n}{(1-x^2)^{n+1}}\,\mathrm{e}^{-2g^2(x)}, \end{aligned}$$

which leads to the desired result. □

Lemma 3.A.5. *For* $x \in (-1,1)$ *and* $\alpha \ge 2$*, we have*

$$\left\|\frac{\mathrm{e}^{-2g^2(x)}}{(1-x^2)^\alpha}\right\|_\infty \le \mathrm{e}^{\sigma_\alpha}$$

with

$$\sigma_\alpha := \frac{1}{4}\alpha^2 + \frac{1}{2} - \ln\left(\frac{1}{2}\alpha + \frac{1}{2}\sqrt{\alpha^2-4}\right).$$

Proof. We set

$$\frac{\mathrm{e}^{-2g^2(x)}}{(1-x^2)^\alpha} = \mathrm{e}^{s_n(x)},$$

where

$$s_n(x) := -2\,\mathrm{arctanh}(x)^2 - \alpha\ln(1-x^2).$$

With the definition of $\operatorname{arctanh}(x)$ we get

$$\begin{aligned} s_n(x) =& -2\left[\frac{1}{2}\ln(1+x)-\frac{1}{2}\ln(1-x)\right]^2-\alpha\ln(1-x)-\alpha\ln(1+x) \\ =& -\frac{1}{2}\left[\ln(1+x)\right]^2+\ln(1+x)\ln(1-x)-\frac{1}{2}\left[\ln(1-x)\right]^2 \\ & -\alpha\ln(1-x)-\alpha\ln(1+x). \end{aligned}$$

Since $s_n(x)$ is symmetric we assume $0 \le x < 1$ and get

$$s_n(x) \le -\frac{1}{2}\left[\ln(1-x)\right]^2-\alpha\ln(1-x)+\ln(1+x)\ln(1-x) =: \tilde{s}_n(x).$$

$\tilde{s}_n(x)$ is strictly increasing in the interval $[0, 0.5]$ for arbitrary $\alpha \in \mathbb{R}_{\ge 2}$. Therefore we may restrict to find an upper bound for $\tilde{s}_n(x)$ in the interval $[0.5, 1[$. With the inequality $\ln(1+x)\ln(1-x) \le -\ln(-\ln(1-x))$ we get

$$\tilde{s}_n(x) \le -\frac{1}{2}\left[\ln(1-x)\right]^2-\alpha\ln(1-x)-\ln(-\ln(1-x)) =: \hat{s}_n(x)$$

in $[0.5, 1[$. The derivative of $\hat{s}_n(x)$ is given by

$$\hat{s}_n'(x) = \frac{\left[\ln(1-x)\right]^2+\alpha\ln(1-x)+1}{(1-x)\ln(1-x)}$$

which has the root

$$x_0 = 1-\mathrm{e}^{-\theta_\alpha},$$

where $\theta_\alpha := \frac{1}{2}\alpha+\frac{1}{2}\sqrt{\alpha^2-4}$. Inserting this above shows that

$$s_n(x) \le \alpha\theta_\alpha-\frac{1}{2}\theta_\alpha^2-\ln\theta_\alpha$$

which leads to the desired result after some straightforward manipulations. □

Lemma 3.A.6. *It holds*

$$\int_{-1}^{1}\left(\ln\frac{4}{1-t^2}\right)^n dt \le 16n!$$

for $n \in \mathbb{N}$.

Proof. We first note that

$$\begin{aligned} &\int_{-1}^{1}|\ln(1-t)|^i\,|\ln(1+t)|^{k-i}dt \\ &\quad= \int_{-1}^{0}|\ln(1-x)|^i\,|\ln(1+t)|^{k-i}dt+\int_{0}^{1}|\ln(1-x)|^i\,|\ln(1+t)|^{k-i}dt \\ &\quad\le (\ln 2)^i\int_{-1}^{0}|\ln(1+t)|^{k-i}dt+(\ln 2)^{k-i}\int_{0}^{1}|\ln(1-t)|^i dt \\ &\quad= (\ln 2)^i\int_{0}^{1}|\ln(t)|^{k-i}dt+(\ln 2)^{k-i}\int_{0}^{1}|\ln(t)|^i dt \\ &\quad= (\ln 2)^i(k-i)!+(\ln 2)^{k-i}i!, \end{aligned}$$

where we used [16, (2.711)] in the last step. With these computations we get

$$\begin{aligned}
\int_{-1}^{1}\left|\left(\ln\frac{4}{1-t^2}\right)^n\right|dt &\le \sum_{k=0}^{n}\binom{n}{k}\int_{-1}^{1}|\ln(1-t^2)|^k(\ln 4)^{n-k}dt \\
&\le \sum_{k=0}^{n}\sum_{i=0}^{k}\binom{n}{k}\binom{k}{i}(\ln 4)^{n-k}\int_{-1}^{1}|\ln(1-t)|^i\,|\ln(1+t)|^{k-i}dt \\
&\le \sum_{k=0}^{n}\sum_{i=0}^{k}\binom{n}{k}\binom{k}{i}(\ln 4)^{n-k}\left((\ln 2)^i(k-i)!+(\ln 2)^{k-i}i!\right) \\
&\le \sum_{k=0}^{n}\binom{n}{k}(\ln 4)^{n-k}\left(k!\sum_{i=0}^{k}\frac{(\ln 2)^i}{i!}+k!\sum_{i=0}^{k}\frac{(\ln 2)^{k-i}}{(k-i)!}\right) \\
&\le 4\sum_{k=0}^{n}\binom{n}{k}(\ln 4)^{n-k}k! \\
&\le 4n!\sum_{k=0}^{n}\frac{(\ln 4)^{n-k}}{(n-k)!}\le 16n!.
\end{aligned}$$

□

References

[1] M. Abramowitz and I. Stegun. *Handbook of Mathematical Functions.* Applied Mathematics Series 55. National Bureau of Standards, U.S. Department of Commerce, 1972.

[2] I. Babuška and J. M. Melenk. The Partition of Unity Method. *Int. J. Numer. Meths. Eng.*, 40:727–758, 1997.

[3] A. Bamberger and T. Ha Duong. Formulation Variationnelle Espace-Temps pur le Calcul par Potientiel Retardé de la Diffraction d'une Onde Acoustique. *Math. Meth. in the Appl. Sci.*, 8:405–435, 1986.

[4] L. Banjai. Multistep and multistage convolution quadrature for the wave equation: Algorithms and experiments. *SIAM J. Sci. Comput.*, 32(5):2964–2994, 2010.

[5] L. Banjai, J. Melenk, and C. Lubich. Runge-Kutta convolution quadrature for operators arising in wave propagation. *Numer. Math.*, 119(1):1–20, 2011.

[6] L. Banjai and S. Sauter. Rapid solution of the wave equation in unbounded domains. *SIAM Journal on Numerical Analysis*, 47:227–249, 2008.

[7] L. Banjai and M. Schanz. Wave Propagation Problems treated with Convolution Quadrature and BEM. Preprint 60/2010, MPI Leipzig.

[8] B. Birgisson, E. Siebrits, and A. Peirce. Elastodynamic Direct Boundary Element Methods with Enhanced Numerical Stability Properties. *Int. J. Num. Meth. Eng.*, 46:871–888, 1999.

[9] M. J. Bluck and S. P. Walker. Analysis of three dimensional transient acoustic wave propagation using the boundary integral equation method. *Int. J. Num. Meth. Eng.*, 39:1419–1431, 1996.

[10] Q. Chen, P. Monk, X. Wang, and D. Weile. Analysis of Convolution Quadrature Applied to the Time-Domain Electric Field Integral Equation. *Submitted*.

[11] P. J. Davies and D. B. Duncan. Averaging techniques for time-marching schemes for retarded potential integral equations. *Appl. Numer. Math.*, 23:291–310, May 1997.

[12] P. J. Davies and D. B. Duncan. Numerical stability of collocation schemes for time domain boundary integral equations. In Carstensen et al., editor, *Computational Electromagnetics*, pages 51–86. Springer, 2003.

[13] Y. Ding, A. Forestier, and T. Ha Duong. A Galerkin scheme for the time domain integral equation of acoustic scattering from a hard surface. *The Journal of the Acoustical Society of America*, 86(4):1566–1572, 1989.

[14] S. J. Dodson, S. P. Walker, and M. J. Bluck. Implicitness and stability of time domain integral equation scattering analysis. *ACES J.*, 13:291–301, 1997.

[15] J. El Gharib. *Problèmes de potentiels retardés pour l'acoustique.* PhD thesis, École Polytechnique, 1999.

[16] I. Gradshteyn and I. Ryzhik. *Table of Integrals, Series, and Products.* Academic Press, 1965.

[17] T. Ha-Duong. On retarded potential boundary integral equations and their discretisation. In *Topics in Computational Wave Propagation: Direct and Iverse Problems*, volume 31 of *Lect. Notes Comput. Sci. Eng.*, pages 301–336. Springer, Berlin, 2003.

[18] T. Ha-Duong, B. Ludwig, and I. Terrasse. A Galerkin BEM for transient acoustic scattering by an absorbing obstacle. *International Journal for Numerical Methods in Engineering*, 57:1845–1882, 2003.

[19] W. Hackbusch, W. Kress, and S. Sauter. Sparse convolution quadrature for time domain boundary integral formulations of the wave equation by cutoff and panel-clustering. In M. Schanz and O. Steinbach, editors, *Boundary Element Analysis*, pages 113–134. Springer, 2007.

[20] W. Hackbusch, W. Kress, and S. Sauter. Sparse convolution quadrature for time domain boundary integral formulations of the wave equation. *IMA, J. Numer. Anal.*, 29:158–179, 2009.

[21] J. C. Nédélec, T. Abboud, and J. Volakis. Stable solution of the retarded potential equations, Applied Computational Electromagnetics Society (ACES) Symposium Digest, 17th Annual Review of Progress, Monterey, 2001.

[22] B. P. Rynne and P. D. Smith. Stability of Time Marching Algorithms for the Electric Field Integral Equation. *J. Electromagnetic Waves and Appl.*, 4:1181–1205, 1990.

[23] S. Sauter and A. Veit. Exact Solutions of Retarded Boundary Integral Equations. Preprint 03-2011, Universität Zürich.

[24] E. P. Stephan, M. Maischak, and E. Ostermann. Transient boundary element method and numerical evaluation of retarded potentials. In *Computational Science - ICCS 2008*, pages 321–330. Springer (5102), 2008.

[25] P. G. Todorov. New explicit formulas for the nth derivative of composite functions. *Pacific J. Math.*, 92(1):217–236, 1981.

[26] L. N. Trefethen. Is Gauss Quadrature Better than Clenshaw-Curtis? *SIAM Rev.*, 50:67–87, February 2008.

[27] A. Veit. A MATLAB code for computing exact solutions of retarded potential equations for a spherical scatterer. 2011. Available via: `https://www.math.uzh.ch/compmath/?exactsolutions`.

[28] X. Wang, R. A. Wildman, D. S. Weile, and P. Monk. A finite difference delay modeling approach to the discretization of the time domain integral equations of electromagnetics. *IEEE Transactions on Antennas and Propagation*, 56(8):2442–2452, 2008.

[29] D. S. Weile, A. A. Ergin, B. Shanker, and E. Michielssen. An accurate discretization scheme for the numerical solution of time domain integral equations. *IEEE Antennas and Propagation Society International Symposium*, 2:741–744, 2000.

[30] D. S. Weile, G. Pisharody, N. W. Chen, B. Shanker, and E. Michielssen. A novel scheme for the solution of the time-domain integral equations of electromagnetics. *IEEE Transactions on Antennas and Propagation*, 52:283–295, 2004.

[31] D. S. Weile, B. Shanker, and E. Michielssen. An accurate scheme for the numerical solution of the time domain electric field integral equation. *IEEE Antennas and Propagation Society International Symposium*, 4:516–519, 2001.

[32] A. Wildman, G. Pisharody, D. S. Weile, S. Balasubramaniam, and E. Michielssen. An accurate scheme for the solution of the time-domain integral equations of electromagnetics using higher order vector bases and bandlimited extrapolation. *IEEE Transactions on Antennas and Propagation*, 52:2973–2984, 2004.

4

[published in Comp. Meth. Appl. Math., 11(3), 2011]

Fast Quadrature Techniques for Retarded Potentials Based on TT/QTT Tensor Approximation

B. N. Khoromskij* S. Sauter† A. Veit‡ §

Abstract

We consider the Galerkin approach for the numerical solution of retarded boundary integral formulations of the three dimensional wave equation in unbounded domains. Recently smooth and compactly supported basis functions in time were introduced which allow the use of standard quadrature rules in order to compute the entries of the boundary element matrix. In this paper we use TT and QTT tensor approximations to increase the efficiency of these quadrature rules. Various numerical experiments show the substantial reduction of the computational cost that is needed to obtain accurate approximations for the arising integrals.

AMS subject classifications: 65F30, 65F50, 65N38, 65F10

Key words: Multi-dimensional problems, tensor approximation, quantized representation of vectors, model reduction, retarded potentials, 3D wave equation, quadrature rules.

4.1 Introduction

Acoustic and electromagnetic scattering problems in three dimensions have a wide range of practical applications in physics and engineering. An important model problem for the

*Max-Planck-Institut für Mathematik in den Naturwissenschaften, Inselstr. 22-26, 04103 Leipzig, Germany, e-mail: bokh@mis.mpg.de

†Institut für Mathematik, Universität Zürich, Winterthurerstrasse 190, CH-8057 Zürich, Switzerland, e-mail: stas@math.uzh.ch

‡Institut für Mathematik, Universität Zürich, Winterthurerstrasse 190, CH-8057 Zürich, Switzerland, e-mail: alexander.veit@math.uzh.ch

§The third author gratefully acknowledges the support given by SNF, No. PDFMP2_127437/1

development of efficient and accurate numerical methods for such types of time-dependent physical applications is the three-dimensional wave equation in unbounded exterior domains. Here, boundary element methods show their natural strength, reducing the problem in the unbounded domain to integral equations on the bounded surface of the scatterer.
The efficient numerical solution of such retarded boundary integral equations has gained growing attention in the last years. Existing approaches include methods based on convolution quadrature (cf. [3, 4, 5, 12, 13, 33, 6]) and methods based on bandlimited interpolation and extrapolation (cf. [35, 34, 36, 38]). Here, we consider a Galerkin method in order to discretize the integral equations in space and time (cf. [2, 7, 9, 10]). It can be shown that the corresponding space-time variational formulation in this approach satisfies a coercivity property which ensures the unconditional stability of conforming Galerkin schemes. Furthermore, this approach is very flexible with regard to the use of variable time stepping and spatially curved scatterers. The standard Galerkin approach uses piecewise polynomial basis functions in time. The drawback of the method in this case is that due to the retarded time argument the domain for the spatial integration is the intersection of (possibly curved) pairs of surface panels with the discrete light cone. The stable numerical handling of these intersections is complicated even for flat panels and might be intractable for curved surface patches. We refer to [8, 22, 30] for examples of quadrature schemes tailored to this problem.
In [27] smooth and compactly supported basis functions in time were introduced. This choice circumvents the problem of integrating on the complicated intersections of the discrete light cone with the spatial surface mesh and allows to apply standard quadrature rules to compute the entries of the boundary element matrix. Due to the compact support of the basis functions the sparsity of the system matrix is maintained. On the other hand this leads to C^∞ but, in general, non-analytic integrands, which makes the quadrature problem more difficult. In general, more quadrature points have to be used as for analytic integrands as they arise, e.g., for boundary element methods applied to elliptic boundary value problems.
In this paper we therefore address the problem how to efficiently evaluate the arising integrals using tensor Gauss quadrature and TT/QTT approximation. Note, that other techniques such as sparse, possibly adaptive quadrature also have the potential to be applied to this problem. Preliminary test with sparse grid quadrature indicates, that our TT/QTT approach is preferable for this class of problems, especially if high accuracies are needed. However an asymptotic complexity analysis still has to be done.
The integrals which define the entries of the block system matrix are defined over pairs of surface panels. They are transformed to the reference triangle in Euclidean space and by applying simplex coordinates the quadrature problems boils down to the approximation of an integral over the four-dimensional unit cube. A tensor quadrature rule applied to these integrals leads to a four dimensional tensor $\mathbf{A}$ of size $N \times N \times N \times N$, whose entries are the values of the integrand evaluated at the different quadrature points.
To reduce the storage and computational costs to handle this large data array, we apply the methods of tensor approximation based on the idea of separation of variables. There are various tensor-product formats which allow the low parametric representation of high-dimensional data. The most commonly used are the canonical, Tucker formats as well as the class of so-called matrix product states (MPS) representations [37, 31, 32] commonly used in high-dimensional quantum computations (see survey paper [17] for more details). Recently these types of tensor formats have attracted much attention in the community of numerical analysis. In particular, the hierarchical Tucker [14], the tensor train (TT) [24] and the tensor chain (TC) [18] formats were considered. In the following we make use of the TT format

applied to both the initial fourth order tensor and to its quantized-TT (QTT) representation. Such representations allow to reduce the asymptotical storage and computational costs of certain bilinear tensor operations from $O(N^4)$ to $O(r^2N)$ or even to $O(r^2 \log N)$ (avoiding the dependence on the grid-size), where r is the small rank parameter, characterizing the separability properties of the target tensor $\mathbf{A}$. Notice that the hierarchical Tucker format was recently applied in the same spirit to computation of certain multivariate integrals arising in boundary element methods [1].
Various numerical experiments show that these tensors have usually a low rank representation in TT and QTT format which reduces the storage and computational cost substantially. The evaluation of the quadrature then corresponds to a simple scalar product of the TT/QTT representation of $\mathbf{A}$ and a rank-1 tensor containing the weights of the quadrature rule. This evaluation can be performed considerably faster compared to the standard approach. In order to compute the TT/QTT approximation of $\mathbf{A}$ directly, without computing $\mathbf{A}$ itself, we apply a TT cross approximation scheme (cf. [25]) in the QTT format. This further reduces the computational cost, since considerably less evaluations of the integrand are required. We perform numerical experiments to show the efficiency of this scheme in our case.
Note that our sparse approximation method for high-dimensional quadrature problems is by no means restricted to the retarded potential integral equation but, potentially, can be applied to a much larger class of problems. We restricted to this application because quadrature is *the* major bottleneck for the direct discretization of retarded potentials.

4.2 Problem Setting

Let $\Omega \subset \mathbb{R}^3$ be a Lipschitz domain with boundary Γ. We consider the homogeneous wave equation

$$\partial_t^2 u - \Delta u = 0 \quad \text{in } \Omega \times [0,T] \tag{4.2.1a}$$

with initial conditions

$$u(\cdot,0) = \partial_t u(\cdot,0) = 0 \quad \text{in } \Omega \tag{4.2.1b}$$

and Dirichlet boundary conditions

$$u = g \quad \text{on } \Gamma \times [0,T] \tag{4.2.1c}$$

on a time interval $[0,T]$ for $T > 0$. In applications, Ω is often the unbounded exterior of a bounded domain. For such problems, the method of boundary integral equations is an elegant tool where this partial differential equation is transformed to an equation on the bounded surface Γ. We employ an ansatz as a *single layer potential* for the solution u

$$u(x,t) := S\phi(x,t) := \int_\Gamma \frac{\phi(y, t - \|x-y\|)}{4\pi\|x-y\|} d\Gamma_y, \quad (x,t) \in \Omega \times [0,T] \tag{4.2.2}$$

with unknown density function ϕ. S is also referred to as *retarded single layer potential* due to the retarded time argument $t - \|x-y\|$ which connects time and space variables.

The ansatz (4.2.2) satisfies the wave equation (4.2.1a) and the initial conditions (4.2.1b). Since the single layer potential can be extended continuously to the boundary Γ, the unknown density function ϕ is determined such that the boundary conditions (4.2.1c) are satisfied. This results in the boundary integral equation for ϕ,

$$\int_\Gamma \frac{\phi(y, t - \|x-y\|)}{4\pi\|x-y\|} d\Gamma_y = g(x,t) \quad \forall (x,t) \in \Gamma \times [0,T]\,. \tag{4.2.3}$$

In order to solve this boundary integral equation numerically we introduce the following space-time variational formulation (cf. [2, 9]): Find ϕ in an appropriate Sobolev space V such that

$$\int_0^T \int_\Gamma \int_\Gamma \frac{\dot{\phi}(y, t - \|x-y\|)\zeta(x,t)}{4\pi\|x-y\|} d\Gamma_y d\Gamma_x dt = \int_0^T \int_\Gamma \dot{g}(x,t)\zeta(x,t) d\Gamma_x dt \tag{4.2.4}$$

for all $\zeta \in V$, where we denote by $\dot{\phi}$ the derivative with respect to time.
Let V_{Galerkin} be a finite dimensional subspace of V being spanned by L basis functions $\{b_i\}_{i=1}^L$ in time and M basis functions $\{\varphi_j\}_{j=1}^M$ in space. This leads to the fully discrete ansatz

$$\phi_{\text{Galerkin}}(x,t) = \sum_{i=1}^{L}\sum_{j=1}^{M} \alpha_i^j \varphi_j(x) b_i(t), \quad (x,t) \in \Gamma \times [0,T]\,, \tag{4.2.5}$$

where α_i^j are the unknown coefficients. Plugging this ansatz in (4.2.4) and rearranging terms shows that this is equivalent to: Find α_i^j for $i = 1, \ldots, L$ and $j = 1, \ldots, M$ such that

$$\sum_{i=1}^{L}\sum_{j=1}^{M} A_{j,l}^{i,k} \alpha_i^j = g_l^k \qquad \forall 1 \le k \le L \quad \forall 1 \le l \le M, \tag{4.2.6}$$

where

$$g_l^k := \int_0^T \int_\Gamma \dot{g}(x,t)\, \varphi_l(x)\, b_k(t) d\Gamma_x dt$$

and

$$A_{j,l}^{i,k} := \int_{\text{supp}(\varphi_l)} \int_{\text{supp}(\varphi_j)} \varphi_j(y)\, \varphi_l(x)\, \psi_{i,k}(\|x-y\|) d\Gamma_y d\Gamma_x. \tag{4.2.7}$$

The function $\psi_{i,k}$ contains the time integration and is defined, for $s > 0$, by

$$\psi_{i,k}(s) := \int_0^T \frac{\dot{b}_i(t-s) b_k(t)}{4\pi s} dt. \tag{4.2.8}$$

Let $\mathcal{G} := \left\{\tau_i : 1 \le i \le \overline{M}\right\}$ denote a finite element mesh on Γ consisting of (possibly curved) triangles. More precisely, we assume that for any $\tau \in \mathcal{G}$, there exists a smooth bijection $\chi_\tau : \widehat{\tau} \to \tau$ from the reference element $\widehat{\tau} := \text{conv}\left\{(0,0)^\intercal, (1,0)^\intercal, (1,1)^\intercal\right\}$ to the surface triangle τ. Then, in the solution process, the following quadrature problem arises: For $\tau, \tilde{\tau} \in \mathcal{G}$ and $1 \le j, l \le M$, compute

$$I_{\tau,\tilde{\tau}}^{i,k}(\varphi_j, \varphi_l) := \int_\tau \int_{\tilde{\tau}} \varphi_j(y)\, \varphi_l(x)\, \psi_{i,k}(\|x-y\|) d\Gamma_y d\Gamma_x, \tag{4.2.9}$$

where φ_j and φ_l, typically, are lifted polynomials, i.e., $\varphi_j \circ \chi_\tau$ and $\varphi_l \circ \chi_{\tilde{\tau}}$ are polynomials on $\widehat{\tau}$.

The definition of smooth and compactly supported temporal shape functions was addressed in [27] and is as follows. Let

$$f(t) := \begin{cases} \frac{1}{2}\,\text{erf}\,(2\,\text{artanh}\, t) + \frac{1}{2} & |t| < 1, \\ 0 & t \le -1, \\ 1 & t \ge 1 \end{cases}$$

and note, that $f \in C^\infty(\mathbb{R})$. Next, we will introduce some scaling. For a function $g \in C^0([-1,1])$ and real numbers $a < b$, we define $g_{a,b} \in C^0([a,b])$ by

$$g_{a,b}(t) := g\left(2\frac{t-a}{b-a} - 1\right).$$

We obtain a bump function on the interval $[a,c]$ with joint $b \in (a,c)$ by

$$\rho_{a,b,c}(t) := \begin{cases} f_{a,b}(t) & a \le t \le b, \\ 1 - f_{b,c}(t) & b \le t \le c, \\ 0 & \text{otherwise.} \end{cases}$$

Let us now consider the closed interval $[0,T]$ and l (not necessarily equidistant) timesteps

$$0 = t_0 < t_1 < \dots t_{l-2} < t_{l-1} = T.$$

We define $\tau_i := [t_{i-1}, t_i]$ for $i = 1, ..., l-1$. Then $\mathcal{T} := \{\omega_i : 1 \le i \le l-1\}$ with

$$\omega_1 := \tau_1, \qquad \omega_l := \tau_{l-1}, \qquad \forall 2 \le i \le l-1 \quad \omega_i := \tau_{i-1} \cup \tau_i$$

defines a cover of $[0,T]$. A smooth partition of unity subordinate to $\mathcal{T}$ then is defined by

$$\varphi_1 := 1 - f_{t_0,t_1}, \quad \varphi_l := f_{t_{l-2,l-1}}, \quad \forall 2 \le i \le l-1 : \varphi_i := \rho_{t_{i-2},t_{i-1},t_i}.$$

Smooth and compactly supported basis functions in time can then be obtained by multiplying these partition of unity functions with suitably scaled Legendre polynomials (cf. [27] for details).

Remark 4.2.1. *In the case of lowest order basis functions in time we have $l = L$ and*

$$b_i(t) = \varphi_i(t) \qquad \text{for} \qquad i = 1, \dots, L.$$

With the above definitions it then holds for $\psi_{i,k}$ as defined in (4.2.8) that:

1. $\operatorname{supp} \psi_{i,k} \subset [t_{k-2} - t_i, t_k - t_{i-2}]$.
2. *In particular, $\psi_{i,k} = 0$ for $k \le i - 2$.*
3. *Let $\mathcal{R}(\tau, \tilde{\tau}) := [\operatorname{dist}(\tau, \tilde{\tau}), \operatorname{maxdist}(\tau, \tilde{\tau})]$, where $\operatorname{maxdist}(\tau, \tilde{\tau}) := \sup_{(x,y)\in\tau\times\tilde{\tau}} \|x - y\|$. Then,*
$$I^{i,k}_{\tau,\tilde{\tau}}(\varphi_j, \varphi_l) = 0 \quad \text{if} \quad \mathcal{R}(\tau, \tilde{\tau}) \cap [t_{k-2} - t_i, t_k - t_{i-2}] = \emptyset.$$

For higher order basis functions in time similar results can be obtained. Let

$$\mathcal{I}(\tau, \tilde{\tau}) := \left\{(i,k) \in \{1, 2, \dots, L\}^2 \mid I^{i,k}_{\tau,\tilde{\tau}}(\varphi_j, \varphi_l) \neq 0\right\}$$

and, vice versa,

$$\mathcal{I}(i,k) := \left\{(\tau, \tilde{\tau}) \in \mathcal{G} \times \mathcal{G} \mid I^{i,k}_{\tau,\tilde{\tau}}(\varphi_j, \varphi_l) \neq 0\right\}.$$

Note that the index sets $\mathcal{I}(\tau, \tilde{\tau})$ and $\mathcal{I}(i,k)$ are sparse.

Our goal is, in the following, to approximate $I^{i,k}_{\tau,\tilde{\tau}}(\varphi_j, \varphi_l)$ efficiently using TT- and QTT-approximations. For simplicity we assume that we have piecewise constant basis functions in

space so that $\operatorname{supp}\varphi_l = \tau$ and $\operatorname{supp}\varphi_k = \tilde{\tau}$ with $\tau, \tilde{\tau} \in \mathcal{G}$. In general these basis functions are lifted piecewise polynomials and typically of low order. Since the use of such low order basis functions in space will not lead to significantly more oscillatory integrands, we do not expect a severe impact of this more general case on the rank decomposition in TT/QTT format. Because simplex coordinates transform triangles to squares, integrals of the form (4.2.9) can be written as

$$\int_\tau \int_{\tilde{\tau}} \psi_{i,k}\left(\|x-y\|\right) d\Gamma_y d\Gamma_x = \tag{4.2.10}$$
$$\int_{[0,1]^4} \underbrace{4|\tau||\tilde{\tau}|\xi_x\xi_y\, \psi_{i,k}(\|\chi_\tau(\xi_x,\xi_x\eta_x) - \chi_{\tilde{\tau}}(\xi_y,\xi_y\eta_y)\|)}_{=:f(\xi_x,\eta_x,\xi_y,\eta_y)} d\eta_y d\xi_y d\eta_x d\xi_x.$$

We apply properly scaled tensor Gauss-Legendre quadrature rules for the numerical approximation of the arising integrals over the four-dimensional unit cube. Let $n_1, n_2, n_3, n_4 \in \mathbb{N}_{>0}$ be the number of Gauss quadrature points in the first/second/third/fourth dimension with nodes

$$(x_{1,i})_{i=1}^{n_1}, (x_{2,j})_{j=1}^{n_2}, (x_{3,k})_{k=1}^{n_3}, (x_{4,l})_{l=1}^{n_4} \in [0,1]$$

and weights

$$(w_{1,i})_{i=1}^{n_1}, (w_{2,j})_{j=1}^{n_2}, (w_{3,k})_{k=1}^{n_3}, (w_{4,l})_{l=1}^{n_4} \in \mathbb{R}.$$

Then,

$$\int_{[0,1]^4} f(\xi_x,\eta_x,\xi_y,\eta_y)\, d\eta_y d\xi_y d\eta_x d\xi_x \approx \sum_{i=1}^{n_1}\sum_{j=1}^{n_2}\sum_{k=1}^{n_3}\sum_{l=1}^{n_4} w_{1,i}w_{2,j}w_{3,k}w_{4,l} f(x_{1,i},x_{2,j},x_{3,k},x_{4,l}). \tag{4.2.11}$$

For simplicity and in order to test the QTT approximation we set $n_1 = n_2 = n_3 = n_4 =: N$ and assume that N is a power of 2. The evaluation of an approximation in the form (4.2.11) requires $O(N^4)$ additions/multiplications and furthermore $O(N^4)$ function evaluations. Since f, or more specifically $\psi_{i,k}$, contains itself an integral, such function evaluations might be expensive. Due to the non-analyticity of f and the need to compute the integrals (4.2.10) accurately in order to obtain stable solutions of the time-domain boundary integral equations, we need a medium number of quadrature points in each direction. Thus, depending on the required accuracy of the approximation, the quadrature problem can become costly. Therefore the question arises if the right hand side in (4.2.11) can be evaluated more efficiently. For this purpose we will investigate, in the following, the TT and QTT low rank approximations to the fourth order tensor $\mathbf{A} = [A(i,j,k,l)]$ defined entrywise by

$$A(i,j,k,l) = f(x_{1,i},x_{2,j},x_{3,k},x_{4,l}), \quad (i,j,k,l) \in \{1,...,N\}^4. \tag{4.2.12}$$

Note that for the singular case, where $\operatorname{dist}(\tau,\tilde{\tau}) = 0$, regularizing coordinate transforms have to be applied to remove the singularity of the kernel function (cf. [29], [26]). In this case, the transformed integral is a sum of integrals over the four-dimensional unit cube and our compression method can be applied also to these cases. For simplicity we restrict in this paper to the approximation of the regular integrals.

4.3 Tensor Approximation of $I_{\tau,\tilde{\tau}}^{i,j}(\varphi_j, \varphi_l)$

In the following we apply the matrix-product states (MPS) type tensor representations in the form of tensor train (TT) and quantized-TT (QTT) formats to represent sparsely the fourth

order coefficients tensor arising in the quadrature approximation of the above integrals (see (4.2.11)).

4.3.1 Matrix-product states (MPS) tensor formats

A tensor of order d is defined as an element of finite dimensional tensor-product Hilbert space $\mathbb{W}_{\mathbf{n}} \equiv \mathbb{W}_{\mathbf{n},d}$ of the d-fold, $N_1 \times ... \times N_d$ real-valued arrays, and equipped with the Euclidean (Frobenius) scalar product $\langle \cdot, \cdot \rangle : \mathbb{W}_{\mathbf{n}} \times \mathbb{W}_{\mathbf{n}} \to \mathbb{R}$. Each tensor in $\mathbb{W}_{\mathbf{n}}$, $\mathbf{n} = (N_1, ..., N_d)$, can be represented componentwise,

$$\mathbf{A} = [A(i_1, ..., i_d)] \quad \text{with} \quad i_\ell \in I_\ell := \{1, ..., N_\ell\},$$

where for the ease of presentation, we mainly consider the equal-size tensors, i.e., $N_\ell = N$ ($\ell = 1, ..., d$). We call the elements of $\mathbb{W}_{\mathbf{n}} = \mathbb{R}^{I_1 \times ... \times I_d}$ as N-d tensors. The dimension of the tensor-product Hilbert space $\mathbb{W}_{\mathbf{n}}$ scales exponentially in d, $\dim \mathbb{W}_{\mathbf{n},d} = N^d$ implying exponential storage cost for a general N-d tensor.

In our application the quadrature coefficients for approximating $I^{i,k}_{\tau,\tilde{\tau}}(\varphi_j, \varphi_l)$ constitute the $N \times N \times N \times N$ tensor $\mathbf{A}$ of order 4 as in (4.2.12), requiring N^4 storage size. Hence, in the case of multiple computations of a tensor and high numerical cost of evaluation a single entry, the calculations become nontractable already for N of order several tens.

The MPS representation of a d-th order tensor reduces the complexity of storage to $O(dr^2N)$, where r is the maximal mode rank [37, 31]. The MPS tensor approximation was proved to be efficient in high-dimensional electronic/molecular structure calculations, in quantum computing and in stochastic PDEs (see survey paper [17] for more details). In the recent mathematical literature the various versions of MPS tensor decomposition were discovered as the hierarchical Tucker [14], the tensor train (TT) [24] and the tensor chain (TC) [18] formats. In the following we make use of the TT format applied to both the initial N-d tensor and to its quantized representation (quantics-TT).

Definition 4.3.1. *(Tensor chain/train format) For a given rank parameter $\mathbf{r} = (r_0, ..., r_d)$, and the respective index sets $J_\ell = \{1, ..., r_\ell\}$ ($\ell = 0, 1, ..., d$), with the periodicity constraints $J_0 = J_d$ (i.e., $r_0 = r_d$), the rank-$\mathbf{r}$ TC format contains all elements $\mathbf{A} = [A(i_1, ..., i_d)] \in \mathbb{W}_{\mathbf{n}}$ which can be represented as the chain of contracted products of 3-tensors over the d-fold product index set $J := \times_{\ell=1}^{d} J_\ell$,*

$$A(i_1, ..., i_d) = \sum_{\alpha_1 \in J_1} \cdots \sum_{\alpha_d \in J_d} A^{(1)}(\alpha_d, i_1, \alpha_1) A^{(2)}(\alpha_1, i_2, \alpha_2) \cdots A^{(d)}(\alpha_{d-1}, i_d, \alpha_d).$$

In the matrix form we have the entrywise MPS representation

$$A(i_1, i_2, \ldots, i_d) = A^{(1)}_{i_1} A^{(2)}_{i_2} \ldots A^{(d)}_{i_d}, \tag{4.3.1}$$

where each $A^{(\ell)}_{i_\ell}$ is $r_{\ell-1} \times r_\ell$ matrix. In the case $J_0 = J_d = \{1\}$, the TC format coincides with TT representation in [24].

The TC/TT format reduces the storage cost of a N-d tensor to $O(dr^2N)$, $r = \max r_\ell$. The important multilinear algebraic operations with TT tensors can be implemented with linear complexity scaling in d and N. In particular, for the Hadamard product we have

$$\mathbf{Z} = \mathbf{X} \circ \mathbf{Y}: \quad Z^{(k)}(i_k) = X^{(k)}(i_k) \otimes Y^{(k)}(i_k),$$

implying the formatted representation of the scalar product (in $O(dr^3N) \ll N^d$ operations)

$$\langle \mathbf{X}, \mathbf{Y} \rangle = \langle \mathbf{X} \circ \mathbf{Y}, \mathbf{1} \rangle.$$

4.3.2 Quantized-TT (QTT) Approximation of N-d tensors

Further reduction of the asymptotic storage complexity can be based on the so-called quantized-TT (QTT) representation obtained from the initial $N \times N \times N \times N$ tensor by simple folding (reshaping) to a higher dimensional $2 \times ... \times 2$ array. It was shown in [18] that the computational gain of the QTT representation is due to the good separability properties of quantized images on a large class of function related tensors. In our application we found numerically the low rank TT/QTT approximations for arising 4th order tensors, indicating nearly the same data compression for both formats. However, the important motivation to use the QTT representation is due to the high efficiency of the QTT-cross approximation scheme ensured by the small mode size (in fact, equals to 2) of the quantized tensors.

We suppose that $N = 2^L$ with some $L = 1, 2, \dots$. The next definition introduces the folding of N-d tensors into the elements (quantized $2 \times ... \times 2$ tensors) of an auxiliary D-dimensional tensor space with $D = d \log_2 N$.

Definition 4.3.2. *([18]) Introduce the binary folding transform of degree $2 \le L$,*

$$\mathcal{F}_{d,L} : \mathbb{W}_{\mathbf{n},d} \to \mathbb{W}_{\mathbf{m},dL}, \quad \mathbf{m} = (\mathbf{m}_1, ..., \mathbf{m}_d), \quad \mathbf{m}_\ell = (m_{\ell,1}, ..., m_{\ell,L}),$$

with $m_{\ell,\nu} = 2$ for $\nu = 1, ..., L$, $(\ell = 1, ..., d)$, that reshapes the initial $\mathbf{n}$-d tensor in $\mathbb{W}_{\mathbf{n},d}$ to elements of the quantized space $\mathbb{W}_{\mathbf{m},dL}$ as follows:
(A) For $d = 1$ a vector $\mathbf{X} = [X(i)]_{i \in I} \in \mathbb{W}_{N,1}$, is reshaped to the element of $\mathbb{W}_{2,L}$ by

$$\mathcal{F}_{1,L} : \mathbf{X} \to \mathbf{Y} = [Y(\mathbf{j})] := [X(i)], \quad \mathbf{j} = \{j_1, ..., j_L\},$$

with $j_\nu \in \{1, 2\}$ for $\nu = 1, ..., L$. For fixed i, $j_\nu = j_\nu(i)$ is defined by $j_\nu - 1 = C_{-1+\nu}$, where the $C_{-1+\nu}$ are found from the binary representation of $i - 1$,

$$i - 1 = C_0 + C_1 2^1 + \dots + C_{L-1} 2^{L-1} \equiv \sum_{\nu=1}^{L} (j_\nu - 1) 2^{\nu-1}.$$

(B) For $d > 1$ the construction is similar.

Notice that the folding transform $\mathcal{F}_{d,L}$ is the linear isometry between $\mathbb{W}_{N,d}$ and $\mathbb{W}_{2,dL}$ (see [18]).

Remark 4.3.3. *Every 2-dL tensor in the quantics space $\mathbb{W}_{2,dL}$ can be represented (approximated) in the low rank TT format. This leads to the so-called QTT representation of N-d tensors. Assuming that $r_k \le r$, $k = 1, ..., dL$, the complexity of the QTT representation can be estimated by $O(dr^2 \log N)$, providing* log*-volume asymptotics compared with the volume size of the initial tensor $O(N^d)$.*

4.3.3 Sketch of numerical TT/QTT approximation

The manifold [15] of rank-$\mathbf{r}$ TT tensors in $\mathbb{W}_{\mathbf{n}}$ is known to be closed in the Frobenius norm [25].

From the computational point of view, one of the most attractive features of TT format is the following: the numerical computation of $r_{k-1} \times r_k$ matrices $A_{i_k}^{(k)}$ in the TT representation (approximation) of a full format tensor $\mathbf{A} = [A(i_1, ..., i_d)]$,

$$A(i_1, i_2, \dots, i_d) = A_{i_1}^{(1)} A_{i_2}^{(2)} \dots A_{i_d}^{(d)},$$

can be implemented by a stable SVD-based algorithm (MATLAB Toolbox `http://spring.inm.rus.ru/osel`). For the completeness of presentation, we sketch the full-to-TT compression algorithm [24], which will be applied in Section 4.4 to our particular fourth order coefficients tensor.

Input: a tensor $\mathbf{A}$ of size $n_1 \times n_2 \cdots \times n_d$ and accuracy bound $\varepsilon > 0$.
1: First unfolding: $N_r = \prod_{k=2}^{d} n_k$, $M := \mathrm{reshape}(\mathbf{A}, [n_1, N_r])$.
2: Compute the truncated SVD of $M \approx U\Lambda V$, so that the approximate rank r ensures

$$\sum_{k=r+1}^{\min(n_1,N_r)} \sigma_k^2 \leq \frac{(\varepsilon \cdot \|\mathbf{A}\|_F)^2}{d-1}.$$

3: Set $A^{(1)} = U$, $M := \Lambda V^T$, $r_1 = r$, and process modes $k = 2, ..., d-1$.
4: **for** $k = 2$ **to** $d-1$ **do**
4a: Construct the next unfolding: $N_r := \frac{N_r}{n_k}$, $M := \mathrm{reshape}(M, [rn_k, N_r])$.
4b: Compute the truncated SVD of $M \approx U\Lambda V$, so that the approximate rank r ensures

$$\sum_{k=r+1}^{\min(n_k,N_r)} \sigma_k^2 \leq \frac{(\varepsilon \cdot \|\mathbf{A}\|_F)^2}{d-1}.$$

4c: Set $r_k = r$ and reshape the matrix U into a tensor:

$$A^{(k)} := \mathrm{reshape}(U, [r_{k-1}, n_k, r_k]).$$

4d: Recompute $M := \Lambda V$.
end for
5: Set $A^{(d)} = M$.
Output: TT cores A_k, $k = 1, \ldots d$, defining a TT ε-approximation to $\mathbf{A}$.

The above algorithm has the numerical complexity $O(n^{d+1})$. In the present paper we directly apply this algorithm to the fourth-order tensor of interest to demonstrate the efficient rank decomposition in the TT format that reduces drastically the storage and computational cost. Moreover, assuming the existence of low-rank TT representation the rank-**r** TT approximation can be computed by the heuristic algorithm called TT-cross approximation [25] avoiding the "curse of dimensionality" (see the numerical example below). This algorithm also applies to QTT format (QTT-cross approximation).

Remark 4.3.4. *Notice that the QTT approximation of the target $N \times N \times N \times N$ tensor $\mathbf{A}$ can be performed by the same decomposition algorithm but applied in the particular setting $n_k = 2$, $d = 4 \log N$. The rank-r QTT-cross approximation takes the advantage of low cost $O(r^4 \log N)$ since, due to the main property of TT-cross algorithm, it calls only for $O(r^2 \log N)$ entries of the initial tensor $\mathbf{A}$. In this way, the generation of the full tensor can be avoided by using the rank-r QTT-cross approximation method that requires to compute only few entries (chosen adaptively) of the target tensor. The numerical results show that the compression is comparable with the complete QTT approximation method (see Section 4.6).*

4.3.4 Computation of $I^{i,j}_{\tau,\tilde{\tau}}(\varphi_j, \varphi_l)$ using TT/QTT approximation

Let us denote the TT and QTT representations of $\mathbf{A}$, defined in (4.2.12), by $\mathbf{A}_{TT}$ and $\mathbf{A}_{QTT}$. An approximation of the integral in (4.2.11) using these representations instead of $\mathbf{A}$ can

be obtained by a simple tensor operation in the quantics space $\mathbb{W}_{2,dL}$, $d = 4$, $L = \log N$, specifically as the scalar product of the rank-1 coefficients tensor $\mathbf{W} = w_1 \otimes w_2 \otimes w_3 \otimes w_4$ with $\mathbf{A}_{TT}$ or $\mathbf{A}_{QTT}$. Let

$$Q_G := \langle \mathbf{W}, \mathbf{A} \rangle = \sum_{i=1}^{N} \sum_{j=1}^{N} \sum_{k=1}^{N} \sum_{l=1}^{N} w_{1,i} w_{2,j} w_{3,k} w_{4,l} f(x_{1,i}, x_{2,j}, x_{3,k}, x_{4,l}), \tag{4.3.2}$$

$$Q_{TT} := \langle \mathbf{W}, \mathbf{A}_{TT} \rangle, \tag{4.3.3}$$

$$Q_{QTT} := \langle \mathbf{W}, \mathbf{A}_{QTT} \rangle, \tag{4.3.4}$$

denote the quadrature formulas based on the different representations of $\mathbf{A}$. As pointed out in Section 4.3.1 the cost to evaluate the scalar products Q_{TT} or Q_{QTT} scales with $O(4r^3N)$, where r is much smaller than N, compared to $O(N^4)$ for the exact evaluation of Q_G. Therefore the approximations Q_{TT} and Q_{QTT} can be computed considerably faster, provided that $\mathbf{A}$ has TT and QTT representations with low rank.
Since $\mathbf{A}_{TT}$ and $\mathbf{A}_{QTT}$ are only approximations of $\mathbf{A}$, the formulas Q_{TT} and Q_{QTT} introduce additional quadrature errors. An important question therefore is how accurate the approximations $\mathbf{A}_{TT/QTT}$ have to be, such that the relative errors

$$E_{G,TT} := \frac{|Q_G - Q_{TT}|}{|Q_G|} \qquad \text{and} \qquad E_{G,QTT} := \frac{|Q_G - Q_{QTT}|}{|Q_G|} \tag{4.3.5}$$

are small and the additional error does not affect the accuracy of the quadrature Q_G.

4.4 Numerical Experiments

In the following, we investigate the compression properties of $\mathbf{A}$ and the accuracy of Q_{TT} and Q_{QTT} using different triangles and time meshes in order to cover various cases, that might occur during the solution of the discrete system (4.2.6) . Therefore, let

$$\tau := \operatorname{conv}\left\{(0,0,0)^{\mathrm{T}}, (1,0,0)^{\mathrm{T}}\ , (1,1,0)^{\mathrm{T}}\ \right\},$$
$$\tilde{\tau} := c_{\text{shift}} + \operatorname{conv}\left\{(1,0,0)^{\mathrm{T}}, (1,\frac{1}{2},1)^{\mathrm{T}}\ , (0,1,\frac{1}{2})^{\mathrm{T}}\ \right\},$$

with $c_{\text{shift}} \in \mathbb{R}$. These triangles will be used for all numerical experiments. Only $c_{\text{shift}} \in \mathbb{R}$ is variable and will be set individually for each case. Furthermore we will define different time grids for each case consisting of six points $t_1 \leq \ldots \leq t_6 \in \mathbb{R}_{\geq 0}$. We then choose basis functions $b(t)$ and $\tilde{b}(t)$ in time such that $\operatorname{supp} b = [t_1, t_3]$ and $\operatorname{supp} \tilde{b} = [t_4, t_6]$. More precisely, b and $\tilde{b}$ will be the smooth bump functions as defined in Section 4.2 multiplied with properly scaled Legendre polynomials of degree 1 (cf. [27]), i.e.,

$$b(t) = \rho_{t_1,t_2,t_3}(t) \left(2\frac{t-t_1}{t_3-t_1} - 1\right) \qquad \text{and} \qquad \tilde{b}(t) = \rho_{t_4,t_5,t_6}(t) \left(2\frac{t-t_4}{t_6-t_4} - 1\right). \tag{4.4.1}$$

Thus, the integrals we want to approximate are of the form

$$I_{\tau,\tilde{\tau}} := \int_{\tau} \int_{\tilde{\tau}} \psi\left(\|x-y\|\right) d\Gamma_y d\Gamma_x, \tag{4.4.2}$$

with

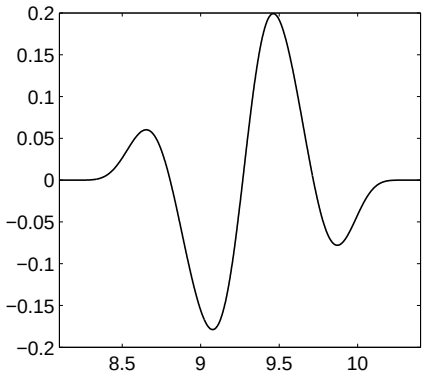

Figure 4.1: *$\psi(s)$ for the time grid given in* (4.4.4).

$$\psi(s) := \int_0^T \frac{\dot{b}(t-s)\tilde{b}(t)}{4\pi s} dt, \tag{4.4.3}$$

where $s \in \mathbb{R}_{>0}$. Note that

$$\operatorname{supp} \psi = [t_4 - t_3, t_6 - t_1].$$

We denote the domain of the spatial integration by

$$S = \left\{ z \in \mathbb{R}^3 \text{ s.t. } z = x - y, x \in \tau, y \in \tilde{\tau} \right\}$$

and define

$$S_{\min} := \min_{z \in S} \|z\| = \operatorname{dist}(\tau, \tilde{\tau}), \qquad S_{\max} := \max_{z \in S} \|z\| = \operatorname{maxdist}(\tau, \tilde{\tau}).$$

It can be easily seen that the position of triangle $\tilde{\tau}$, i.e. c_{shift}, has to be chosen such that $[S_{\min} S_{\max}] \cap [t_4 - t_3, t_6 - t_1] \neq \emptyset$ in order to obtain $I_{\tau,\tilde{\tau}} \neq 0$ (cf. Remark 4.2.1). In the following we will perform numerical experiments for the following cases:

1. $S_{\min} < t_4 - t_3$ and $S_{\max} < t_6 - t_1$. Here, the domain S is only partially enlighted from one side (cf. Figure 4.2). The case $S_{\min} > t_4 - t_3$ and $S_{\max} > t_6 - t_1$ leads to similar numerical results in our example and will not be treated separately.

2. $S_{\min} > t_4 - t_3$ and $S_{\max} < t_6 - t_1$. In this case the domain S is completely enlighted (cf. Figure 4.4).

3. $S_{\min} < t_4 - t_3$ and $S_{\max} > t_6 - t_1$. Here, the discrete light cone is a narrow strip (cf. Figure 4.6).

4. $S_{\min}$ small. In this case we examine how small distances between the triangles influence the compression rates.

5. At last we consider the case of higher order basis functions in time and therefore a more oscillatory function ψ.

Remark 4.4.1. *The following numerical experiments were performed using MATLAB on an Intel Q8200 processor, 4Gb RAM. The TT/QTT approximations of the tensor* $\mathbf{A}$ *were computed using the TT-toolbox 1.0 for MATLAB written by I. Oseledets (*`http://spring.inm.rus.ru/osel`*).*

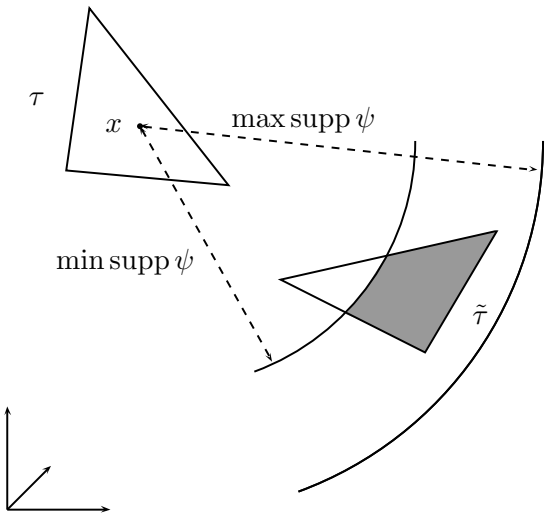

Figure 4.2: *Enlighted region for fixed $x \in \tau$ in Case 1.*

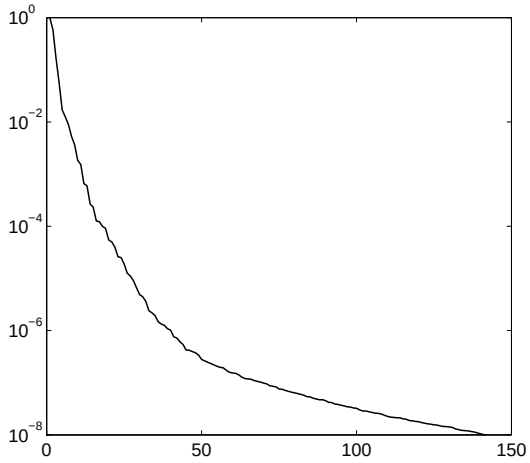

Figure 4.3: *Relative singular values of* $\mathbf{B}$*: Nonzero entries of* $\mathbf{B}$*:* $\approx$ *50%.*

4.4.1 Case 1: Partially enlighted integration domain

For this case we define the time grid

$$t_1 = 0.6, \quad t_2 = 1.2, \quad t_3 = 1.7, \quad t_4 = 9.8, \quad t_5 = 10.5, \quad t_6 = 11.0 \tag{4.4.4}$$

and $c_{\text{shift}} = 4.4$ such that $S_{\min} \approx 7.2$ and $S_{\max} \approx 9.6$. This choice of the parameters leads to a situation as illustrated in Figure 4.2. The integration domain is only partially enlighted from one side, which leads (depending of the choice of c_{shift}) to many zero entries in the resulting tensor $\mathbf{A}$. In this example c_{shift} was chosen such that approximately 50% of the entries of $\mathbf{A}$ are nonzero.
Since we are mostly concerned with far field integrals we expect that a fixed number of quadrature points leads to a sufficiently high accuracy of the approximations. For the near field integrals we expect that the number of quadrature points has to be asymptotically increased, e.g., in a logarithmic way. However a rigorous theoretical analysis of the influence of the quadrature error on the total discretization error is still open. For the approximation of $I_{\tau,\tilde{\tau}}$ we set $N = 32$, i.e., we use 32 Gauss quadrature points in each direction leading to a tensor $\mathbf{A}$ with $\text{size}(\mathbf{A}) = 32 \times 32 \times 32 \times 32$. In order to compute singular values we reshape $\mathbf{A}$ to a matrix $\mathbf{B}$ of size $32^2 \times 32^2$. Note, that in many cases the number of quadrature points can be chosen lower in order to obtain accurate approximations.
The table below shows the efficiency of the TT-approximation $\mathbf{A}_{TT}$ and the QTT-approximation $\mathbf{A}_{QTT}$ of $\mathbf{A}$. We listed the mean ranks of the corresponding cores for different approximation accuracies. We additionally computed the singular value decomposition of $\mathbf{B}$ and listed the number of relative singular values that are greater than the prescribed accuracy. The decay of the singular values is shown in Figure 4.3.

Accuracy	Mean rank of $\mathbf{A}_{TT}$	Mean rank of $\mathbf{A}_{QTT}$	Rel. SV of $\mathbf{B}$
10^{-2}	5.7	8.0	7
10^{-3}	9.4	15.2	12
10^{-4}	13.0	23.1	18
10^{-5}	18.7	33.4	28
10^{-6}	25.4	45.5	41

It can be observed that the ranks of the TT- and QTT-approximation are small, especially for low and medium accuracies. The low ranks in this case could be found also for other configurations of the numerical experiment. In general it can be noticed that the compression in this case is better if many entries of $\mathbf{A}$ are zero or in other words that the enlighted part of the integration domain is small. (That a sparse $\mathbf{A}$ however does not necessarily lead to good compression rates can be seen in Section 4.4.3).
In the next table we compare the time that is needed to compute the approximations Q_G, Q_{TT} and Q_{QTT} for different accuracies of the TT- and QTT-approximation. We assume that $\mathbf{A}$, $\mathbf{A}_{TT}$, and $\mathbf{A}_{QTT}$ are given in each case, so that only the different scalar products (4.3.2)-(4.3.4) have to be evaluated. Furthermore we compute the relative errors $E_{G,TT}$ and $E_{G,QTT}$ (cf. (4.3.5)) in order to see the effect of the additional approximation on the quadrature result.

Accuracy	Time Q_G	Time Q_{TT}	$E_{G,TT}$	Time Q_{QTT}	$E_{G,QTT}$
10^{-2}	100	1.3	$2 \cdot 10^{-3}$	9.8	$2 \cdot 10^{-4}$
10^{-3}	100	1.3	$4 \cdot 10^{-5}$	10.1	$1 \cdot 10^{-4}$
10^{-4}	100	1.4	$2 \cdot 10^{-6}$	10.3	$6 \cdot 10^{-6}$
10^{-5}	100	1.5	$1 \cdot 10^{-7}$	10.8	$2 \cdot 10^{-7}$
10^{-6}	100	1.6	$7 \cdot 10^{-8}$	11.2	$4 \cdot 10^{-8}$

It can be seen above that the evaluation of Q_{TT} and Q_{QTT} is considerably faster than the evaluation of Q_G due to the low ranks of $\mathbf{A}_{TT}$ and $\mathbf{A}_{QTT}$ and the induced low number of arithmetic operations that are needed to compute the corresponding scalar products. Furthermore it can be observed that the errors $E_{G,TT}$ and $E_{G,QTT}$ are small even for low and medium accuracies of the TT- and QTT-approximation. In this case it is sufficient to determine $\mathbf{A}_{TT}$ and $\mathbf{A}_{QTT}$ with relatively low accuracy in order to obtain accurate approximations for Q_G. On the one hand this is advantageous since we benefit from low ranks in this case and on the other hand the computation of $\mathbf{A}_{TT}$ and $\mathbf{A}_{QTT}$ directly via TT/QTT cross approximation becomes cheaper as well (cf. Section 4.4.6).

4.4.2 Case 2: Completely enlighted integration domain

For this case we again use the time grid (4.4.4) and set $c_{\text{shift}} = 5.1$ such that $S_{\min} \approx 8.42$ and $S_{\max} \approx 10.28$. We are therefore in the situation where the integration domain $\tau \times \tilde{\tau}$ is completely enlighted (cf. Figure 4.4). Thus, $\mathbf{A}$ is in general densely populated with no vanishing entries. We set again $N = 32$ and compute the mean ranks of the TT- and QTT approximation of $\mathbf{A}$. The decay of the relative singular values of the reshaped matrix $\mathbf{B}$ is shown in Figure 4.5.

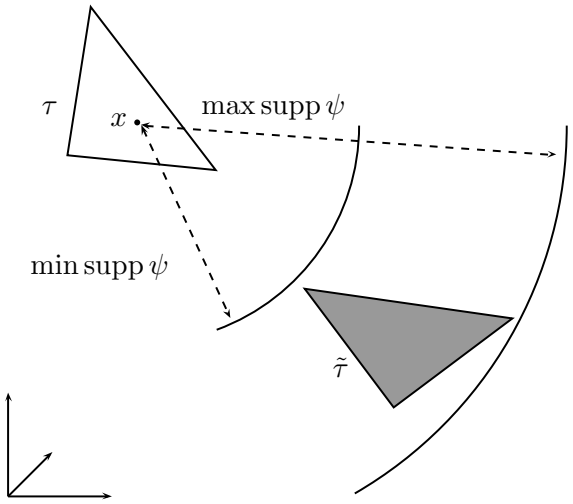

Figure 4.4: *Enlighted region for fixed $x \in \tau$ in Case 2.*

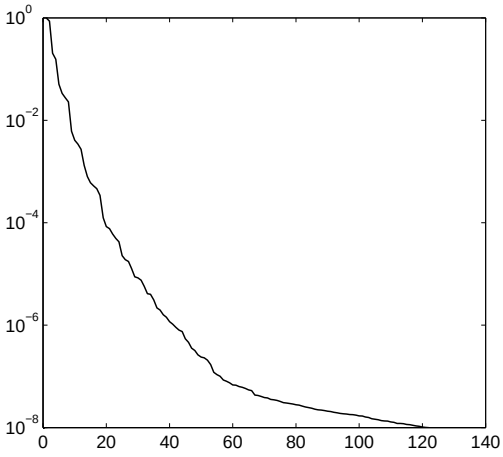

Figure 4.5: *Relative singular values of* $\mathbf{B}$*. Non-zero entries of* $\mathbf{B}$*: 100%.*

The results of the numerical experiments indicate that the compression rates in this case are very similar to Case 1. Thus a fully populated tensor $\mathbf{A}$ does not have a severe negative impact on the ranks of $\mathbf{A}_{TT}$ and $\mathbf{A}_{QTT}$ compared to a situation where the integration domain ist only partially enlighted and similar basis functions in time are used.

Accuracy	Mean rank of $\mathbf{A}_{TT}$	Mean rank of $\mathbf{A}_{QTT}$	Rel. SV of $\mathbf{B}$
10^{-2}	6.7	10.4	9
10^{-3}	9.8	18.2	14
10^{-4}	13.4	29.1	20
10^{-5}	18.4	40.5	29
10^{-6}	25.0	53.3	42

The next table shows the time that is needed to compute the different approximations of $I_{\tau,\tilde{\tau}}$. Thereby we again assume that $\mathbf{A}$,$\mathbf{A}_{TT}$ and $\mathbf{A}_{QTT}$ are given for each accuracy.

Accuracy	Time Q_G	Time Q_{TT}	$E_{G,TT}$	Time Q_{QTT}	$E_{G,QTT}$
10^{-2}	100	1.3	$7 \cdot 10^{-3}$	10.0	$5 \cdot 10^{-2}$
10^{-3}	100	1.4	$1 \cdot 10^{-3}$	10.3	$4 \cdot 10^{-4}$
10^{-4}	100	1.4	$8 \cdot 10^{-5}$	10.6	$4 \cdot 10^{-5}$
10^{-5}	100	1.5	$3 \cdot 10^{-6}$	10.8	$3 \cdot 10^{-6}$
10^{-6}	100	1.7	$4 \cdot 10^{-8}$	11.3	$1 \cdot 10^{-8}$

As expected the evaluation of the scalar product using the TT- and QTT approximation is considerably faster. Furthermore, the relative errors $E_{G,TT}$ and $E_{G,QTT}$ are, as in the previous case, small for medium accuracies of $\mathbf{A}_{TT}$ and $\mathbf{A}_{QTT}$.

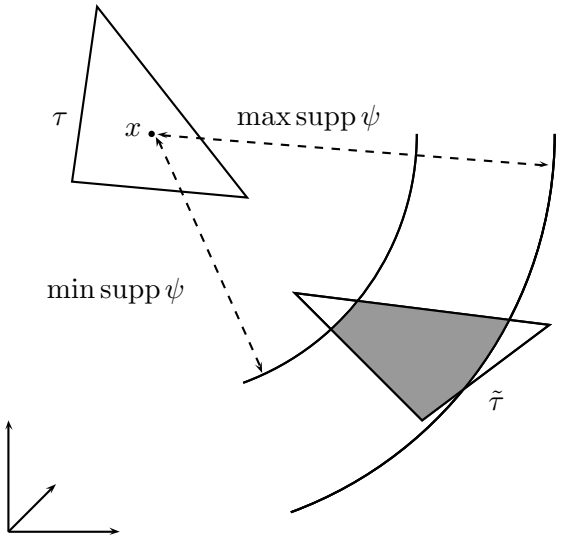

Figure 4.6: *Enlighted region for fixed $x \in \tau$ in Case 3.*

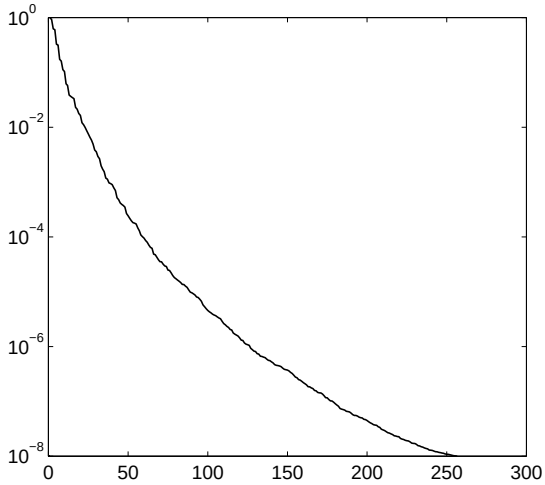

Figure 4.7: *Relative singular values of* $\mathbf{B}$*. Non-zero entries of* $\mathbf{B}$*:* $\approx 64\%$*.*

4.4.3 Case 3: Narrow discrete light cone

Here we want to examine how a narrow discrete light cone, i.e., the support of ψ is a small interval, influences the compression rates. Therefore we consider the time mesh

$$t_1 = 0.6, \quad t_2 = 0.8, \quad t_3 = 1.0, \quad t_4 = 10.3, \quad t_5 = 10.45, \quad t_6 = 10.7$$

such that $\operatorname{supp}\psi = [9.3, 10.1]$. Choosing $c_{\text{shift}} = 5.4$ leads to the case where $S_{\min} < 9.3$ and $S_{\max} > 10.1$. We are thus in the situation illustrated in Figure 4.6. We set again $N = 32$ and compute the mean ranks of the TT- and QTT approximation of $\mathbf{A}$ which has approximately 64% nonzero entries. The decay of the relative singular values of the reshaped matrix $\mathbf{B}$ is shown in Figure 4.7.

Accuracy	Mean rank of $\mathbf{A}_{TT}$	Mean rank of $\mathbf{A}_{QTT}$	Rel. SV of $\mathbf{B}$
10^{-2}	14.4	21.8	23
10^{-3}	23.3	46.8	37
10^{-4}	33.2	69.7	60
10^{-5}	44.3	97.1	89
10^{-6}	57.0	130.1	126

As one can see in the table above, the compression rates are worse than in the previous cases. This is not surprising since ψ has the same oscillatory behavior as before but varies on a smaller interval. The approximation of the tensor $\mathbf{A}$, which is based on the evaluation of ψ at different points in $\tau \times \tilde{\tau}$ and not only in a narrow strip containing the discrete light cone, is therefore clearly more difficult. This is confirmed by various numerical experiments. The narrower the discrete light cone is, the higher are the mean ranks of the TT- and QTT approximation of $\mathbf{A}$ in general. This case is therefore an example where a more sparse $\mathbf{A}$ does not lead to better compression rates.

Although the mean ranks of $\mathbf{A}_{TT}$ and $\mathbf{A}_{QTT}$ are larger here than in the previous cases, the compression is still good enough to reduce the computing times of the quadratures considerably.

Accuracy	Time Q_G	Time Q_{TT}	$E_{G,TT}$	Time Q_{QTT}	$E_{G,QTT}$
10^{-2}	100	1.3	$4 \cdot 10^{-1}$	9.0	$6 \cdot 10^{-1}$
10^{-3}	100	1.4	$1 \cdot 10^{-2}$	9.5	$2 \cdot 10^{-2}$
10^{-4}	100	1.6	$1 \cdot 10^{-4}$	10.2	$1 \cdot 10^{-3}$
10^{-5}	100	1.8	$5 \cdot 10^{-5}$	11.1	$5 \cdot 10^{-5}$
10^{-6}	100	2.1	$1 \cdot 10^{-6}$	12.4	$1 \cdot 10^{-6}$

Another effect that can be observed here is, that the errors $E_{G,TT}$ and $E_{G,QTT}$ decay slower than before. The approximations of $\mathbf{A}$ have therefore to be computed with higher accuracy in order to obtain good approximations of Q_G.

4.4.4 Case 4: Near field integrals

We now want to test the compression rates in the case where the triangles in (4.4.2) are close to each other. Since the integrand in (4.4.2) is weakly singular for $x = y$, the convergence rates of standard quadrature rules deteriorate for $\operatorname{dist}(\tau, \tilde{\tau}) \to 0$. We examine if low distances between the triangles also have a negative influence on the compression rates of the TT- and QTT-approximation. In order to test this numerically we use the triangles $\tau, \tilde{\tau}$ as before and set $c_{\text{shift}} = 1$. In this case we have

$$\operatorname{dist}(\tau, \tilde{\tau}) \approx 1.44 \qquad \text{and} \qquad \operatorname{maxdist}(\tau, \tilde{\tau}) \approx 3.20.$$

As time grid we choose

$$t_1 = 0.6, \quad t_2 = 1.2, \quad t_3 = 1.9, \quad t_4 = 4.2, \quad t_5 = 4.7, \quad t_6 = 5.7,$$

such that $\operatorname{supp} \psi = [2.3, 5.1]$. Thus, we are in the case of a partially enlighted integration domain as in Case 1. Setting again $N = 32$, we obtain the following mean ranks for $\mathbf{A}_{TT}$ and $\mathbf{A}_{QTT}$.

Accuracy	Mean rank of $\mathbf{A}_{TT}$	$E_{G,TT}$	Mean rank of $\mathbf{A}_{QTT}$	$E_{G,QTT}$
10^{-2}	5.5	$4 \cdot 10^{-3}$	7.4	$1 \cdot 10^{-3}$
10^{-3}	9.1	$2 \cdot 10^{-4}$	13.6	$6 \cdot 10^{-4}$
10^{-4}	13.8	$2 \cdot 10^{-6}$	22.1	$4 \cdot 10^{-5}$
10^{-5}	20.0	$9 \cdot 10^{-7}$	33.2	$5 \cdot 10^{-7}$
10^{-6}	27.4	$1 \cdot 10^{-8}$	46.0	$3 \cdot 10^{-8}$

As we can see above small distances between the triangles τ and $\tilde{\tau}$ do not have an influence on the compression rates of the TT- and QTT approximation and that the ranks are comparable to those in Case 1. Note however that the number of Gauss points N usually has to be chosen larger for such near field integrals in order to preserve a certain accuracy of the quadrature rule (cf. [26]).

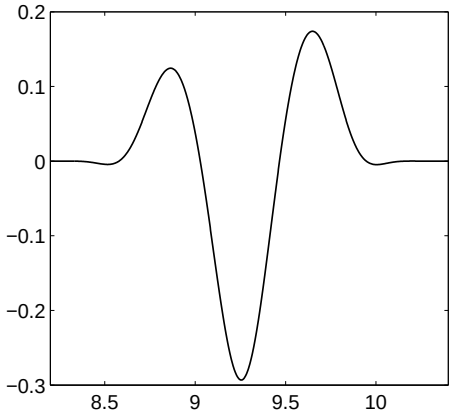

Figure 4.8: *Plot of $\psi_{high,1}$.*

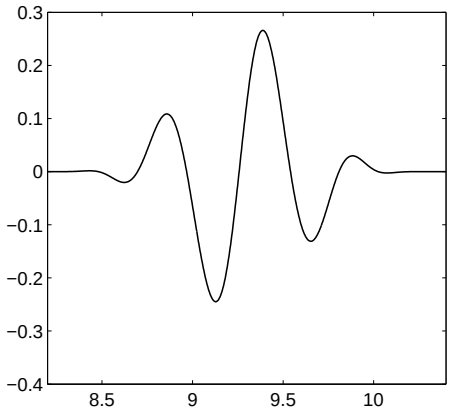

Figure 4.9: *Plot of $\psi_{high,2}$.*

As in Case 1, $E_{G,TT}$ and $E_{G,QTT}$ are quickly decreasing such that a relatively low accuracy of $\mathbf{A}_{TT}$ and $\mathbf{A}_{QTT}$ is sufficient for the quadrature. The computing times for Q_{TT} and Q_{QTT} are very similar to those in Case 1 and we therefore refrain from listing them here.

4.4.5 Case 5: Higher order basis functions in time

At last we examine the case of a higher order of the basis functions than considered before. Therefore we adopt the setting in Case 1, i.e., we use the time grid (4.4.4) and set c_{shift}=4.4. Instead of using the basis function in (4.4.1) we first set

$$b(t) = \rho_{t_1,t_2,t_3}(t) P_2\left(2\frac{t-t_1}{t_3-t_1} - 1\right) \qquad \text{and} \qquad \tilde{b}(t) = \rho_{t_4,t_5,t_6}(t) P_3\left(2\frac{t-t_4}{t_6-t_4} - 1\right),$$

where P_p denotes Legendre polynomials of degree p. We denote the corresponding function ψ in (4.4.3) by $\psi_{\text{high},1}$ (cf. Figure 4.8). As a second example we choose

$$b(t) = \rho_{t_1,t_2,t_3}(t) P_5\left(2\frac{t-t_1}{t_3-t_1} - 1\right) \qquad \text{and} \qquad \tilde{b}(t) = \rho_{t_4,t_5,t_6}(t) P_5\left(2\frac{t-t_4}{t_6-t_4} - 1\right).$$

As above we denote the corresponding ψ in (4.4.3) by $\psi_{\text{high},2}$ (cf. Figure 4.9). In the following we list the mean ranks and the relative errors for both settings.

Accuracy	Mean rank of $\mathbf{A}_{TT}$	$E_{G,TT}$	Mean rank of $\mathbf{A}_{QTT}$	$E_{G,QTT}$
10^{-2}	4.7	$4 \cdot 10^{-3}$	7.0	$3 \cdot 10^{-3}$
10^{-3}	8.5	$6 \cdot 10^{-5}$	13.3	$2 \cdot 10^{-4}$
10^{-4}	12.5	$4 \cdot 10^{-5}$	22.1	$6 \cdot 10^{-5}$
10^{-5}	18.3	$6 \cdot 10^{-6}$	32.2	$1 \cdot 10^{-5}$
10^{-6}	24.7	$6 \cdot 10^{-7}$	44.6	$1 \cdot 10^{-6}$

The table above shows the results for case $\psi_{\text{high},1}$. As we can see the mean ranks are not affected by the higher order of the basis functions in this example. They are even slightly lower than in Case 1. This is due to the fact that $\psi_{\text{high},1}$ is not considerably more oscillating

than ψ in Case 1 even though Legendre polynomials of higher order are involved. In order to see a negative effect of higher order basis function we have to consider Legendre polynomials of degree 5, i.e. $\psi_{\text{high},2}$, as the next table shows.

Accuracy	Mean rank of $\mathbf{A}_{TT}$	$E_{G,TT}$	Mean rank of $\mathbf{A}_{QTT}$	$E_{G,QTT}$
10^{-2}	5.5	$5 \cdot 10^{-1}$	9.1	$6 \cdot 10^{-1}$
10^{-3}	10.7	$1 \cdot 10^{-2}$	16.8	$3 \cdot 10^{-3}$
10^{-4}	14.3	$1 \cdot 10^{-3}$	26.8	$7 \cdot 10^{-5}$
10^{-5}	20.8	$4 \cdot 10^{-5}$	37.7	$2 \cdot 10^{-5}$
10^{-6}	27.5	$1 \cdot 10^{-5}$	50.9	$2 \cdot 10^{-5}$
10^{-7}	44.3	$5 \cdot 10^{-7}$	77.6	$1 \cdot 10^{-6}$

Also here we can see that the compression rates are not considerably worse than before or in Case 1 even though $\psi_{\text{high},2}$ is more oscillatory now. A negative aspect that becomes evident, however, is the slower decrease of $E_{G,TT}$ and $E_{G,QTT}$.

4.4.6 Example on QTT-cross approximation

As it was mentioned in Remark 4.3.4 the rank-r QTT-cross approximation takes the advantage of the log-volume cost $O(r^4 \log N)$ requiring an evaluation of only $O(r^2 \log N) \ll N^4$ entries. In the following we give the numerical illustration on QTT-cross approximation for Case 1 above. The next table presents the results of ε-QTT-cross approximation of the target tensor $\mathbf{A}$ of size $32 \times 32 \times 32 \times 32$. We give the CPU time (sec.), QTT and TT ε-ranks and the relative storage size for the obtained TT and QTT approximations. In all cases the storage cost of QTT representation is lower than those for the TT-format.

ε	10^{-6}	10^{-5}	10^{-4}
Time (sec.)	10.4	6.3	3.1
QTT-rank	31	21	14
TT-rank	18	13	9
stor(TT)/stor(QTT)	1.14	1.17	1.24

Finally we notice that the numerical evaluation of the full tensor $\mathbf{A}$ amounts to 321 seconds. For the evaluation of the tensor entries we approximated ψ in (4.4.3) using Gauss quadrature with 100 points. This high order of approximation is necessary in order to maintain the smoothness of the integrand which is crucial for the good compression rates observed above. Note that an accurate approximation of the 1-dimensional function $\psi(s)$ on a suitable interval by simpler functions, e.g., (piecewise) polynomials, could lead to a further reduction of the computing times.

4.5 Conclusion

In this paper, we have presented a new method for the efficient evaluation of the integrals which arise from the direct discretization of retarded potential integral operators. Since

the integrands are C^∞ but, in general, not analytic the number of quadrature points is relatively large while the total number of such integrals is huge during the generation of the system matrix. We have introduced the TT and the QTT representations for the four-dimensional quadrature tensors arising from the evaluation of the (transformed) integrands at the quadrature points in the four-dimensional unit cube. We have systematically tested the sensitivity of the algorithm with respect a) to different cases how the smeared discrete light cone intersects the spatial mesh, b) to the distance of the surface panels inducing different nearly-singular behaviors of the integrands, and c) to the polynomial degree of the temporal approximation. In all cases the compression by the TT and QTT representation is impressive.

Since both, the TT and the QTT formats require as input the full tensor it is important to substitute the corresponding full-to-TT and full-to-QTT approximation algorithms by their adaptive cross versions. We have performed numerical experiments which show that the compression rates by the adaptive TT-cross and QTT-cross representations are comparable with the original ones while the generation of the full tensor can be avoided.

Acknowledgement. The authors are thankful to Dr. I. Oseledets (INM RAS, Moscow) for the assistance with the QTT-cross-approximation MATLAB routine.

References

[1] J. Ballani. Fast evaluation of singular BEM integrals based on tensor approximations. Preprint 77/2010, MPI MiS, Leipzig 2010.

[2] A. Bamberger and T. Ha Duong. Formulation Variationnelle Espace-Temps pur le Calcul par Potientiel Retardé de la Diffraction d'une Onde Acoustique. *Math. Meth. in the Appl. Sci.*, 8:405–435, 1986.

[3] L. Banjai. Multistep and multistage convolution quadrature for the wave equation: Algorithms and experiments. *SIAM J. Sci. Comput.*, 32(5):2964–2994, 2010.

[4] L. Banjai and S. Sauter. Rapid solution of the wave equation in unbounded domains. *SIAM Journal on Numerical Analysis*, 47:227–249, 2008.

[5] L. Banjai and M. Schanz. Wave Propagation Problems treated with Convolution Quadrature and BEM. Preprint 60/2010, MPI Leipzig.

[6] Q. Chen, P. Monk, X. Wang, and D. Weile. Analysis of Convolution Quadrature Applied to the Time-Domain Electric Field Integral Equation. *Submitted.*

[7] Y. Ding, A. Forestier, and T. Ha Duong. A Galerkin scheme for the time domain integral equation of acoustic scattering from a hard surface. *The Journal of the Acoustical Society of America*, 86(4):1566–1572, 1989.

[8] J. El Gharib. *Problèmes de potentiels rétardes pour l'acoustique.* PhD thesis, École Polytechnique, 1999.

[9] T. Ha-Duong. On retarded potential boundary integral equations and their discretisation. In *Topics in Computational Wave Propagation: Direct and Iverse Problems*, volume 31 of *Lect. Notes Comput. Sci. Eng.*, pages 301–336. Springer, Berlin, 2003.

[10] T. Ha-Duong, B. Ludwig, and I. Terrasse. A Galerkin BEM for transient acoustic scattering by an absorbing obstacle. *International Journal for Numerical Methods in Engineering*, 57:1845–1882, 2003.

[11] W. Hackbusch, B. N. Khoromskij, S. Sauter, and E. Tyrtyshnikov. Use of Tensor Formats in Elliptic Eigenvalue Problems. Preprint 78, MPI MiS, Leipzig 2008. Numer. Lin. Alg. Appl., 2011, DOI: 10.1002/nla.793.

[12] W. Hackbusch, W. Kress, and S. Sauter. Sparse convolution quadrature for time domain boundary integral formulations of the wave equation by cutoff and panel-clustering. In M. Schanz and O. Steinbach, editors, *Boundary Element Analysis*, pages 113–134. Springer, 2007.

[13] W. Hackbusch, W. Kress, and S. Sauter. Sparse convolution quadrature for time domain boundary integral formulations of the wave equation. *IMA, J. Numer. Anal.*, 29:158–179, 2009.

[14] W. Hackbusch and S. Kühn. A new scheme for the tensor representation. *J. of Fourier analysis and applications*, 15:706–722, 2009.

[15] S. Holtz, T. Rohwedder, and R. Schneider. On manifold of tensors of fixed TT-rank. Technical Report 61, TU Berlin, 2010.

[16] B. N. Khoromskij. Introduction to Tensor Numerical Methods in Scientific Computing. Lecture Notes, University/ETH Zürich, Preprint 06-2011, Universität Zürich 2011, pp. 1-238.

[17] B. N. Khoromskij. Tensors-structured Numerical Methods in Scientific Computing: Survey on Recent Advances. Preprint 21/2010, MPI MIS Leipzig 2010 (submitted).

[18] B. N. Khoromskij. $O(d \log N)$-Quantics Approximation of N-d Tensors in High-Dimensional Numerical Modeling. *Constructive Approximation*, pages 1–24, 2011. DOI: 10.1007/s00365-011-9131-1. Preprint 55/2009 MPI MIS, Leipzig 2009.

[19] B. N. Khoromskij, V. Khoromskaia, and H.-J. Flad. Numerical Solution of the Hartree-Fock Equation in Multilevel Tensor-structured Format. *SIAM J. on Sci. Comp.*, 33(1):45–65, 2011.

[20] B. N. Khoromskij and I. Oseledets. Quantics-TT approximation of elliptic solution operators in higher dimensions. Preprint MPI MIS 79/2009, Leipzig 2009. To appear in Rus. J. of Numerical Math., 2010.

[21] T. G. Kolda and B. W. Bader. Tensor decompositions and applications. *SIAM Review*, 51/3:455–500, 2009.

[22] J. C. Nédélec, T. Abboud, and J. Volakis. Stable solution of the retarded potential equations, Applied Computational Electromagnetics Society (ACES) Symposium Digest, 17th Annual Review of Progress, Monterey, 2001.

[23] I. V. Oseledets. Approximation of $2^d \times 2^d$ matrices using tensor decomposition. *SIAM J. Matrix Anal. Appl.*, 31(4):2130–2145, 2010.

[24] I. V. Oseledets and E. E. Tyrtyshnikov. Breaking the Curse of Dimensionality, or How to Use SVD in Many Dimensions. *SIAM J. Sci. Comp.*, 31:3744–3759, 2009.

[25] I. V. Oseledets and E. E. Tyrtyshnikov. TT-cross approximation for multidimensional arrays. *Lin. Alg. and its Applications*, 432:70–88, 2010.

[26] S. Sauter and C. Schwab. *Boundary Element Methods.* Springer, Heidelberg, 2010.

[27] S. Sauter and A. Veit. Adaptive Time Discretization for Retarded Potentials. Preprint 04-2011, Universität Zürich.

[28] S. Sauter and A. Veit. Explicit Solutions of Retarded Boundary Integral Equations. Preprint 03-2011, Universität Zürich.

[29] S. A. Sauter. *Über die effiziente Verwendung des Galerkinverfahrens zur Lösung Fredholmscher Integralgleichungen.* PhD thesis, Inst. f. Prakt. Math., Universität Kiel, 1992.

[30] E. P. Stephan, M. Maischak, and E. Ostermann. Transient boundary element method and numerical evaluation of retarded potentials. In *Computational Science - ICCS 2008*, pages 321–330. Springer (5102), 2008.

[31] G. Vidal. Efficient classical simulation of slightly entangled quantum computations. *Phys. Rev. Lett.*, 91(14):147902–1 147902–4, 2003.

[32] H. Wang and M. Thoss. Multilayer formulation of the multiconfiguration time-dependent Hartree theory. *J. Chem. Phys.*, 119:1289–1299, 2003.

[33] X. Wang, R. A. Wildman, D. S. Weile, and P. Monk. A finite difference delay modeling approach to the discretization of the time domain integral equations of electromagnetics. *IEEE Transactions on Antennas and Propagation*, 56(8):2442–2452, 2008.

[34] D. S. Weile, A. A. Ergin, B. Shanker, and E. Michielssen. An accurate discretization scheme for the numerical solution of time domain integral equations. *IEEE Antennas and Propagation Society International Symposium*, 2:741–744, 2000.

[35] D. S. Weile, G. Pisharody, N. W. Chen, B. Shanker, and E. Michielssen. A novel scheme for the solution of the time-domain integral equations of electromagnetics. *IEEE Transactions on Antennas and Propagation*, 52:283–295, 2004.

[36] D. S. Weile, B. Shanker, and E. Michielssen. An accurate scheme for the numerical solution of the time domain electric field integral equation. *IEEE Antennas and Propagation Society International Symposium*, 4:516–519, 2001.

[37] S. R. White. Density-matrix algorithms for quantum renormalization groups. *Phys. Rev. B*, 48(14):10345–10356, 1993.

[38] A. Wildman, G. Pisharody, D. S. Weile, S. Balasubramaniam, and E. Michielssen. An accurate scheme for the solution of the time-domain integral equations of electromagnetics using higher order vector bases and bandlimited extrapolation. *IEEE Transactions on Antennas and Propagation*, 52:2973–2984, 2004.

5

[Preprint 14-2011, Institute of Mathematics, University of Zurich]

Numerical Solution of Exterior Maxwell Problems by Galerkin BEM and Runge-Kutta Convolution Quadrature

J. Ballani* L. Banjai† S. Sauter‡ A. Veit§

Abstract

In this paper we consider time-dependent electromagnetic scattering problems from conducting objects. We discretize the time-domain electric field integral equation using Runge-Kutta convolution quadrature in time and a Galerkin method in space. We analyze the involved operators in the Laplace domain and obtain convergence results for the fully discrete scheme. Numerical experiments indicate the sharpness of the theoretical estimates.

AMS subject classifications: 78A45, 65N38, 65R20

Key words: Electromagnetic scattering, boundary integral equations, Runge-Kutta convolution quadrature, boundary element methods.

5.1 Introduction

Electromagnetic scattering problems in three dimensions have a wide range of practical applications in physics and engineering, prominent examples being magnetic resonance imaging,

*Max-Planck-Institut für Mathematik in den Naturwissenschaften, Inselstr. 22-26, 04103 Leipzig, Germany, e-mail: Jonas.Ballani@mis.mpg.de

†Max-Planck-Institut für Mathematik in den Naturwissenschaften, Inselstr. 22-26, 04103 Leipzig, Germany, e-mail: Lehel.Banjai@mis.mpg.de

‡Institut für Mathematik, Universität Zürich, Winterthurerstrasse 190, CH-8057 Zürich, Switzerland, e-mail: stas@math.uzh.ch

§Institut für Mathematik, Universität Zürich, Winterthurerstrasse 190, CH-8057 Zürich, Switzerland, e-mail: alexander.veit@math.uzh.ch

remote sensing systems or global positioning systems. The efficient and accurate numerical solution of such wave propagation phenomena in the time-domain has gained growing attention in the last years. Since such problems are typically formulated in unbounded domains the method of integral equations is an elegant tool to transform the underlying set of partial differential equations into time-domain boundary integral equations (TDBIEs) on the bounded surface of the scatterer.

Although the numerical solution of TDBIEs has been pursued since the 1960s (cf. [15]), their use was unpopular for a long time due to the need to deal with distributional fundamental solutions and due to stability problems of the resulting implementations. More recent numerical methods have overcome these stability issues. Important discretization techniques include Galerkin methods based on space-time variational formulations (cf. [3, 30, 36, 2, 1, 16, 33]) and methods based on bandlimited interpolation and extrapolation (cf. [40, 39, 41, 42]).

An alternative approach to solve TDBIEs numerically is based on convolution quadrature. Developed more than 20 years ago (cf. [23, 24]), convolution quadrature based on linear multistep methods has been applied to numerous problems (cf. [25, 7, 35, 34, 38, 12]); fast numerical implementations were developed in [18, 17, 20] . For a review on convolution quadrature and its applications we refer to [26, 8]. The advantages of this discretization scheme for TDBIEs include its excellent stability properties and the fact that only the Laplace transform of the time-domain fundamental solution is used and thus distributional kernels are avoided. An important assumption for the stability of convolution quadrature is the A-stability of the underlying time-discretization method. Since A-stable linear multistep methods cannot exceed a convergence order of 2, convolution quadratures based on Runge-Kutta methods have recently been considered and analyzed in order to obtain high order schemes (cf. [27, 4, 5, 6]). Most related to our work is [12] where multistep methods are considered for the time discretization and an error analysis is presented. Some of the stability estimates could be improved in our paper so that the regularity assumptions with respect to time are relaxed.

In this paper we are interested in the propagation of time-dependent electromagnetic fields in a homogeneous medium arising from the scattering of incoming waves at a perfectly conducting obstacle. In order to solve the resulting time-domain electric field integral equation (EFIE) numerically we use Runge-Kutta convolution quadrature for the time discretization and a Galerkin method for the discretization in space. The aim of this paper is, for the first time, to fully analyze this numerical method. We do this by first analyzing the Laplace domain EFIE operator $\mathcal{V}$ to show that the inverse operator can be polynomially bounded by

$$\left\|\mathcal{V}^{-1}(s)\right\| \leq C(\sigma_0)\,\frac{|s|}{\operatorname{Re} s}$$

for $\operatorname{Re} s \geq \sigma_0 > 0$ and some $\sigma_0 > 0$. This allows us to use the analysis of Runge-Kutta convolution quadrature in [6] to obtain convergence estimates for the semi-discrete scheme. For the space discretization we use the classical Raviart-Thomas elements of lowest order. Using the results of the semi-discrete case we finally obtain convergence results for the fully discrete scheme. We perform numerical test with a spherical scatterer. The results indicate the sharpness of the derived convergence estimates.

5.2 Sobolev Spaces and Trace Theorems

Let Ω_- be an open bounded set in $\mathbb{R}^3$ with Lipschitz boundary Γ, unitary outer normal $\mathbf{n}$, and complement $\Omega_+ := \mathbb{R}^3 \setminus \overline{\Omega_-}$. The inner product of two vectors $\mathbf{a}, \mathbf{b} \in \mathbb{C}^3$ is denoted

by $\mathbf{a}.\mathbf{b}$, $\mathbf{a}\times\mathbf{b}$ is the usual vectorial product. Let Ω either be Ω_- or Ω_+. For $u\in \mathrm{L}^2(\Omega)$ or $\mathbf{v}\in\mathbf{L}^2(\Gamma):=\mathrm{L}^2(\Omega)^3$, let

$$\|u\|_{0,\Omega}=\left(\int_\Omega |u(\mathbf{x})|^2\,d\mathbf{x}\right)^{1/2}\quad\text{resp.}\quad \|\mathbf{v}\|_{0,\Omega}=\left(\sum_{i=1}^3\|v_i\|_{0,\Omega}^2\right)^{1/2}$$

be the norms of $u,\mathbf{v}$ in these spaces. We define the following Hilbert spaces with their associated graph norms:

$$\begin{aligned}\mathbf{H}(\mathrm{curl},\Omega)&:=\left\{\mathbf{v}\in\mathbf{L}^2(\Gamma),\,\mathrm{curl}\,\mathbf{v}\in\mathbf{L}^2(\Gamma)\right\},\\ \|\mathbf{v}\|_{\mathrm{curl},\Omega}&=\left(\|\mathbf{v}\|_{0,\Omega}^2+\|\mathrm{curl}\,\mathbf{v}\|_{0,\Omega}^2\right)^{1/2}\end{aligned}$$

and in a similar manner

$$\begin{aligned}\mathbf{H}(\mathrm{div},\Omega)&:=\left\{\mathbf{v}\in\mathbf{L}^2(\Gamma),\,\mathrm{div}\,\mathbf{v}\in\mathrm{L}^2(\Omega)\right\},\\ \|\mathbf{v}\|_{\mathrm{div},\Omega}&=\left(\|\mathbf{v}\|_{0,\Omega}^2+\|\mathrm{div}\,\mathbf{v}\|_{0,\Omega}^2\right)^{1/2}.\end{aligned}$$

We will further require the $\mathbf{L}^2(\Gamma)$ space of tangential fields,

$$\mathbf{L}_t^2(\Gamma):=\{\mathbf{v}\in\mathbf{L}^2(\Gamma)|\mathbf{n}.\mathbf{v}=0\text{ on }\Gamma\}$$

and the following trace operators Π_τ and γ_τ mapping $\mathscr{D}(\overline{\Omega})=\{\phi|_\Omega\mid\phi\in C^\infty_{comp}(\mathbb{R}^3)\}$ to $\mathbf{L}_t^2(\Gamma)$

$$\Pi_\tau:\mathbf{u}\mapsto\mathbf{n}\times(\mathbf{u}\times\mathbf{n})|_\Gamma\quad\text{and}\quad\gamma_\tau:\mathbf{u}\mapsto\mathbf{u}|_\Gamma\times\mathbf{n}.$$

Adhering to [11], we define the following Hilbert spaces

$$V:=\mathbf{H}^{1/2}(\Gamma),\qquad V_\gamma:=\gamma_\tau(V),\qquad V_\Pi:=\Pi_\tau(V),$$

with norms that assure the continuity of the trace operators

$$\|\boldsymbol{\lambda}\|_{V_\gamma}=\inf_{\mathbf{u}\in V}\{\|\mathbf{u}\|_V\mid\gamma_\tau(\mathbf{u})=\boldsymbol{\lambda}\}$$

and

$$\|\boldsymbol{\lambda}\|_{V_\Pi}=\inf_{\mathbf{u}\in V}\{\|\mathbf{u}\|_V\mid\Pi_\tau(\mathbf{u})=\boldsymbol{\lambda}\}.$$

Further, we denote by V_Π' and V_γ' the respective dual spaces with $\mathbf{L}_t^2(\Gamma)$ as the pivot space and their natural norms. We are now ready, see [11], to introduce the following Hilbert spaces on Γ:

$$\begin{aligned}\mathbf{H}^{-1/2}(\mathrm{div}_\Gamma,\Gamma)&:=\{\mathbf{v}\in V_\gamma'\mid\mathrm{div}_\Gamma\,\mathbf{v}\in H^{-1/2}(\Gamma)\},\\ \mathbf{H}^{-1/2}(\mathrm{curl}_\Gamma,\Gamma)&:=\{\mathbf{v}\in V_\Pi'\mid\mathrm{curl}_\Gamma\,\mathbf{v}\in H^{-1/2}(\Gamma)\}\end{aligned}$$

with norms defined as

$$\begin{aligned}\|\mathbf{v}\|_{-1/2,\mathrm{div}_\Gamma}&:=\left\{\|\mathbf{v}\|_{V_\gamma'}^2+\|\mathrm{div}_\Gamma\,\mathbf{v}\|_{H^{-1/2}(\Gamma)}^2\right\}^{1/2},\\ \|\mathbf{v}\|_{-1/2,\mathrm{curl}_\Gamma}&:=\left\{\|\mathbf{v}\|_{V_\Pi'}^2+\|\mathrm{curl}_\Gamma\,\mathbf{v}\|_{H^{-1/2}(\Gamma)}^2\right\}^{1/2}.\end{aligned}\tag{5.2.1}$$

The unknown densities which arise in the boundary integral equations for the Maxwell problem are traces of vector fields in $\mathbf{H}(\mathrm{curl},\Omega_+)$. The following theorem shows that $\mathbf{H}^{-1/2}(\mathrm{div}_\Gamma,\Gamma)$ and $\mathbf{H}^{-1/2}(\mathrm{curl}_\Gamma,\Gamma)$ are the correct spaces for these densities.

Theorem 5.2.1. *Let $\Omega \in \{\Omega_-, \Omega_+\}$. The trace mappings*

$$\Pi_\tau^\Omega : \mathbf{H}(\mathrm{curl}, \Omega) \;\to\; \mathbf{H}^{-1/2}(\mathrm{curl}_\Gamma, \Gamma)$$

and

$$\gamma_\tau^\Omega : \mathbf{H}(\mathrm{curl}, \Omega) \;\to\; \mathbf{H}^{-1/2}(\mathrm{div}_\Gamma, \Gamma)$$

are continuous and surjective. Moreover, there exist continuous liftings for these trace operators in $\mathbf{H}(curl, \Omega)$.

For a proof we refer to [11, Theorem 4.1]. As an important consequence of Theorem 5.2.1 we get the following *Green's formula*. For this, we put $\mathbf{H}^{-1/2}(\mathrm{curl}_\Gamma, \Gamma)$ and $\mathbf{H}^{-1/2}(\mathrm{div}_\Gamma, \Gamma)$ in duality when $\mathbf{L}_t^2(\Omega)$ is used as pivot space (cf. [11, Section 5]). More precisely, the usual $\mathbf{L}_t^2(\Gamma)$ scalar product can be continuously extended to a sesqui-linear duality pairing

$$(\cdot,\cdot)_\Gamma : \mathbf{H}^{-1/2}(\mathrm{div}_\Gamma, \Gamma) \times \mathbf{H}^{-1/2}(\mathrm{curl}_\Gamma, \Gamma) \to \mathbb{C}$$

by means of Green's formula: For all $\mathbf{u}, \mathbf{v} \in \mathbf{H}(\mathrm{curl}, \Omega)$

$$\mathrm{sign}\,(\Omega) \int_\Omega (\overline{\mathbf{u}} \,.\, \mathrm{curl}\, \mathbf{v} - \mathrm{curl}\, \overline{\mathbf{u}} \,.\, \mathbf{v})\, d\mathbf{x} = \left(\gamma_\tau^\Omega \mathbf{u}, \Pi_\tau^\Omega \mathbf{v}\right)_\Gamma \quad \text{with} \quad \mathrm{sign}\,(\Omega) := \begin{cases} -1, & \Omega = \Omega_+, \\ +1, & \Omega = \Omega_-. \end{cases} \tag{5.2.2}$$

Note that the complex conjugation in $(\cdot,\cdot)_\Gamma$ is on the first argument. This will be of importance in Section 5.4.4.

For bounded, smooth domains, Green's formula is proved in [28] and for Lipschitz domains in [9, 11]. For exterior domains Ω_+, this follows by employing a cutoff function and the dense embedding

$$\left\{ u|_{\Omega_+} : u \in C^\infty_{\mathrm{comp}}(\mathbb{R}^3) \right\} \hookrightarrow \mathbf{H}\,(\mathrm{curl}, \Omega)$$

and applying Green's formula for bounded domains.

Finally, as another consequence of the duality of the two trace spaces $\mathbf{H}^{-1/2}(\mathrm{div}_\Gamma, \Gamma)$ and $\mathbf{H}^{-1/2}(\mathrm{curl}_\Gamma, \Gamma)$ with $\mathbf{L}_t^2(\Gamma)$ as the pivot space (see (36) in [11]) we have the identities

$$\|\mathbf{u}\|_{-1/2,\mathrm{div}} = \sup_{\boldsymbol{\varphi} \in \mathbf{H}^{-1/2}(\mathrm{curl}_\Gamma, \Gamma)} \frac{|(\mathbf{u}, \boldsymbol{\varphi})_\Gamma|}{\|\boldsymbol{\varphi}\|_{-1/2,\mathrm{curl}}} \tag{5.2.3a}$$

and

$$\|\mathbf{v}\|_{-1/2,\mathrm{curl}} = \sup_{\boldsymbol{\varphi} \in \mathbf{H}^{-1/2}(\mathrm{div}_\Gamma, \Gamma)} \frac{|(\mathbf{v}, \boldsymbol{\varphi})_\Gamma|}{\|\boldsymbol{\varphi}\|_{-1/2,\mathrm{div}}}. \tag{5.2.3b}$$

Remark 5.2.2. *In the remainder of the paper we may, in order to enhance readability, use both the classical notation $\mathbf{n} \times (\cdot \times \mathbf{n})$ and $\cdot \times \mathbf{n}$ and the notation Π_τ and γ_τ, even though strictly speaking only the latter should be used.*

5.3 Integral Formulation for Exterior Scattering Problems

In the following we will be concerned with the propagation of time-dependent electromagnetic fields near a perfectly conducting body. We consider three-dimensional exterior scattering problems in a homogeneous, isotropic medium with constant, positive electric permittivity ε and constant, positive magnetic permeability μ. Furthermore we assume that there are no external sources.

Let Ω_- be a three-dimensional perfectly conducting object with bounded Lipschitz surface Γ and let $(\mathbf{E}^{\text{inc}}, \mathbf{H}^{\text{inc}})$ be an incident electromagnetic field. The scattered field $(\mathbf{E}, \mathbf{H})$ satisfies the time dependent Maxwell equations:

$$-\varepsilon \frac{\partial \mathbf{E}}{\partial t} + \operatorname{curl} \mathbf{H} = \mathbf{0} \quad \text{in } \mathbb{R}_+ \times \Omega_+, \tag{5.3.1}$$

$$\mu \frac{\partial \mathbf{H}}{\partial t} + \operatorname{curl} \mathbf{E} = \mathbf{0} \quad \text{in } \mathbb{R}_+ \times \Omega_+, \tag{5.3.2}$$

$$\operatorname{div} \mathbf{E} = \operatorname{div} \mathbf{H} = 0 \quad \text{in } \mathbb{R}_+ \times \Omega_+, \tag{5.3.3}$$

with boundary conditions

$$(\mathbf{E} + \mathbf{E}^{\text{inc}}) \times \mathbf{n} = \mathbf{0} \quad \text{on } \mathbb{R}_+ \times \Gamma \tag{5.3.4}$$

and initial conditions

$$\mathbf{E}(t, \mathbf{x}) = \mathbf{H}(t, \mathbf{x}) = \mathbf{0} \quad \text{for } t \leq 0 \text{ and } \mathbf{x} \in \Omega_+.$$

Since our problem is formulated in unbounded domains we use the method of integral equations to transform this set of partial differential equations to integral equations on the bounded surface of the scatterer. These can be derived by inverse Laplace transformation of the more widely known frequency domain integral representations, see (5.6.4–6) in [28], as we explain next. The application of the Laplace transform, i.e., $\hat{\mathbf{E}} := \mathscr{L}\mathbf{E} = \int_0^t \mathrm{e}^{-st}\, \mathbf{E}(\cdot, t) dt$, to equations (5.3.1) and (5.3.2) leads to

$$-\varepsilon s \hat{\mathbf{E}} + \operatorname{curl} \hat{\mathbf{H}} = \mathbf{0} \quad \text{in } \Omega_+,$$

$$\mu s \hat{\mathbf{H}} + \operatorname{curl} \hat{\mathbf{E}} = \mathbf{0} \quad \text{in } \Omega_+,$$

with boundary condition

$$(\hat{\mathbf{E}} + \hat{\mathbf{E}}^{\text{inc}}) \times \mathbf{n} = \mathbf{0} \qquad \text{on } \Gamma.$$

The boundary integral representation for the solution of the above Laplace domain boundary value problem is given by

$$\hat{\mathbf{E}}(\mathbf{y}) = -s\mu \int_\Gamma K(s, \mathbf{x} - \mathbf{y}) \mathbf{j}(\mathbf{x}) d\Gamma_{\mathbf{x}} + \frac{1}{\varepsilon} \nabla \int_\Gamma K(s, \mathbf{x} - \mathbf{y}) \frac{1}{s} \operatorname{div}_\Gamma \mathbf{j}(\mathbf{x}) d\Gamma_{\mathbf{x}}, \tag{5.3.5}$$

$$\hat{\mathbf{H}}(\mathbf{y}) = \operatorname{curl} \int_\Gamma K(s, \mathbf{x} - \mathbf{y}) \mathbf{j}(\mathbf{x}) d\Gamma_{\mathbf{x}}, \tag{5.3.6}$$

where the free space Green's function for the Helmholtz operator is given by

$$K(s, \mathbf{z}) := \frac{\mathrm{e}^{-s\sqrt{\varepsilon\mu}\|\mathbf{z}\|}}{4\pi \|\mathbf{z}\|}. \tag{5.3.7}$$

Taking the inverse Laplace transform of the above formulation gives the time-domain electric field integral equation (EFIE):

$$\begin{aligned} \mathbf{E}(t, \mathbf{y}) = &-\mu \int_0^t \int_\Gamma k(t - \tau, \mathbf{x} - \mathbf{y})\, \partial_t \mathbf{j}(\tau, \mathbf{x})\, d\Gamma_{\mathbf{x}}\, d\tau \\ &- \frac{1}{\varepsilon} \nabla \int_0^t \int_\Gamma k(t - \tau, \mathbf{x} - \mathbf{y})\, q(\tau, \mathbf{x})\, d\Gamma_{\mathbf{x}}\, d\tau \end{aligned} \tag{5.3.8}$$

$$\mathbf{H}(t,\mathbf{y}) = \operatorname{curl} \int_0^t \int_\Gamma k(t-\tau, \mathbf{x}-\mathbf{y})\, \mathbf{j}(\tau,\mathbf{x})\, d\Gamma_{\mathbf{x}}\, d\tau$$

for $\mathbf{y} \in \Omega_+ \setminus \Gamma$, involving the electric surface current density $\mathbf{j}$, the charge density q

$$q(t,\mathbf{x}) = -\int_0^t \operatorname{div}_\Gamma \mathbf{j}(\tau,\mathbf{x}) d\tau, \tag{5.3.9}$$

and the time domain free space Green's function

$$k(t,\mathbf{z}) := \mathscr{L}^{-1}\{K(\cdot,\mathbf{z})\}(t) = \frac{\delta(t-\sqrt{\varepsilon\mu}\|\mathbf{z}\|)}{4\pi\|\mathbf{z}\|}, \tag{5.3.10}$$

where δ denotes the Dirac delta function. It can be easily checked that for any $\mathbf{j}$ and q satisfying (5.3.9), $\mathbf{E}$ and $\mathbf{H}$ given by the representation formula (5.3.8) satisfy (5.3.1), (5.3.2), and (5.3.3). The initial conditions are also satisfied since we assume that $\mathbf{j}(\tau,\mathbf{y}) = \mathbf{0}$ and $q(\tau,\mathbf{y}) = 0$ for $\tau \le 0$ and $\mathbf{y} \in \Omega_+ \setminus \Gamma$. The unknown density functions are now determined via the boundary condition (5.3.4). This requires the extension of $\mathbf{E} \times \mathbf{n}$ to the boundary Γ which can be done continuously (cf. [28]). The resulting integral equation we have to solve reads

$$\begin{aligned} -\mu\Pi_\tau \int_0^t \int_\Gamma k(t-\tau,\mathbf{x}-\mathbf{y})\mathbf{j}_t(\tau,\mathbf{x})\, d\Gamma_{\mathbf{x}} d\tau \\ -\frac{1}{\varepsilon}\nabla_\Gamma \int_0^t \int_\Gamma k(t-\tau,\mathbf{x}-\mathbf{y}) q(\tau,\mathbf{x})\, d\Gamma_{\mathbf{x}} d\tau = \mathbf{n}(\mathbf{y}) \times \mathbf{g}(t,\mathbf{y}) \quad \text{for } (t,\mathbf{y}) \in \mathbb{R}\times\Gamma, \end{aligned} \tag{5.3.11}$$

with

$$\mathbf{g} := -\mathbf{E}^{\text{inc}} \times \mathbf{n}, \tag{5.3.12}$$

$\mathbf{j}_t = \partial_t \mathbf{j}$, and ∇_Γ the surface gradient.

In order to eliminate the unknown q and for further reasons that will become apparent in the next section, see Remark 5.4.3, we differentiate both sides of the above equation with respect to time to obtain

$$\begin{aligned} -\mu\Pi_\tau \int_0^t \int_\Gamma k(t-\tau,\mathbf{x}-\mathbf{y})\mathbf{j}_{tt}(\tau,\mathbf{x})\, d\Gamma_{\mathbf{x}} d\tau \\ +\frac{1}{\varepsilon}\nabla_\Gamma \int_0^t \int_\Gamma k(t-\tau,\mathbf{x}-\mathbf{y}) \operatorname{div}_\Gamma \mathbf{j}(\tau,\mathbf{x})\, d\Gamma_{\mathbf{x}} d\tau = \mathbf{n}(\mathbf{y}) \times \mathbf{g}_t(t,\mathbf{y}) \end{aligned} \tag{5.3.13}$$

which we have to solve for all $(t,\mathbf{y}) \in \mathbb{R}\times\Gamma$. Note that this integral equation contains only the unknown electric surface current density $\mathbf{j}$.

5.4 Numerical Discretization

5.4.1 Time Discretization

For the time discretization we will make use of convolution quadrature based on a Runge-Kutta method. An m-stage Runge-Kutta method in the standard Butcher tableau notation can be described by the matrix $\mathbf{A} = (a_{ij})_{i,j=1}^m \in \mathbb{R}^{m\times m}$ and the vectors $\mathbf{b} = (b_1, b_2, \ldots, b_m)^T \in$

$\mathbb{R}^m$ and $\mathbf{c} = (c_1, c_2, \ldots, c_m)^T$. The corresponding Runge-Kutta discretization of the initial value problem $y' = f(t, y), y(0) = y_0$, is then given by

$$Y_{ni} = y_n + \Delta t \sum_{j=1}^{m} a_{ij} f(t_n + c_j \Delta t, Y_{nj}), \qquad i = 1, \ldots, m,$$

$$y_{n+1} = y_n + \Delta t \sum_{j=1}^{m} b_j f(t_n + c_j \Delta t, Y_{nj});$$

here $\Delta t > 0$ is the time-step and $t_j = j\Delta t$. The values Y_{ni} and y_n are approximations to $y(t_n + c_i \Delta t)$ and $y(t_n)$, respectively. This Runge-Kutta method is said to be of (classical) order $p \geq 1$ and stage order q if for sufficiently smooth right-hand sides f,

$$Y_{0i} - y(c_i \Delta t) = O(\Delta t^{q+1}), \text{ for } i = 1, \ldots, m, \quad \text{and} \quad y_1 - y(t_1) = O(\Delta t^{p+1}), \tag{5.4.1}$$

as $\Delta t \to 0$. Using the notation

$$\mathbb{1} = (1, 1, \ldots, 1)^T,$$

the Runge-Kutta method is said to be A-stable if $\mathbf{I} - z\mathbf{A}$ is non-singular for $\operatorname{Re} z \leq 0$ and the stability function

$$R(z) = 1 + z\mathbf{b}^T(\mathbf{I} - z\mathbf{A})^{-1}\mathbb{1} \tag{5.4.2}$$

satisfies $|R(z)| \leq 1$ for $\operatorname{Re} z \leq 0$. Note that if $\mathbf{A}^{-1}$ exists, then $R(\infty) = 1 - \mathbf{b}^T\mathbf{A}^{-1}\mathbb{1}$.

In order to use the convergence results proved in [6], we make the following assumptions on the Runge-Kutta methods.

Assumption 5.4.1. *a. The Runge-Kutta method is A-stable with (classical) order $p \geq 1$ and stage order $q \leq p$.*

b. The stability function satisfies $|R(\mathrm{i}y)| < 1$ for all real $y \neq 0$.

c. $R(\infty) = 0$.

d. The Runge-Kutta coefficient matrix $\mathbf{A}$ is invertible.

Radau IIA and Lobatto IIIC are examples of methods satisfying all of the above assumptions with $q = m$ and $p = 2m - 1$ for Radau IIA and $q = m - 1$ and $p = 2m$ for Lobatto IIIC. For possible relaxation of these conditions and deeper meaning of them see [6].

Convolution quadrature is a method for the discretization of continuous convolutions

$$u(t) = K(\partial_t)g := \int_0^t k(t - \tau)g(\tau)d\tau \tag{5.4.3}$$

that uses only the Laplace transformed kernel $K(s) = (\mathscr{L}k)(s)$, the so-called transfer function. The importance of the transfer function is highlighted by the operational notation $K(\partial_t)g$.

The Runge-Kutta based convolution quadrature approximation to $u(t_n + c_\ell \Delta t), \ell = 1, \ldots, m$, is given by

$$\begin{pmatrix} u_{n1} \\ \vdots \\ u_{nm} \end{pmatrix} = \left(K(\underline{\partial_t}^{\Delta t})g\right)_n := \sum_{j=0}^{n} \mathbf{W}_{n-j}^{\Delta t}(K) \begin{pmatrix} g(t_j + c_1 \Delta t) \\ \vdots \\ g(t_j + c_m \Delta t) \end{pmatrix}. \tag{5.4.4}$$

Here, the matrix convolution weights $\mathbf{W}_j^{\Delta t}(K)$ are defined implicitly through a generating function

$$K\left(\frac{\chi(\zeta)}{\Delta t}\right) = \sum_{j=0}^{\infty} \mathbf{W}_j^{\Delta t}(K)\zeta^j, \tag{5.4.5}$$

with

$$\chi(\zeta) = \mathbf{A}^{-1} - \zeta \mathbf{A}^{-1}\mathbb{1}\mathbf{b}^T\mathbf{A}^{-1}. \tag{5.4.6}$$

The approximation at t_{n+1} is given simply by $u_{n+1} = \mathbf{b}^T\mathbf{A}^{-1}(u_{n\ell})_{\ell=1}^m$, i.e.,

$$u_{n+1} := \mathbf{b}^T\mathbf{A}^{-1}\left(K(\underline{\partial_t}^{\Delta t})g\right)_n. \tag{5.4.7}$$

Note that for stiffly accurate Runge-Kutta methods like Radau IIA or Lobatto IIIC we have $\mathbf{b}^T\mathbf{A}^{-1} = (0,0,\ldots,0,1)^T$ and therefore (5.4.7) simplifies to $u_{n+1} = u_{nm}$ in this case.

Applying this time-discretization to (5.3.13) we obtain the semi-discretized equations

$$\begin{aligned} &-\sum_{j=0}^{n} \mu\,\Pi_\tau \int_\Gamma \mathbf{W}_{n-j}^{(2)}(\mathbf{x}-\mathbf{y}) \begin{pmatrix} \mathbf{j}(t_j + c_1\Delta t, \mathbf{x}) \\ \vdots \\ \mathbf{j}(t_j + c_m\Delta t, \mathbf{x}) \end{pmatrix} d\Gamma_{\mathbf{x}} \\ &\quad + \sum_{j=0}^{n} \frac{1}{\varepsilon}\nabla_\Gamma \int_\Gamma \mathbf{W}_{n-j}(\mathbf{x}-\mathbf{y}) \begin{pmatrix} \operatorname{div}_\Gamma \mathbf{j}(t_j + c_1\Delta t, \mathbf{x}) \\ \vdots \\ \operatorname{div}_\Gamma \mathbf{j}(t_j + c_m\Delta t, \mathbf{x}) \end{pmatrix} d\Gamma_{\mathbf{x}} = (\mathbf{n}\times\mathbf{g}_t)_n, \end{aligned} \tag{5.4.8}$$

with

$$(\mathbf{n}\times\mathbf{g}_t)_n(\mathbf{y}) := \begin{pmatrix} \mathbf{n}(\mathbf{y}) \times \mathbf{g}_t(t_n + c_1\Delta t, \mathbf{y}) \\ \vdots \\ \mathbf{n}(\mathbf{y}) \times \mathbf{g}_t(t_n + c_m\Delta t, \mathbf{y}) \end{pmatrix}$$

and the weights $\mathbf{W}_j = (w_{j,k,\ell})_{1\le k,\ell\le m}$ and $\mathbf{W}_j^{(2)} = \left(w_{j,k,\ell}^{(2)}\right)_{1\le k,\ell\le m}$ defined by

$$K(\chi(\zeta)/\Delta t, \mathbf{z}) = \sum_{j=0}^{\infty} \mathbf{W}_j(\mathbf{z})\zeta^j, \quad (\chi(\zeta)/\Delta t)^2 K(\chi(\zeta)/\Delta t, \mathbf{z}) = \sum_{j=0}^{\infty} \mathbf{W}_j^{(2)}(\mathbf{z})\zeta^j, \tag{5.4.9}$$

where K is again as in (5.3.7). The importance of using the differentiated formulation (5.3.13) instead of (5.3.11) can be seen from the following proposition.

Proposition 5.4.2. *Under the above assumptions on the Runge-Kutta method, there exists a constant $c > 0$ such that for any $\epsilon > 0$ and all $\mathbf{z} \in \mathbb{R}^3$ with $\|\mathbf{z}\| < R$ it holds*

$$\|\mathbf{W}_j(\mathbf{z})\| \le \epsilon, \qquad \textit{for all } j > \max\left(\frac{cR}{\Delta t}, \log\frac{1}{\epsilon}\right)$$

and

$$\|\mathbf{W}_j^{(2)}(\mathbf{z})\| \le \epsilon, \qquad \textit{for all } j > \max\left(\frac{cR}{\Delta t}, \log\frac{1}{\epsilon} + \log\frac{1}{\Delta t}\right).$$

Proof. By Cauchy's integral formula it holds

$$\mathbf{W}_j(\mathbf{z}) = \frac{1}{4\pi \|\mathbf{z}\|} \frac{1}{2\pi \mathrm{i}} \oint_C \mathrm{e}^{-\chi(\zeta)\|\mathbf{z}\|/\Delta t} \zeta^{-j-1} d\zeta = \frac{1}{4\pi \|\mathbf{z}\|} \sum_{\ell=j}^{\infty} \frac{(\|\mathbf{z}\|/\Delta t)^\ell}{\ell!} \frac{1}{2\pi \mathrm{i}} \oint_C (-\chi(\zeta))^\ell \zeta^{-j-1} d\zeta.$$

For the contour C we may use the unit circle and obtain the bound

$$\|\mathbf{W}_j(\mathbf{z})\| \leq \frac{1}{4\pi \|\mathbf{z}\|} \sum_{\ell=j}^{\infty} \frac{(a\|\mathbf{z}\|/\Delta t)^\ell}{\ell!}, \qquad \text{with } a = \max_{|\zeta|=1} \|\chi(\zeta)\|.$$

Using Stirling's approximation finally we obtain a crude bound

$$\begin{aligned} \|\mathbf{W}_j(\mathbf{z})\| &\leq \frac{1}{4\pi \|\mathbf{z}\|} \sum_{\ell=j}^{\infty} \left(\frac{a\,\mathrm{e}\,\|\mathbf{z}\|}{\ell \Delta t} \right)^\ell \leq \frac{1}{4\pi \|\mathbf{z}\|} \left(\frac{a\,\mathrm{e}\,\|\mathbf{z}\|}{j\Delta t} \right)^j \frac{1}{1 - (a\,\mathrm{e}\,\|\mathbf{z}\|/j\Delta t)} \\ &= \frac{a\,\mathrm{e}}{4\pi j \Delta t} \left(\frac{a\,\mathrm{e}\,\|\mathbf{z}\|}{j\Delta t} \right)^{j-1} \frac{1}{1 - (a\,\mathrm{e}\,\|\mathbf{z}\|/j\Delta t)}. \end{aligned}$$

Assuming for example that $j > 2a\,\mathrm{e}\,R/\Delta t$ we obtain that

$$\|\mathbf{W}_j(\mathbf{z})\| \leq C \frac{1}{R} 2^{-j}$$

from which the first bound follows directly. Similar reasoning gives the result for $\mathbf{W}_j^{(2)}$. □

Remark 5.4.3. *The above proposition shows that for large enough j, the weights $\mathbf{W}_j$ and $\mathbf{W}_j^{(2)}$ are exponentially close to zero. In order to eliminate q from (5.3.11) we could have simply substituted for q the conservation law (5.3.9). This would, however, have introduced the integration operator $1/s$ and since $(\chi(\zeta))^{-1} = \mathbf{A} + \frac{\zeta}{1-\zeta} \mathbb{1}\mathbf{b}^T$ it is not difficult to see that weights for this operator do not converge to zero.*

5.4.2 Convergence of the semi-discrete scheme

Let us define the Laplace domain EFIE operator on the boundary $\mathcal{V}(s) : \mathbf{H}^{-1/2}(\mathrm{div}_\Gamma, \Gamma) \to \mathbf{H}^{-1/2}(\mathrm{curl}_\Gamma, \Gamma)$ by

$$\begin{aligned} \left(\mathcal{V}(s) \hat{\mathbf{j}} \right)(\mathbf{y}) := & -\mu \Pi_\tau \int_\Gamma s^2 K(s, \mathbf{x}-\mathbf{y}) \hat{\mathbf{j}}(\mathbf{x})\, d\Gamma_{\mathbf{x}} \\ & + \frac{1}{\varepsilon} \nabla_\Gamma \int_\Gamma K(s, \mathbf{x}-\mathbf{y})\, \mathrm{div}_\Gamma \hat{\mathbf{j}}(\mathbf{x})\, d\Gamma_{\mathbf{x}}, \qquad \mathbf{y} \in \Gamma. \end{aligned} \tag{5.4.10}$$

Further denote by $\mathcal{S}(s) : \mathbf{H}^{-1/2}(\mathrm{div}_\Gamma, \Gamma) \to \mathbf{H}(\mathrm{curl}, \Omega_+)$ the operator

$$\begin{aligned} \left(\mathcal{S}(s) \hat{\mathbf{j}} \right)(\mathbf{y}) := & -\mu \int_\Gamma s\, K(s, \mathbf{x}-\mathbf{y}) \hat{\mathbf{j}}(\mathbf{x})\, d\Gamma_{\mathbf{x}} \\ & + \frac{1}{\varepsilon} \nabla \int_\Gamma \frac{1}{s} K(s, \mathbf{x}-\mathbf{y})\, \mathrm{div}_\Gamma \hat{\mathbf{j}}(\mathbf{x})\, d\Gamma_{\mathbf{x}}, \qquad \mathbf{y} \in \Omega^+. \end{aligned} \tag{5.4.11}$$

Note that $\mathcal{V}(s)$ is the tangential trace of the differentiated domain operator $\mathcal{S}(s)$:

$$\mathcal{V}(s) = s \Pi_\tau \mathcal{S}(s).$$

Therefore, using the operational notation (5.4.3), the continuous system (5.3.13) can be written in short-hand as: Find $\mathbf{j}$ such that

$$\mathcal{V}(\partial_t)\mathbf{j} = \mathbf{n} \times \mathbf{g}_t, \tag{5.4.12}$$

and its Runge-Kutta discretization as: Find $\mathbf{j}^{\Delta t}$ such that

$$\left(\mathcal{V}(\underline{\partial_t}^{\Delta t})\mathbf{j}^{\Delta t}\right)_n = (\mathbf{n} \times \mathbf{g}_t)_n.$$

Using the composition rule

$$K_2K_1(\underline{\partial_t}^{\Delta t})g = K_2(\underline{\partial_t}^{\Delta t})K_1(\underline{\partial_t}^{\Delta t})g, \tag{5.4.13}$$

see [5], we see that the unknown density is in fact given by

$$(\mathbf{j}^{\Delta t})_n = \begin{pmatrix} \mathbf{j}_{n1}^{\Delta t} \\ \vdots \\ \mathbf{j}_{nm}^{\Delta t} \end{pmatrix} = \left(\mathcal{V}^{-1}(\underline{\partial_t}^{\Delta t})\mathbf{n} \times \mathbf{g}_t\right)_n$$

and

$$\mathbf{j}_{n+1}^{\Delta t} := \mathbf{b}^T\mathbf{A}^{-1}\left(\mathcal{V}^{-1}(\underline{\partial_t}^{\Delta t})\mathbf{n} \times \mathbf{g}_t\right)_n.$$

Finally, using the definition of $\mathcal{S}(s)$ (recall that $\mathcal{V}(s) = s\Pi_\tau\mathcal{S}(s)$) we have that

$$\mathbf{E} = \mathcal{S}\mathcal{V}^{-1}(\partial_t)\,\mathbf{n} \times \mathbf{g}_t$$

and the discrete approximation $\mathbf{E}_{n+1}^{\Delta t} \approx \mathbf{E}(t_{n+1}, \cdot)$ of the electric field is given by

$$\mathbf{E}_{n+1}^{\Delta t} = \mathbf{b}^T\mathbf{A}^{-1}\left(\mathcal{S}\mathcal{V}^{-1}(\underline{\partial_t}^{\Delta t})\mathbf{n} \times \mathbf{g}_t\right)_n.$$

It is consequently possible to deduce convergence results just from properties of $\mathcal{V}^{-1}(s)$ and $\mathcal{S}(s)$ in the Laplace domain.

Theorem 5.4.4. *There exists $\sigma_0 > 0$ such that the following statements hold.*

(a) The inverse operator $\mathcal{V}^{-1}(s) : \mathbf{H}^{-1/2}(\mathrm{curl}_\Gamma, \Gamma) \to \mathbf{H}^{-1/2}(\mathrm{div}_\Gamma, \Gamma)$ is analytic for $\mathrm{Re}\, s > 0$ and bounded in the operator norm as

$$\left\|\mathcal{V}^{-1}(s)\right\| \leq C(\sigma_0)\,\frac{|s|}{\mathrm{Re}\, s} \qquad \text{for } \mathrm{Re}\, s \geq \sigma_0 > 0. \tag{5.4.14}$$

(b) An upper bound for the operator norm of $\mathcal{V}(s) : \mathbf{H}^{-1/2}(\mathrm{div}_\Gamma, \Gamma) \to \mathbf{H}^{-1/2}(\mathrm{curl}_\Gamma, \Gamma)$ is given by

$$\|\mathcal{V}(s)\| \leq C(\sigma_0)\,\frac{|s|^3}{\mathrm{Re}\, s}. \tag{5.4.15}$$

(c) For any $\mathbf{y} \in \Omega_+$, the field point evaluation $\delta_{\mathbf{y}}\mathcal{S}(s) : \mathbf{H}^{-1/2}(\mathrm{div}_\Gamma, \Gamma) \to \mathbb{C}^3$ is analytic for $\mathrm{Re}\, s > 0$ and bounded as

$$\|\delta_{\mathbf{y}}\mathcal{S}(s)\| \leq C(\sigma_0, \mathrm{dist}(\mathbf{y}, \Gamma))\, \mathrm{e}^{-\mathrm{Re}\, s\, \mathrm{dist}(\mathbf{y}, \Gamma)}\, |s|^2 \qquad \text{for } \mathrm{Re}\, s \geq \sigma_0 > 0.$$

Proof. We follow the ideas of [3] and extend them from the acoustic case to the present case of Maxwell operators. Similar arguments can be found in the master's thesis of one of the authors [37, Prop. 3.5], see also the PhD theses [29] and [36]. The definitions of the single layer operators in these references differ slightly, for example $\mathcal{V}(s) = sR(s)$, where $R(s)$ is as in [37, (3.10)]. In our proof C will denote a generic constant which is allowed to change from one line to the next.

For $\boldsymbol{\varphi} \in \mathbf{H}^{-1/2}(\mathrm{div}_\Gamma, \Gamma)$, we define $\boldsymbol{\psi} := \mathcal{V}(s)\boldsymbol{\varphi}$. Let $\mathbf{h} \in \mathbf{H}(\mathrm{curl}, \Omega)$ denote a lifting of $\boldsymbol{\psi} \in \mathbf{H}^{-1/2}(\mathrm{curl}_\Gamma, \Gamma)$, i.e., $\boldsymbol{\psi} = \Pi_\tau \mathbf{h}$; a proof of the existence of a continuous lifting operator can be found in [28, 36]. We relate this equation to the following exterior and interior, time-harmonic Maxwell problem. Let $\Omega \in \{\Omega_-, \Omega_+\}$. Find $(\mathbf{E}_\Omega, \mathbf{H}_\Omega) \in \mathbf{H}(\mathrm{curl}, \Omega) \times \mathbf{H}(\mathrm{curl}, \Omega)$ such that

$$\begin{aligned} -s\varepsilon\mathbf{E}_\Omega + \mathrm{curl}\ \mathbf{H}_\Omega &= \mathbf{0} && \text{in } \Omega, \\ s\mu\mathbf{H}_\Omega + \mathrm{curl}\ \mathbf{E}_\Omega &= \mathbf{0} && \text{in } \Omega, \\ \mathbf{E}_\Omega \times \mathbf{n} &= \frac{1}{s}\mathbf{h} \times \mathbf{n} && \text{on } \Gamma. \end{aligned} \tag{5.4.16}$$

This problem admits a unique solution for all $\mathrm{Re}\, s > 0$ as proved, e.g., in [36] and [37, Lemma 3.3]. In the following we will make use of the scaled norm

$$\|\mathbf{E}_\Omega\|^2_{\mathrm{curl},\Omega,s} := \int_\Omega |\mathrm{curl}\, \mathbf{E}_\Omega|^2 + |\sqrt{\mu\varepsilon} s \mathbf{E}_\Omega|^2 \, d\mathbf{x}.$$

Then, we have, see [28, Theorem 5.5.1],

$$\Pi_\tau \mathbf{h} = s\Pi_\tau^\Omega \mathbf{E}_\Omega \quad \text{and} \quad \boldsymbol{\varphi} = \gamma_\tau^{\Omega_-}\mathbf{H}_{\Omega_-} - \gamma_\tau^{\Omega_+}\mathbf{H}_{\Omega_+}. \tag{5.4.17}$$

Hence, by Green's formula

$$\begin{aligned} \mathrm{Re}\,(-s\boldsymbol{\varphi}, \mathcal{V}(s)\boldsymbol{\varphi})_\Gamma &= \mathrm{Re}\,(-s\boldsymbol{\varphi}, \Pi_\tau \mathbf{h})_\Gamma \qquad (5.4.18) \\ &= \mathrm{Re}\left[\left(-s\gamma_\tau^{\Omega_-}\mathbf{H}_{\Omega_-}, s\Pi_\tau^{\Omega_-}\mathbf{E}_{\Omega_-}\right)_\Gamma - \left(-s\gamma_\tau^{\Omega_+}\mathbf{H}_{\Omega_+}, s\Pi_\tau^{\Omega_+}\mathbf{E}_{\Omega_+}\right)_\Gamma\right] \\ &= -\,\mathrm{Re} \sum_{\Omega\in\{\Omega_-,\Omega_+\}} |s|^2 \int_\Omega (\overline{\mathbf{H}}_\Omega \,.\, \mathrm{curl}\, \mathbf{E}_\Omega - \mathrm{curl}\, \overline{\mathbf{H}}_\Omega \,.\, \mathbf{E}_\Omega)\, d\mathbf{x} \\ &= \sum_{\Omega\in\{\Omega_-,\Omega_+\}} \mathrm{Re} \int_\Omega \frac{s}{\mu} |\mathrm{curl}\, \mathbf{E}_\Omega|^2 + \overline{s}\, |s|^2 \varepsilon\, |\mathbf{E}_\Omega|^2 \, d\mathbf{x} \\ &= \frac{\mathrm{Re}\, s}{\mu} \|\mathbf{E}\|^2_{\mathrm{curl},\Omega_-\cup\Omega_+,s}\,. \qquad (5.4.19) \end{aligned}$$

To estimate $\boldsymbol{\varphi}$ in terms of $\mathbf{E}$ we pick any $\boldsymbol{\zeta} \in \mathbf{H}^{-1/2}(\mathrm{curl}_\Gamma, \Gamma)$ and denote by $\mathbf{u}_{\Omega_-} \in \mathbf{H}(\mathrm{curl}, \Omega_-)$, resp. $\mathbf{u}_{\Omega_+} \in \mathbf{H}(\mathrm{curl}, \Omega_+)$ the interior and exterior lifting of $\boldsymbol{\zeta}$, i.e., $\boldsymbol{\zeta} = \Pi_\tau^{\Omega_-}\mathbf{u}_{\Omega_-} = \Pi_\tau^{\Omega_+}\mathbf{u}_{\Omega_+}$. The continuity of the lifting operator implies

$$\|\mathbf{u}_{\Omega_\pm}\|_{\mathrm{curl},\Omega_\pm} \le C\|\boldsymbol{\zeta}\|_{-1/2,\mathrm{curl}}.$$

We employ Green's identity to obtain

$$\begin{aligned} |(\boldsymbol{\varphi}, \boldsymbol{\zeta})_\Gamma| &= \left|\left(\gamma_\tau^{\Omega_-}\mathbf{H}_{\Omega_-}, \Pi_\tau^{\Omega_-}\mathbf{u}_{\Omega_-}\right)_\Gamma - \left(\gamma_\tau^{\Omega_+}\mathbf{H}_{\Omega_+}, \Pi_\tau^{\Omega_+}\mathbf{u}_{\Omega_+}\right)_\Gamma\right| \\ &= \left|\sum_{\Omega\in\{\Omega_-,\Omega_+\}} \int_\Omega (\overline{\mathbf{H}_\Omega} \,.\, \mathrm{curl}\, \mathbf{u}_\Omega - \mathrm{curl}\, \overline{\mathbf{H}_\Omega} \,.\, \mathbf{u}_\Omega)\, d\mathbf{x}\right| \end{aligned}$$

$$
\begin{aligned}
&= \left| \sum_{\Omega\in\{\Omega_-,\Omega_+\}} \int_\Omega \left(\frac{1}{\bar{s}\mu} \operatorname{curl} \overline{\mathbf{E}_\Omega} \,.\, \operatorname{curl} \mathbf{u}_\Omega + \bar{s}\varepsilon \overline{\mathbf{E}_\Omega} \,.\, \mathbf{u}_\Omega \right) d\mathbf{x} \right| \\
&\leq \frac{1}{|s|\mu} \|\mathbf{E}\|_{\operatorname{curl},\Omega_-\cup\Omega_+,s} \|\mathbf{u}\|_{\operatorname{curl},\Omega_-\cup\Omega_+,s} \\
&\leq \frac{1}{\mu} \max\left(\sqrt{\varepsilon\mu}, \frac{1}{\operatorname{Re} s} \right) \|\mathbf{E}\|_{\operatorname{curl},\Omega_-\cup\Omega_+,s} \|\mathbf{u}\|_{\operatorname{curl},\Omega_-\cup\Omega_+} \\
&\leq \frac{C}{\mu} \max\left(\sqrt{\varepsilon\mu}, \frac{1}{\operatorname{Re} s} \right) \|\mathbf{E}\|_{\operatorname{curl},\Omega_-\cup\Omega_+,s} \|\boldsymbol{\zeta}\|_{-1/2,\operatorname{curl}}.
\end{aligned}
$$

Hence, from (5.2.3a) we conclude that

$$
\|\boldsymbol{\varphi}\|_{-1/2,\operatorname{div}} \leq \frac{C}{\mu} \max\left(\sqrt{\mu\varepsilon}, \frac{1}{\sigma_0} \right) \|\mathbf{E}\|_{\operatorname{curl},\Omega_-\cup\Omega_+,s}
$$

holds. The combination with (5.4.19) finally leads to

$$
\operatorname{Re}\left(-s\boldsymbol{\varphi}, \mathcal{V}(s)\,\boldsymbol{\varphi} \right)_\Gamma \geq C \min\left(\sqrt{\frac{\mu}{\varepsilon}}, \mu\sigma_0^2 \right) \operatorname{Re} s \, \|\boldsymbol{\varphi}\|^2_{-1/2,\operatorname{div}}. \tag{5.4.20}
$$

The Lax-Milgram lemma in the form [32, Lemma 2.1.51 with the definition of ellipiticty as in (2.43)] gives

$$
\left\| (s\mathcal{V}(s))^{-1} \right\| \leq C \max\left(\sqrt{\frac{\varepsilon}{\mu}}, \frac{1}{\mu\sigma_0^2} \right) \frac{1}{\operatorname{Re} s}.
$$

Multiplying by $|s|$ leads to the asserted bound of $\mathcal{V}^{-1}(s)$ in the operator norm.

Now, for any $\boldsymbol{\psi} \in \mathbf{H}^{-1/2}(\operatorname{curl}_\Gamma, \Gamma)$ we set $\boldsymbol{\varphi} := \mathcal{V}^{-1}(s)\,\boldsymbol{\psi}$. Let $(\mathbf{E}_\Omega, \mathbf{H}_\Omega)$ denote the solution of (5.4.16) for this choice of $\boldsymbol{\psi}$ and corresponding lifting $\mathbf{h}$. Note that the relations (5.4.17) also hold for this case. Again by Green's formula and the continuity of the trace mapping $\Pi_\tau^\Omega : \mathbf{H}(\operatorname{curl},\Omega) \to \mathbf{H}^{-1/2}(\operatorname{curl}_\Gamma,\Gamma)$ we get the estimate

$$
\begin{aligned}
\operatorname{Re}\left(-s\mathcal{V}^{-1}(s)\,\boldsymbol{\psi}, \boldsymbol{\psi} \right)_\Gamma &= \frac{\operatorname{Re} s}{\mu} \|\mathbf{E}\|^2_{\operatorname{curl},\Omega_-\cup\Omega_+,s} \\
&\geq C \min\left(\frac{1}{\mu}, \varepsilon\sigma_0^2 \right) \operatorname{Re} s \, \|\mathbf{E}\|^2_{\operatorname{curl},\Omega_-\cup\Omega_+} \\
&\geq C \min\left(\frac{1}{\mu}, \varepsilon\sigma_0^2 \right) \operatorname{Re} s \, \|\Pi_\tau \mathbf{E}\|^2_{-1/2,\operatorname{curl}} \\
&= C \min\left(\frac{1}{\mu}, \varepsilon\sigma_0^2 \right) \frac{\operatorname{Re} s}{|s|^2} \|\boldsymbol{\psi}\|^2_{-1/2,\operatorname{curl}}.
\end{aligned} \tag{5.4.21}
$$

Similarly as for $\mathcal{V}^{-1}(s)$, this now gives the required estimate for $\|\mathcal{V}(s)\|$.

To prove the third bound we can proceed as in the acoustic case discussed in [6, Lemma 5.1]:

$$
\begin{aligned}
|\mathcal{S}(s)\mathbf{v}(\mathbf{y})| &\leq \mu|s| \left\| \frac{\mathrm{e}^{-s\|\cdot-\mathbf{y}\|}}{4\pi\|\cdot-\mathbf{y}\|} \right\|_{H^{1/2}(\Gamma)} \|\mathbf{v}\|_{H^{-1/2}(\Gamma)} + \frac{1}{|s|\varepsilon} \left\| \nabla \frac{\mathrm{e}^{-s\|\cdot-\mathbf{y}\|}}{4\pi\|\cdot-\mathbf{y}\|} \right\|_{H^{1/2}(\Gamma)} \|\operatorname{div}_\Gamma \mathbf{v}\|_{H^{-1/2}(\Gamma)} \\
&\leq \left(\mu^2|s|^2 \left\| \frac{\mathrm{e}^{-s\|\cdot-\mathbf{y}\|}}{4\pi\|\cdot-\mathbf{y}\|} \right\|^2_{H^{1/2}(\Gamma)} + \frac{1}{|s|^2\varepsilon^2} \left\| \nabla \frac{\mathrm{e}^{-s\|\cdot-\mathbf{y}\|}}{4\pi\|\cdot-\mathbf{y}\|} \right\|^2_{H^{1/2}(\Gamma)} \right)^{1/2} \|\mathbf{v}\|_{-1/2,\operatorname{div}_\Gamma}.
\end{aligned}
$$

It is not difficult to show that, see [6, Lemma 5.1],

$$\left\| \frac{\mathrm{e}^{-s\|\cdot-\mathbf{y}\|}}{4\pi\|\cdot-\mathbf{y}\|} \right\|_{H^{1/2}(\Gamma)} \leq C(\sigma_0, \mathrm{dist}(\mathbf{y},\Gamma))|s|\,\mathrm{e}^{-\mathrm{Re}\,s\,\mathrm{dist}(\mathbf{y},\Gamma)}$$

and hence

$$\left\| \nabla \frac{\mathrm{e}^{-s\|\cdot-\mathbf{y}\|}}{4\pi\|\cdot-\mathbf{y}\|} \right\|_{H^{1/2}(\Gamma)} \leq C(\sigma_0, \mathrm{dist}(\mathbf{y},\Gamma))|s|^2\,\mathrm{e}^{-\mathrm{Re}\,s\,\mathrm{dist}(\mathbf{y},\Gamma)}\,.$$

Combining the three estimates gives the required result. □

In the following we will derive error estimates for the Runge-Kutta convolution quadrature approximation of the computation of the electric surface current density

$$\mathbf{j} = \mathcal{V}^{-1}(\partial_t)\,(\mathbf{n}\times\mathbf{g}_t) \tag{5.4.22}$$

and the corresponding field point evaluation

$$\mathbf{E}\,(\mathbf{y}) = \delta_{\mathbf{y}}\mathcal{S}\mathcal{V}^{-1}(\partial_t)\mathbf{n}\times\mathbf{g}_t \tag{5.4.23}$$

where $\mathbf{g} = -\mathbf{E}^{\mathrm{inc}}\times\mathbf{n}$. The transfer function for problem (5.4.22) is given (and estimated) by

$$\|\mathcal{V}^{-1}(s)\| \leq C\,(\sigma_0)\,\frac{|s|}{\mathrm{Re}\,s},$$

where for (5.4.23) it is

$$\left\|\delta_{\mathbf{y}}\mathcal{S}\,(s)\,\mathcal{V}^{-1}(s)\right\| \leq C(\sigma_0, \mathrm{dist}(\mathbf{y},\Gamma))\,\mathrm{e}^{-\mathrm{Re}\,s\,\mathrm{dist}(\mathbf{y},\Gamma)}\,\frac{|s|^3}{\mathrm{Re}\,s}.$$

In [6] it has been proved that the Runge-Kutta convolution quadrature for a transfer function that is bounded by $C|s|^{\mu}/\,(\mathrm{Re}\,s)^{\nu}$ for some real μ and $\nu \geq 0$ converges at the rate $O(\Delta t^{q+1-\mu+\nu})$. Hence, these estimates imply the following result.

Definition 5.4.5. *Let $W_0^{r,1}\,(0,T;X)$ denote the space of functions g on $(0,T)$ with values in the Banach space X and the r-th weak derivative in $L^1\,(0,T)$ and with $g\,(0) = g'\,(0) = \ldots = g^{(r-1)}\,(0) = 0$ equipped with the norm*

$$\left\|g^{(r)}\right\|_{L^1(0,T)} = \int_0^T \|g^{(r)}(t)\|_X dt.$$

Theorem 5.4.6.

(a) Let $r > p+3$ and $\mathbf{g} \in W_0^{r+1,1}([0,T];\mathbf{H}^{-1/2}(\mathrm{curl}_\Gamma,\Gamma))$. Then, under the above conditions on the Runge-Kutta method there exists $\bar{t} \geq 0$ such that for $0 < \Delta t < \bar{t}$ and $t \in [0,T]$,

$$\left\|\mathbf{j}_n^{\Delta t}(\cdot) - \mathbf{j}(t_n,\cdot)\right\|_{-1/2,\mathrm{div}_\Gamma} \leq C\Delta t^{\min(p,q+1)} \int_0^t \|\partial_t^{r+1}\mathbf{g}(\tau,\cdot)\|_{-1/2,\mathrm{curl}_\Gamma} d\tau.$$

(b) Let $r > p+5$ and assume further that $\mathbf{g} \in W_0^{r+1,1}([0,T];\mathbf{H}^{-1/2}(\mathrm{curl}_\Gamma,\Gamma))$. Then for any $\mathbf{y} \in \Omega^+$

$$\left\|\mathbf{E}_n^{\Delta t}(\mathbf{y}) - \mathbf{E}(t_n,\mathbf{y})\right\| \leq C\Delta t^p \int_0^t \|\partial_t^{r+1}\mathbf{g}(\tau,\cdot)\|_{-1/2,\mathrm{curl}_\Gamma} d\tau.$$

Remark 5.4.7. *The statement of the theorem on convergence of Runge-Kutta based convolution quadrature as given in [6], requires the data $\mathbf{g}$ to be in the space $C^r([0,T])$ of r-times continuously differentiable functions. The proof is, however, easily seen to hold also for data $\mathbf{g}$ in spaces $W_0^{r,1}([0,T])$.*

5.4.3 Spatial Discretization

For the rest of the paper we assume Ω_- to be a bounded polyhedron. In this case the spaces V_Π and V_γ can be explicitly characterized, see [9, 10]. We equip the boundary Γ of Ω_- with a surface boundary element mesh $\mathcal{G}_h$ (in the sense of, e.g., [32]), where h denotes the mesh width. We assume that the surface mesh is aligned with edges of Γ, i.e. the edges of Γ are covered by a subset of triangle edges. Let

$$\mathcal{G}_h := \{\tau_\ell\}_{\ell=1}^{\tilde{M}}$$

be such a triangulation with $\Gamma = \bigcup_{\ell=1}^{\tilde{M}} \overline{\tau_\ell}$. The set of triangle edges is denoted by

$$\mathcal{E}_h := \{e_i\}_{i=1}^{M}.$$

The triangulation is assumed to be conforming i.e. two panels $\overline{\tau_\ell}$ and $\overline{\tau_k}$ either coincide, they share a common edge, a common vertex or they are disjoint. In order to discretize our problem we have to define a suitable finite dimensional boundary element space

$$V_h \subset \mathbf{H}^{-1/2}(\mathrm{div}_\Gamma, \Gamma).$$

We use here the classical Raviart-Thomas elements of lowest order, which we denote by $\mathcal{RT}_0(\mathcal{G}_h)$, see [31].

Let a basis of $\mathcal{RT}_0(\mathcal{G}_h)$ be given by $\{\mathbf{b}_1, \mathbf{b}_2, \ldots, \mathbf{b}_M\}$. We define the block matrices $\underline{\underline{\mathbf{W}}}_k \in \mathbb{C}^{mM\times mM}$ for $1 \le i, j \le m$ by

$$\left(\underline{\underline{\mathbf{W}}}_k\right)_{i,j} := \left(\mu \int_\Gamma \int_\Gamma \left(\mathbf{W}_k^{(2)}(\mathbf{x}-\mathbf{y})\right)_{i,j} (\mathbf{b}_e(\mathbf{x})\,,\, \mathbf{b}_f(\mathbf{y}))\; d\Gamma_{\mathbf{x}} d\Gamma_{\mathbf{y}} \right.$$
$$\left. + \frac{1}{\varepsilon} \int_\Gamma \int_\Gamma (\mathbf{W}_k(\mathbf{x}-\mathbf{y}))_{i,j}\, \mathrm{div}_\Gamma\, \mathbf{b}_e(\mathbf{x}) \overline{\mathrm{div}_\Gamma\, \mathbf{b}_f(\mathbf{y})} d\Gamma_{\mathbf{x}} d\Gamma_{\mathbf{y}} \right)_{e,f=1}^{M} \in \mathbb{C}^{M\times M},$$

where $(\cdot,\cdot)$ refers to the standard inner product in $\mathbb{C}^3$. For $1 \le i \le m$, we define the right-hand sides $\mathbf{r}_{k,i} \in \mathbb{C}^M$ by

$$\mathbf{r}_{k,i} := \left(\int_\Gamma \left(\mathbf{b}_f, \mathbf{E}_t^{\mathrm{inc}}(t_k + c_i\Delta t, \mathbf{y})\right) d\Gamma_{\mathbf{y}} \right)_{f=1}^{M}$$

and form the block vectors $\underline{\mathbf{R}}_k := (\mathbf{r}_{k,i})_{i=1}^m \in \mathbb{C}^{mM}$. Then, the Galerkin discretization of (5.4.8) is given by seeking, for $0 \le k \le N$, the block vectors $\underline{\mathbf{J}}_k = (\mathbf{j}_{k,i})_{i=1}^m$ with $\mathbf{j}_{k,i} = (j_{k,i,e})_{e=1}^M \in \mathbb{C}^M$ such that

$$\sum_{j=0}^{n} \underline{\underline{\mathbf{W}}}_{n-j} \underline{\mathbf{J}}_j = \underline{\mathbf{R}}_n \qquad \forall 0 \le n \le N.$$

The temporal Runge-Kutta convolution quadrature, spatial Galerkin approximation to the electric surface current densities $\underline{\mathbf{j}}_k(\mathbf{x}) := (\mathbf{j}\,(t_k + c_i\Delta t, \mathbf{x}))_{i=1}^m$ at time points $t_k + c_i\Delta t$, $1 \le i \le m$, then is given by

$$\underline{\mathbf{j}}_k(\mathbf{x}) \approx \underline{\mathbf{j}}_k^{\Delta t,h}(\mathbf{x}) := \left(\sum_{e=1}^{M} j_{k,i,e} \mathbf{b}_e(\mathbf{x}) \right)_{i=1}^{m}. \tag{5.4.24}$$

In order to obtain approximations at t_{k+1} and not only at stage values, under the assumption $R(\infty) = 0$ on the Runge-Kutta method, note that

$$\mathbf{j}\left(t_{k+1}, \mathbf{x}\right) \approx \mathbf{j}_{k+1}^{\Delta t,h}\left(\mathbf{x}\right) := \mathbf{b}^T \mathbf{A}^{-1} \underline{\mathbf{j}}_k^{\Delta t,h}(\mathbf{x})$$

due to (5.4.7). For stiffly stable RK methods, such as the Radau IIA method, $b^T A^{-1} = (0, 0, \ldots, 0, 1)^T$ and $c_m = 1$, so that

$$\mathbf{j}_{k+1}^{\Delta t,h} = \mathbf{j}_{km}^{\Delta t,h}.$$

5.4.4 Convergence of the fully discrete scheme

The Galerkin discretization of the variational problem (5.4.12) in the Laplace domain is given by finding $\hat{\mathbf{j}}^h = \hat{\mathbf{j}}^h\left(s\right) \in \mathcal{RT}_0(\mathcal{G}_h)$ such that

$$\left(\boldsymbol{\zeta}, \mathcal{V}(s)\hat{\mathbf{j}}^h\right)_\Gamma = \left(\boldsymbol{\zeta}, s\,\mathbf{n} \times \hat{\mathbf{g}}\right)_\Gamma \qquad \forall \boldsymbol{\zeta} \in \mathcal{RT}_0(\mathcal{G}_h). \tag{5.4.25}$$

Let $P_{0,h} : \mathbf{L}_t^2(\Gamma) \to \mathcal{RT}_0(\mathcal{G}_h)$ and $P_{\mathrm{div},h} : \mathbf{H}^{-1/2}(\mathrm{div}_\Gamma, \Gamma) \to \mathcal{RT}_0(\mathcal{G}_h)$ denote the orthogonal projections. Then, the semi-discrete Galerkin discretization in the time domain can be written as

$$\mathcal{V}_h\left(\partial_t\right)\mathbf{j}^h = P_{0,h}\mathbf{n} \times \mathbf{g}_t,$$

where

$$\mathcal{V}_h\left(s\right) := P_{0,h}\mathcal{V}\left(s\right)P_{0,h}^\star : \mathcal{RT}_0(\mathcal{G}_h) \to \mathcal{RT}_0(\mathcal{G}_h).$$

The operator $\mathcal{V}_h\left(s\right)$ is invertible as we state in the next result.

Lemma 5.4.8. *For $s \in \mathbb{C}$ with $\mathrm{Re}\, s \geq \sigma_0 > 0$, the discrete Laplace domain Galerkin variational problem (5.4.25) has a unique solution $\hat{\mathbf{j}}^h\left(s\right) \in \mathcal{RT}_0(\mathcal{G}_h)$ with the stability estimate in the operator norm*

$$\left\|\mathcal{V}_h^{-1}\left(s\right)\right\| \leq C\left(\sigma_0\right)\frac{|s|}{\mathrm{Re}\, s}. \tag{5.4.26}$$

Proof. Since $\mathcal{V}(s)$ is coercive, (5.4.20), the same estimate holds for $\|\mathcal{V}_h^{-1}(s)\|$ as for $\|\mathcal{V}^{-1}(s)\|$. □

Hence,

$$\mathcal{V}_h\left(\partial_t\right)\left(\mathbf{j}^h - P_{\mathrm{div},h}\mathbf{j}\right) = P_{0,h}\mathcal{V}\left(\partial_t\right)\left(I - P_{\mathrm{div},h}\right)\mathbf{j}$$

and the composition rule $K_2(\partial_t)K_1(\partial_t)g = K_2K_1(\partial_t)g$ gives us

$$\mathbf{j}^h - P_{\mathrm{div},h}\mathbf{j} = \mathcal{V}_h^{-1}\left(\partial_t\right)P_{0,h}\mathcal{V}\left(\partial_t\right)\left(I - P_{\mathrm{div},h}\right)\mathbf{j}. \tag{5.4.27}$$

The representation (5.4.27) along with the discrete stability estimate (5.4.26) allow to employ Parseval's formula in the following form.

Lemma 5.4.9. *Let $K\left(s\right)$ be analytic and bounded by $|K\left(s\right)| \leq M\,|s|^\mu$ for all $s \in \mathbb{C}$ with $\mathrm{Re}\, s \geq \sigma_0 > 0$. Then, for $r > \mu$ the convolution operator $K\left(\partial_t\right)$ is a bounded linear operator*

$$K\left(\partial_t\right) : W_0^{r,1}\left(0,T\right) \to W_0^{r-\mu,1}\left(0,T\right).$$

Further for any $r > \mu + 1$

$$K\left(\partial_t\right) : W_0^{r,1}\left(0,T\right) \to C\left([0,T]\right)$$

is also a bounded operator.

Proof. The first statement is a direct consequence of the definition of the spaces $W_0^{r,1}$, whereas the second statement is proved in [25, Lemma 2.2]. □

In combination with both continuous stability estimates (5.4.14), (5.4.15), we obtain for $r > 5$

$$\left\|\mathbf{j}^h(t) - P_{\mathrm{div},h}\mathbf{j}(t)\right\|_{-1/2,\mathrm{div}_\Gamma} \leq C(\sigma_0, T)\left\|(I - P_{\mathrm{div},h})\mathbf{j}\right\|_{\mathbf{W}_0^{r,1}\left([0,T];\mathbf{H}^{-1/2}(\mathrm{div}_\Gamma,\Gamma)\right)}, \qquad (5.4.28)$$

i.e., quasi-optimality with respect to the space discretization. Now, we can formulate the following theorem.

Theorem 5.4.10. *Let a Runge-Kutta based convolution quadrature be applied in time and a Galerkin method with lowest order Raviart-Thomas elements be applied in space to the equation $\mathcal{V}(\partial_t)\mathbf{j} = \mathbf{n} \times \mathbf{g}_t$. Under the conditions on the Runge-Kutta method stated in Assumption 5.4.1, the following hold:*

(a) Let $\mathbf{g} \in W_0^{r,1}((0,T);\mathbf{H}_{-1/2}(curl_\Gamma))$ with $r > p+4$, where p is the (classical) order of the Runge-Kutta method. Then, the fully discrete method converges with

$$\begin{aligned}\left\|\mathbf{j}(t_k) - \mathbf{j}_k^{\Delta t,h}\right\|_{-1/2,\mathrm{div}} &\leq C(\Delta t)^{\min\{p,q+1\}}\int_0^t \|\partial_t^{r+1}\mathbf{g}(\tau,\cdot)\|_{-1/2,\mathrm{curl}_\Gamma}d\tau \\ &\quad + C(\sigma_0,T)\left\|(I - P_{\mathrm{div},h})\mathbf{j}\right\|_{\mathbf{W}_0^{r,1}\left([0,T];\mathbf{H}^{-1/2}(\mathrm{div}_\Gamma,\Gamma)\right)}.\end{aligned}$$

(b) Let $\mathbf{g} \in W_0^{r,1}((0,T);\mathbf{H}_{-1/2}(curl_\Gamma))$ with $r > p+5$, where p is the (classical) order of the Runge-Kutta method. Further, let $\hat{\mathbf{w}}_{\mathcal{S},i}$ be the solution of the problem: Find $\hat{\mathbf{w}}_{\mathcal{S},i} \in \mathbf{H}^{-1/2}(\mathrm{div}_\Gamma,\Gamma)$ such that

$$(\hat{\mathbf{w}}_{\mathcal{S},i}, \mathcal{V}(s)\boldsymbol{\zeta})_\Gamma = \ell(\boldsymbol{\zeta}) \qquad \forall \boldsymbol{\zeta} \in \mathbf{H}^{-1/2}(\mathrm{div}_\Gamma,\Gamma),$$

where $\ell(\cdot)$ is the linear functional defined by

$$\ell(\boldsymbol{\zeta}) = \delta_{\mathbf{y}}\mathcal{S}_i(s)(\boldsymbol{\zeta}).$$

If for some $-1/2 \leq \kappa \leq 1$, $\hat{\mathbf{w}}_{\mathcal{S},i} \in \mathbf{H}^\kappa(\mathrm{div}_\Gamma,\Gamma)$ and $\|\hat{\mathbf{w}}_{\mathcal{S},i}\|_{\kappa,div_\Gamma} \leq C|s|^{\alpha_\kappa}$ for $Re\, s > \sigma_0$ and $\mathbf{j} \in W_0^{\alpha_\kappa+8,1}([0,T];\mathbf{H}^{-1/2}(div_\Gamma,\Gamma))$, then for any $\mathbf{y} \in \Omega^+$ and $i = 1,2,3$, it holds

$$\begin{aligned}\left|\mathbf{E}_i(t_k,\mathbf{y}) - \mathbf{E}_{k,i}^{\Delta t,h}(\mathbf{y})\right| &\leq C\Delta t^p\int_0^t \|\partial_t^{r+1}\mathbf{g}(\tau,\cdot)\|_{-1/2,\mathrm{curl}_\Gamma}d\tau \\ &\quad + C(\sigma_0,T)\left\|(I - P_{\mathrm{div},h})\mathbf{j}\right\|_{\mathbf{W}_0^{\alpha_\kappa+8,1}\left([0,T];\mathbf{H}^{-1/2}(\mathrm{div}_\Gamma,\Gamma)\right)} \times \\ &\quad \|I - P_{div,h}\|_{H^\kappa(div_\Gamma)\leftarrow H^{-1/2}(div_\Gamma)}\end{aligned}$$

Proof. Let us first remark that assumptions on $\mathbf{g}$ in both (a) and (b) together with Lemma 5.4.9 imply $\mathbf{j} \in W_0^{r,1}([0,T];\mathbf{H}^{-1/2}(\mathrm{curl}_\Gamma,\Gamma))$, where $r > p+4 \geq 5$ so that (5.4.28) can be applied.

We employ a triangle inequality to obtain

$$\left\|\mathbf{j}(t_k) - \mathbf{j}_k^{\Delta t,h}\right\|_{-1/2,\mathrm{div}_\Gamma} \leq \left\|\mathbf{j}(t_k) - \mathbf{j}^h(t_k)\right\|_{-1/2,\mathrm{div}_\Gamma} + \left\|\mathbf{j}^h(t_k) - \mathbf{j}_k^{\Delta t,h}\right\|_{-1/2,\mathrm{div}_\Gamma}.$$

The first term can be estimated by a best-approximation estimate in space by using (5.4.28):

$$\begin{aligned}\left\|\mathbf{j}\left(t_k\right)-\mathbf{j}^h\left(t_k\right)\right\|_{-1/2,\mathrm{div}_\Gamma} &\leq \left\|\mathbf{j}\left(t_k\right)-P_{\mathrm{div},h}\mathbf{j}\left(t_k\right)\right\|_{-1/2,\mathrm{div}_\Gamma}+\left\|P_{\mathrm{div},h}\mathbf{j}\left(t_k\right)-\mathbf{j}^h\left(t_k\right)\right\|_{-1/2,\mathrm{div}_\Gamma}\\ &\leq \left(1+C\left(\sigma_0,T\right)\right)\left\|\left(I-P_{\mathrm{div},h}\right)\mathbf{j}\right\|_{\mathbf{W}_0^{r,1}\left([0,T];\mathbf{H}^{-1/2}(\mathrm{div}_\Gamma,\Gamma)\right)}.\end{aligned}$$

Note that

$$\mathbf{j}^h-\mathbf{j}^{\Delta t,h}=\left(\mathcal{V}_h^{-1}\left(\partial_t\right)-\mathcal{V}_h^{-1}(\underline{\partial_t}^{\Delta t})\right)P_{0,h}\left(\mathbf{n}_\mathbf{y}\times\partial_t\mathbf{g}\right).$$

Since $\mathcal{V}_h^{-1}\left(s\right)$ has the same analyticity and growth behaviour as $\mathcal{V}^{-1}\left(s\right)$ with respect to $s\in\mathbb{C}$ with $\mathrm{Re}\, s\geq\sigma_0>0$ we can apply Theorem 5.4.6 verbatim for the operator $\mathcal{V}_h^{-1}\left(s\right)$ to obtain

$$\left\|\mathbf{j}^h\left(t_k\right)-\mathbf{j}_k^{\Delta t,h}\right\|_{-1/2,\mathrm{div}_\Gamma}\leq C\left(\Delta t\right)^{\min\{p,q+1\}}\int_0^t\|\partial_t^{r+1}\mathbf{g}(\tau,\cdot)\|_{-1/2,\mathrm{curl}_\Gamma}d\tau.$$

For the estimate in b) we start again with a triangle inequality and denote

$$\left|\mathbf{E}_i(t_k,\mathbf{y})-\mathbf{E}_{k,i}^{\Delta t,h}(\mathbf{y})\right|\leq\left|\mathbf{E}_i(t_k,\mathbf{y})-\mathbf{E}_i^h(t_k,\mathbf{y})\right|+\left|\mathbf{E}_i^h(t_k,\mathbf{y})-\mathbf{E}_{k,i}^{\Delta t,h}(\mathbf{y})\right|. \tag{5.4.29}$$

The second difference can be written as

$$\mathbf{E}_i^h(t_k,\mathbf{y})-\mathbf{E}_{k,i}^{\Delta t,h}(\mathbf{y})=\left(\delta_\mathbf{y}\mathcal{S}_i\mathcal{V}_h^{-1}\left(\partial_t\right)-\delta_\mathbf{y}\mathcal{S}_i\mathcal{V}_h^{-1}\left(\underline{\partial_t}^{\Delta t}\right)\right)P_{0,h}\left(\mathbf{n}_\mathbf{y}\times\mathbf{g}_t\right).$$

From Theorem 5.4.6 we deduce

$$\left|\mathbf{E}_i^h(t_k,\mathbf{y})-\mathbf{E}_{k,i}^{\Delta t,h}(\mathbf{y})\right|\leq C\Delta t^p\int_0^t\|\partial_t^{r+1}\mathbf{g}(\tau,\cdot)\|_{-1/2,\mathrm{curl}_\Gamma}d\tau.$$

For the first term in the right-hand side of (5.4.29) we employ an Aubin-Nitsche type argument as, e.g., described in [32, Theorem 4.2.14]. We consider $\delta_\mathbf{y}\mathcal{S}_i\left(s\right)$ as a linear functional on $\mathbf{H}^{-1/2}(\mathrm{div}_\Gamma,\Gamma)$. With the definition of $\hat{\mathbf{w}}_{\mathcal{S},i}\in\mathbf{H}^{-1/2}(\mathrm{div}_\Gamma,\Gamma)$ above we have

$$\delta_\mathbf{y}\mathcal{S}_i\left(s\right)\left(\widehat{\mathbf{j}}-\widehat{\mathbf{j}}^h\right)=\left(\hat{\mathbf{w}}_{\mathcal{S},i},\mathcal{V}(s)\left(\widehat{\mathbf{j}}-\widehat{\mathbf{j}}^h\right)\right)_\Gamma.$$

By using Galerkin orthogonality and the assumptions $\hat{\mathbf{w}}_{\mathcal{S},i}\in\mathbf{H}^\kappa(\mathrm{div}_\Gamma,\Gamma)$ and $\|\hat{\mathbf{w}}_{\mathcal{S},i}\|_{\kappa,\mathrm{div}_\Gamma}\leq C|s|^{\alpha_\kappa}$ we obtain

$$\begin{aligned}\left|\delta_\mathbf{y}\mathcal{S}_i\left(s\right)\left(\widehat{\mathbf{j}}-\widehat{\mathbf{j}}^h\right)\right| &= \left|\left(\left(I-P_{\mathrm{div},h}\right)\hat{\mathbf{w}}_{\mathcal{S},i},\mathcal{V}(s)\left(\widehat{\mathbf{j}}-\widehat{\mathbf{j}}^h\right)\right)_\Gamma\right|\\ &\leq C|s|^{\alpha_\kappa}\left\|\mathcal{V}\left(s\right)\left(\widehat{\mathbf{j}}-\widehat{\mathbf{j}}^h\right)\right\|_{-1/2,\mathrm{curl}_\Gamma}\left\|I-P_{\mathrm{div},h}\right\|_{H^\kappa(\mathrm{div}_\Gamma)\leftarrow H^{-1/2}(\mathrm{div}_\Gamma)}\\ &\leq C|s|^{\alpha_\kappa+3}\left\|\widehat{\mathbf{j}}-\widehat{\mathbf{j}}^h\right\|_{-1/2,\mathrm{div}_\Gamma}\left\|I-P_{\mathrm{div},h}\right\|_{H^\kappa(\mathrm{div}_\Gamma)\leftarrow H^{-1/2}(\mathrm{div}_\Gamma)}.\end{aligned}$$

Taking into account that $\hat{\mathbf{E}}\left(s,\mathbf{y}\right)=\delta_\mathbf{y}\mathcal{S}\left(s\right)\widehat{\mathbf{j}}$ holds, we obtain

$$\begin{aligned}\left|\mathbf{E}_i(t_k,\mathbf{y})-\mathbf{E}_i^h(t_k,\mathbf{y})\right| \leq C\left(\sigma_0,T\right)&\left\|\mathbf{j}-\mathbf{j}^h\right\|_{\mathbf{W}_0^{\alpha_\kappa+4,1}\left([0,T];\mathbf{H}^{-1/2}(\mathrm{div}_\Gamma,\Gamma)\right)}\times\\ &\left\|I-P_{\mathrm{div},h}\right\|_{H^\kappa(\mathrm{div}_\Gamma)\leftarrow H^{-1/2}(\mathrm{div}_\Gamma)}.\end{aligned}$$

Finally

$$\begin{aligned}\left\|\mathbf{j}-\mathbf{j}^h\right\|_{\mathbf{W}_0^{\alpha_\kappa+4,1}\left([0,T];\mathbf{H}^{-1/2}(\mathrm{div}_\Gamma,\Gamma)\right)} &\leq \left\|\mathbf{j}^h-P_{\mathrm{div},h}\mathbf{j}\right\|_{\mathbf{W}_0^{\alpha_\kappa+4,1}\left([0,T];\mathbf{H}^{-1/2}(\mathrm{div}_\Gamma,\Gamma)\right)}\\ &\quad+\left\|\left(I-P_{\mathrm{div},h}\right)\mathbf{j}\right\|_{\mathbf{W}_0^{\alpha_\kappa+4,1}\left([0,T];\mathbf{H}^{-1/2}(\mathrm{div}_\Gamma,\Gamma)\right)}\end{aligned}$$

and using (5.4.27)

$$\left\|\mathbf{j}^h - P_{\mathrm{div},h}\mathbf{j}\right\|_{\mathbf{W}_0^{\alpha_\kappa+4,1}\left([0,T];\mathbf{H}^{-1/2}(\mathrm{div}_\Gamma,\Gamma)\right)} \leq C\,\|(I-P_{\mathrm{div},h})\mathbf{j}\|_{\mathbf{W}_0^{\alpha_\kappa+8,1}\left([0,T];\mathbf{H}^{-1/2}(\mathrm{div}_\Gamma,\Gamma)\right)}\,. \qquad \square$$

Remark 5.4.11. *In the case of full regularity, the term* $\|(I-P_{\mathrm{div},h})\,\mathbf{j}\|_{\mathbf{W}_0^{r,1}\left([0,T];\mathbf{H}^{-1/2}(\mathrm{div}_\Gamma,\Gamma)\right)}$ *can be estimated by* $\mathcal{O}\left(h^{3/2}\right)$*. However, in the considered case of polyhedral surfaces, the regularity of the solution is typically reduced (cf. [11], [19]).*

From Theorem 5.4.4, it follows that the assumption on the growth behaviour of $\hat{w}_{S,i}$ *is satisfied with* $\alpha_\kappa = 3$ *for* $\kappa = -1/2$*. For* $0 \leq \kappa \leq 1$*, the growth estimate requires a shifted version of Theorem 5.4.4. We skipped this analysis in order not to overload this paper.*

5.5 Numerical Experiments

In all of the numerical experiments, we will consider scattering by a perfect conductor when the incident wave is given by

$$\mathbf{E}^{\mathrm{inc}}(t,\mathbf{x}) = \hat{\mathbf{p}}\cos\left(2\pi f_0\left[t-\mathbf{x}\cdot\hat{\mathbf{k}}/c\right]\right)\,\exp\left[-\frac{(t-\mathbf{x}\cdot\hat{\mathbf{k}}/c-t_p)^2}{2\sigma^2}\right].$$

Here f_0 is the center frequency, $\hat{\mathbf{k}}$ the direction of travel, $\hat{\mathbf{p}}$ polarization, $\sigma = 6/(2\pi f_{bw})$, and $t_p = 6\sigma$. In all of the examples the scatterer will be the unit sphere. For a number of numerical experiments with the convolution quadrature applied to EFIE and CFIE on different scatterers, we refer the reader to [38].

5.5.1 Scattering by a spherical conductor

In the first example, we consider a spherical scatterer of radius 1m and centered at the origin. The center frequency is chosen as $f_0 = 200$ MHz, bandwidth $f_{bw} = 150$ MHz, polarization $\hat{\mathbf{p}} = (1,0,0)$, direction of travel $\hat{\mathbf{k}} = (0,0,1)$, and the length of time computation $T = 6\times10^{-8}s$. Due to the spherical shape of the scatterer, the problem can be approximated accurately and cheaply by Fourier transformation of frequency domain solutions obtained by Mie series [14]. Thus obtained numerical solution will play the role of the exact solution in the calculation of errors.

For the time discretization we have used the 3-stage Radau IIA convolution quadrature. In space, the lowest order Raviart-Thomas elements were used. The computation of the resulting matrices and their storage in $\mathcal{H}$-matrix format were done using a modification of the HLIBpro library written by Ronald Kriemann; see [21, 22] and the website `www.hlibpro.org`. The spatial discretization was chosen sufficiently fine so that no significant change in the error could be observed, the largest calculation had $M = 12288$ spatial degrees of freedom. Since the operator $\mathcal{V}(s)$ satisfies the coercivity result (cf. (5.4.20)), an equivalent norm to $\|\cdot\|_{-1/2,\mathrm{div}}$ is given by

$$\|\boldsymbol{\varphi}\|^2_{-1/2,\mathrm{div}} \sim (\boldsymbol{\varphi}, -\mathcal{V}(1)\boldsymbol{\varphi})_{L^2(\Gamma)}\,.$$

The latter can then be estimated via a Galerkin discretization of the operator $\mathcal{V}(1)$. Finally, the error in time and space is computed as

$$e_{N,\Gamma} := \left(\Delta t\sum_{j=0}^{N}\|\boldsymbol{\varphi}_e(\cdot,t_j)-\boldsymbol{\varphi}_N(\cdot,t_j)\|^2_{-1/2,\mathrm{div}}\right)^{1/2},$$

where φ_e denotes the solution obtained by Mie series. The results thereby obtained are given in Table 5.1.

N	5	10	20	30	40	50
$e_{N,\Gamma}$	9.9	1.4	1.4×10^{-1}	3.4×10^{-2}	1.2×10^{-2}	5.0×10^{-3}
order	–	2.8	3.4	3.4	3.7	3.8

Table 5.1: *Convergence of the 3-stage Radau IIA based convolution quadrature for the EFIE formulation of scattering by a spherical conductor.*

The 3-stage Radau IIA method has stage order $q = 3$, therefore the theory stated in preceding sections predicts the order of convergence to be $O(\Delta t^4)$. The results in Table 5.1 indeed suggest that this convergence order is obtained in the limit in this example.

Finally, let us note that the parameters defining the incident wave have been chosen so that interior resonances of the unit sphere can be excited, see [13]. Still, no adverse effect could be seen in using the EFIE instead of the CFIE.

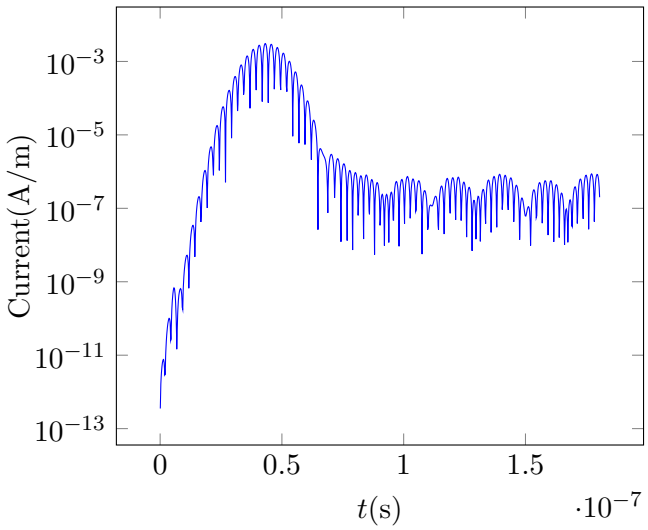

Figure 5.1: *Magnitude of the current at a point on the perfectly conducting sphere induced by an incident wave with center frequency $f_0 = 200MHz$.*

5.5.2 Scattering by a spherical conductor: low frequency instability

In the previous example, the incident wave contained very little near low frequencies. In order to investigate possible instability induced by low-frequency breakdown, for the next computation we change the center frequency to $f_0 = 0$. With a spatial discretization of 6348 degrees of freedom, computational time interval increased to 1.8×10^{-7}, and 400 times steps of the three stage Radau IIA convolution quadrature, the magnitude of the current at a point on the sphere is shown in Figure 5.2. For reference we also show the current for the previous example in Figure 5.1. In Figure 5.1 we see that after $t \approx 0.8 \times 10^{-7}$ the current magnitude seems to stagnate. In reality the current should go to zero, but when

implementing convolution quadrature as described in [24, 4], there is a limit in the accuracy that can be obtained. Therefore we do not expect the numerical current to go to zero, but in the second example the current increases. The convergence analysis allows for such an increase to happen since all the constants in the error estimates depend on the length of the computational time interval T, see [6]. Still, such increase has not been observed in the acoustic case, therefore we expect that the infinite dimensional kernel of the curl curl operator is guilty for this instability.

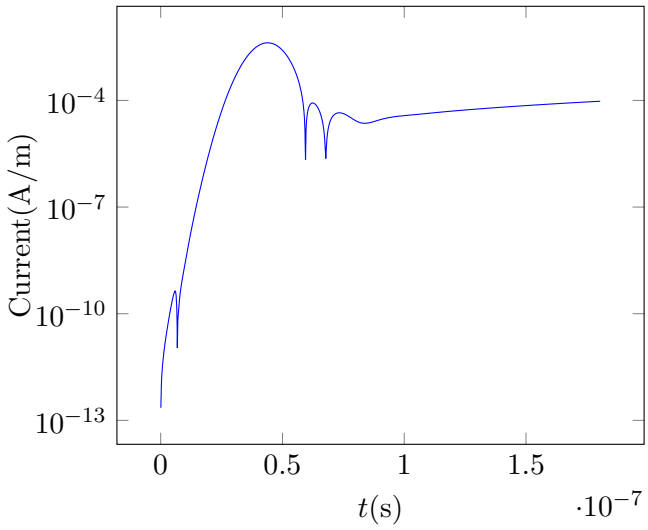

Figure 5.2: *Magnitude of the current at a point on the perfectly conducting sphere induced by an incident wave with center frequency* $f_0 = 0$.

5.6 Conclusion

We described and analysed a numerical method for solving time-domain boundary integral equations arising in electromagnetic scattering which is based on Runge-Kutta convolution quadrature in time and Galerkin BEM for the spatial discretization. We obtained error estimates for the semi-discrete scheme by exploiting that the transfer function in the Laplace domain is bounded by $C|s|/(\mathrm{Re}\ s)$ and therefore the error analysis in [6] can be applied. For the spatial discretization we used the classical Raviart-Thomas elements of lowest order. Using the properties of the involved operators in the Laplace domain we derived convergence estimates for the fully discrete scheme. We performed numerical experiments in the case of a perfectly conducting spherical scatterer. The observed convergence behaviour of the method indicates that the derived error estimates are sharp. The numerical results also showed a possible instability developing if the incident wave excites low frequency modes. The current analysis does not fully describe this phenomenon.

Acknowledgment

The second author gratefully acknowledges the helpful discussions he had with Qiang Chen while visiting University of Delaware.

The fourth author gratefully acknowledges the support given by SNF, No. PDFMP2_127437/1.

References

[1] T. Abboud, J. Nédélec, and J. Volakis. Stable solution of the retarded potential equations. *Proc. 17th Ann. Rev. Progress in Appl. Comp. Electromagnetics, Monterey, CA, March 2001*, pages 146–151, 2001.

[2] A. Bachelot, L. Bounhoure, and A. Pujols. Couplage éléments finis-potentiels retardés pour la diffraction électromagnétique par un obstacle hétérogène. *Numer. Math.*, 89:257–306, 2001.

[3] A. Bamberger and T. H. Duong. Formulation Variationnelle Espace-Temps pur le Calcul par Potientiel Retardé de la Diffraction d'une Onde Acoustique. *Math. Meth. in the Appl. Sci.*, 8:405–435, 1986.

[4] L. Banjai. Multistep and multistage convolution quadrature for the wave equation: Algorithms and experiments. *SIAM J. Sci. Comput.*, 32(5):2964–2994, 2010.

[5] L. Banjai and C. Lubich. An error analysis of Runge-Kutta convolution quadrature. *BIT*, 51(3):483–496, 2011.

[6] L. Banjai, J. Melenk, and C. Lubich. Runge-Kutta convolution quadrature for operators arising in wave propagation. *Numer. Math.*, 119(1):1–20, 2011.

[7] L. Banjai and S. Sauter. Rapid solution of the wave equation in unbounded domains. *SIAM Journal on Numerical Analysis*, 47:227–249, 2008.

[8] L. Banjai and M. Schanz. Wave Propagation Problems treated with Convolution Quadrature and BEM. *accepted for publication*, 2011.

[9] A. Buffa and P. Ciarlet. On traces for functional spaces related to Maxwell's equations. part I: an integration by parts formula in Lipschitz polyhedra. *Mathematical Methods in the Applied Sciences*, 24:9–30, 2001.

[10] A. Buffa and P. Ciarlet, Jr. On traces for functional spaces related to Maxwell's equations. II. Hodge decompositions on the boundary of Lipschitz polyhedra and applications. *Math. Methods Appl. Sci.*, 24(1):31–48, 2001.

[11] A. Buffa, M. Costabel, and D. Sheen. On traces for $H(\mathrm{curl},\Omega)$ in Lipschitz domains. *J. Math. Anal. Appl.*, 276:845–867, 2002.

[12] Q. Chen, P. Monk, X. Wang, and D. Weile. Analysis of Convolution Quadrature Applied to the Time-Domain Electric Field Integral Equation. *Submitted.*

[13] W. C. Chew, J.-M. Jin, E. Michielssen, and J. M. Song. *Fast and Efficient Algorithms in Computational Electromagnetics.* Artech House, Boston, London, 2001.

[14] V. A. Erma. Exact solution for the scattering of electromagnetic waves from conductors of arbitrary shape. II. General case. *Phys. Rev. (2)*, 176:1544–1553, 1968.

[15] M. Friedman and R. Shaw. Diffraction of pulses by cylindrical obstacles of arbitrary cross section. *J. Appl. Mech*, 29:40–46, 1962.

[16] T. Ha-Duong. On retarded potential boundary integral equations and their discretisation. In *Topics in Computational Wave Propagation: Direct and Iverse Problems*, volume 31 of *Lect. Notes Comput. Sci. Eng.*, pages 301–336. Springer, Berlin, 2003.

[17] W. Hackbusch, W. Kress, and S. Sauter. Sparse convolution quadrature for time domain boundary integral formulations of the wave equation by cutoff and panel-clustering. In M. Schanz and O. Steinbach, editors, *Boundary Element Analysis*, pages 113–134. Springer, 2007.

[18] W. Hackbusch, W. Kress, and S. Sauter. Sparse convolution quadrature for time domain boundary integral formulations of the wave equation. *IMA, J. Numer. Anal.*, 29:158–179, 2009.

[19] R. Hiptmair and C. Schwab. Natural Boundary Element Methods for the Electric Field Integral Equation on Polyhedra. *SIAM Journal on Numerical Analysis*, 40:66–86, 2002.

[20] W. Kress and S. Sauter. Numerical treatment of retarded boundary integral equations by sparse panel clustering. *IMA J. Numer. Anal.*, 28(1):162–185, 2008.

[21] R. Kriemann. HLIBpro C language interface. Technical Report 10/2008, MPI for Mathematics in the Sciences, Leipzig, 2008.

[22] R. Kriemann. HLIBpro user manual. Technical Report 9/2008, MPI for Mathematics in the Sciences, Leipzig, 2008.

[23] C. Lubich. Convolution Quadrature and Discretized Operational Calculus I. *Numerische Mathematik*, 52:129–145, 1988.

[24] C. Lubich. Convolution Quadrature and Discretized Operational Calculus II. *Numerische Mathematik*, 52:413–425, 1988.

[25] C. Lubich. On the multistep time discretization of linear initial-boundary value problems and their boundary integral equations. *Numerische Mathematik*, 67(3):365–389, 1994.

[26] C. Lubich. Convolution quadrature revisited. *BIT Numerical Mathematics*, 44:503–514, 2004.

[27] C. Lubich and A. Ostermann. Runge-Kutta methods for parabolic equations and convolution quadrature. *Math. Comp.*, 60(201):105Ű131, 1993.

[28] J. C. Nédélec. *Acoustic and Electromagnetic Equations*. Springer-Verlag, 2001.

[29] A. Pujols. *Equations intégrales Espace-Temps pour le système de Maxwell Application au calcul de la Surface Equivalente Radar*. PhD thesis, L'Universite Bordeaux I, 1991.

[30] A. Pujols. Time Dependent Integral Method for Maxwell Equations. *Rapport CESTA/SI A. P. 6589*, 1991.

[31] P. Raviart and J. Thomas. A mixed finite element method for 2-nd order elliptic problems. *Mathematical aspects of finite element methods (Springer Lecture Notes in Mathematics)*, 606:292–315, 1977.

[32] S. Sauter and C. Schwab. *Boundary Element Methods*. Springer, 2010.

[33] S. Sauter and A. Veit. Adaptive Time Discretization for Retarded Potentials. Preprint 04-2011, Universität Zürich.

[34] A. Schädle, M. López-Fernández, and C. Lubich. Fast and oblivious convolution quadrature. *SIAM J. Sci. Comput.*, 28(2):421–438, 2006.

[35] M. Schanz. Wave Propagation in Viscoelastic and Poroelastic Continua. A Boundary Element Approach. In *Lecture Notes in Applied and Computational Mechanics 2*. Springer, 2001.

[36] I. Terrasse. *Résolution mathématique et numérique des équations de Maxwell instationnaires par une méthode de potentiels retardés*. PhD thesis, Ecole polytechnique, 1993.

[37] A. Veit. Convolution quadrature for time-dependent Maxwell equations. Master's thesis, University of Zurich, 2009.

[38] X. Wang, R. Wildman, D. Weile, and P. Monk. A finite difference delay modeling approach to the discretization of the time domain integral equations of electromagnetics. *IEEE Transactions on Antennas and Propagation*, 56(8):2442–2452, 2008.

[39] D. S. Weile, A. Ergin, B. Shanker, and E. Michielssen. An accurate discretization scheme for the numerical solution of time domain integral equations. *IEEE Antennas and Propagation Society International Symposium*, 2:741–744, 2000.

[40] D. S. Weile, G. Pisharody, N. W. Chen, B. Shanker, and E. Michielssen. A novel scheme for the solution of the time-domain integral equations of electromagnetics. *IEEE Transactions on Antennas and Propagation*, 52:283–295, 2004.

[41] D. S. Weile, B. Shanker, and E. Michielssen. An accurate scheme for the numerical solution of the time domain electric field integral equation. *IEEE Antennas and Propagation Society International Symposium*, 4:516–519, 2001.

[42] A. Wildman, G. Pisharody, D. S. Weile, S. Balasubramaniam, and E. Michielssen. An accurate scheme for the solution of the time-domain integral equations of electromagnetics using higher order vector bases and bandlimited extrapolation. *IEEE Transactions on Antennas and Propagation*, 52:2973–2984, 2004.